ROLES OF THE ESTROGEN RECEPTORS AND THE NUCLEAR MATRIX IN BREAST CANCER DEVELOPMENT AND TAMOXIFEN RESISTANCE

by

Miranda Jean Sarachine

B.S. Biology, Allegheny College, 2004

Submitted to the Graduate Faculty of

The University of Pittsburgh School of Medicine in partial fulfillment

of the requirements for the degree of

Doctor of Philosophy

University of Pittsburgh

2009

UNIVERSITY OF PITTSBURGH

SCHOOL OF MEDICINE

This dissertation was presented

by

Miranda Jean Sarachine

It was defended on

September 10th, 2009

and approved by

Bruce Freeman, Ph.D., Pharmacology and Chemical Biology

Thomas Conrads, Ph.D., Pharmacology and Chemical Biology

Jean Latimer, Ph.D., Obstetrics, Gynecology, and Women's Health

Guillermo Romero, Ph.D., Pharmacology and Chemical Biology

Billy W. Day, Ph.D., Major Thesis Advisor, Pharmaceutical Sciences

ROLES OF THE ESTROGEN RECEPTORS AND THE NUCLEAR MATRIX IN BREAST CANCER DEVELOPMENT AND TAMOXIFEN RESISTANCE

Miranda Jean Sarachine, PhD

University of Pittsburgh, 2009

In the United States in 2009, 192,370 women are expected to be diagnosed with invasive breast cancer, and 62,280 with *in situ* disease. About 70% of these cases are estrogen receptor positive (ER+). There are two isoforms of the ER, α and β, that differ somewhat in structure and action. ERβ expression plays a protective role in breast cancer, and selective targeting of this isoform would have many beneficial effects. Tamoxifen has long been the standard of care for patients with ER+ breast cancer. A major problem with tamoxifen is the development of drug resistance. One of the mechanisms proposed for the development of tamoxifen resistance involves the loss of ERβ expression.

The first objective of this study was to screen a library of biphenyl *C*-cyclopropylalkylamides for their ability to function as ERβ-selective ligands. Two compounds were identified with modest selectivity for ERβ and anti-proliferative effects in breast cancer cells where they inhibited expression of c-Myc.

The nuclear matrix (NM), the structural scaffolding of the nucleus, plays a major role in many fundamental processes of the cell. Using the ER+ breast cancer cell line MCF-7 and an antiestrogen resistant derivative, along with subtype selective ER ligands, alterations in the abundance of specific proteins present in the NM were identified using a mass spectrometry (MS)-based relative quantitative methodology. Some of the most interesting proteins with altered abundance are NuMA, serpin H1, hnRNP R, and dynein heavy chain 5. These proteins

may represent putative biomarkers to customize treatment. The alterations also provide a mechanistic understanding of tamoxifen resistance.

The NM was also investigated by MS in the earliest stage of breast cancer, ductal carcinoma *in situ* (DCIS), utilizing novel cell lines derived from normal (breast reduction), DCIS, and non-diseased contralateral breast surgical specimens. Two of the interesting proteins found to be altered in DCIS were HSP90 and EEF1D. These studies may provide biomarkers to aid in the diagnosis and treatment of breast cancer. In addition by understanding the mechanism behind the development of breast cancer, prevention becomes a possibility.

TABLE OF CONTENTS

LIST OF TABLES

LIST OF FIGURES

ACKNOWLEDGEMENTS

Special thanks goes to my advisor, Dr. Billy W. Day, for his guidance and support over the past several years. He has truly helped develop me into an independent researcher, for which I will always be grateful. He also gave me the opportunity to take on exciting new projects and was there to provide advice whenever I needed it. Additionally, I acknowledge all the members of the Day lab for their support over the years, including Jelena Janjic for getting me started in the lab, and particularly Brianne Raccor and Hikmat Daghestani, who have also become great friends. I am also grateful to Drs. Jean Latimer and Steve Grant for providing much support and scientific advice throughout our collaboration with their lab. I also thank Amie Benson, Nicole Myers-Gonzalez, Nancy Lalanne, and Tim Furphee for their assistance in the Latimer lab.

I would like to acknowledge my committee for all of their valuable feedback throughout my dissertation work and writing. I also want to thank the proteomics core lab staff for taking the time to provide their advice and support. Thankfully, John, Chris, and Guy were always willing to come along for a coffee break. All of the support staff in the Interdisciplinary Biomedical Sciences Graduate Program, the Pharmacology department, and the School of Pharmacy have helped in one way or another by answering questions, ordering supplies, or helping with forms.

I would also like to thank my friends for all their support:

- Neil, my running partner and big brother, I can't thank you enough for how great of a friend you have become. I truly do not know how I would have made it though these years without you. I can't thank you enough for being such a good friend and helping me to grow these past few years.
- Hikmat, you have been a great friend both inside and out of lab. Thank you so much for all your support and help; you are a major reason I made it. I'll really miss you.
- Nisa, our emails back and forth really helped me get through the tough times. You are such a great friend. Visit soon!
- Carolyn, Christi, Joe, Jared, Arlee, Austin, Brian, Bart, Mike, Vicki, Lauren, Derek, and the rest of the 2009 PSL softball champs, you guys were a blast to play with and great friends. Thanks for the support!
- Kristen & Kelly, I'm so thankful I got to spend so much time with you guys over the past couple years. I expect a visit soon, because I'm going to miss you guys and Pony so much! And Kristen, I'll keep working on the business ideas.
- Amy, thanks for being a great friend for over 20 years now!
- Brian, thanks for the funny texts that always gave me a reason to smile.
- Brianne, lab has not been the same without you. I'm looking forward to joining you out west and hopefully hanging out more. Thanks for your support whenever I needed it.
- Nicole, thank you so much for all your help in lab and also for being there to listen to whatever I had to talk about. I'm going to miss you so much.

The network of family I have around me is truly why I am where I am today and I will forever be indebted to them. My first thank you goes to my late grandma, Rita Moorman, who was my inspiration to get involved in breast cancer research, and is the reason I am in this current position. Additionally I wish to thank my late grandfather, Ed Sarachine (Pappy), who was another great motivator in my life and never far from my thoughts and my grandmother, Lucia Sarachine, for her emails throughout grad school that always made me smile. Her constant support and love have meant so much. To all my aunts, uncles and cousins who have had encouraging words whenever I needed them, know that I appreciate you all, especially my Aunt Linda, who has always been interested in my research and supported me through all of it, even making the trip out here to see me present it, and even you, Uncle Ray…I think I'm finally done with school! I also want to thank the Falso family, who I consider my second family, for their support and love over the last six years. I'm grateful to my brother Stevie for his support and for letting me scream from the bleachers at his hockey games as my escape from science. My sister Melanie (and Gomer) deserve thanks for always listening to me and putting up with my craziness like nobody else can. And finally my parents, Ann and Steve, who I cannot even begin to thank for the love they have shown me and the support they have provided. I have accomplished all that I have in my life because of the opportunities they have given me. I am so lucky that I was able to find such a strong program close to Pittsburgh, because it allowed me to spend time with my heroes. I hope to someday be as great at parenting. I know I am going far away for the next step in life, but you will always be in my heart.

Finally, I would like to thank Paul Falso, who despite being almost 3,000 miles away the last four years has managed to be my strongest supporter. Paul has helped me stay sane and provided me with an escape whenever I needed it. I will never be able to thank him enough for

all that he has done for me. His love and care are a major reason I have been able to achieve this accomplishment. His passion for his work has always been inspirational to me, and I'm truly grateful. We have some great times ahead.

ABBREVIATIONS

2D-LC-MS/MS - two dimensional-liquid chromatography-mass spectrometry/mass spectrometry
AF1 - activation function 1
AF2 - activation function 2
AI - aromatase inhibitor
AKT - protein kinase B
ARE - antioxidant response element
ASCO - American Society of Clinical Oncology
ATCC - American Type Culture Collection
BCA - bicinchoninic acid
BMP-6 - bone morphogenetic protein 6
BRL - breast reduction line
BTL - breast tumor line
CEA - cardioembryonic antigen
CFBS - colostrum free bovine serum
CGH - comparative genomic hybridization
CID - collision-induced disassociation
cisplatin - *cis*-diamminedichloroplatinum (II)
CKB - creatine kinase B
DBD - DNA binding domain
DCIS - ductal carcinoma *in situ*
DPN – diarylpropionitrile
E2 - 17β-estradiol
ECM - extracellular matrix
EEF1D - eukaryotic translation elongation factor 1 delta
EGFR - epidermal growth factor receptor
ELISA – enzyme-linked immunosorbent assays
ER - estrogen receptor
ERE - estrogen response element
ES2 - fluorescent E2 derivative
ESA - epithelial specific antigen

FBS - fetal bovine serum
FFPE - formalin-fixed, paraffin-embedded
FP - fluorescence polarization
GI_{50} - 50% growth inhibition
GO - gene ontology
H2O2 - hydrogen peroxide
HER2 - human epidermal growth factor receptor 2
HET - HSP27-ERE-TATA-binding protein
HMEC - human mammary epithelial cell
hnRNP - heterogeneous nuclear ribonucleoprotein
HPV - human papillomavirus
HSP - heat shock protein
IF - intermediate filament
IGF-IR - insulin-like growth factor-1 receptor
iTRAQ - isobaric tags for relative and absolute quantitation
LBD - ligand binding domain
LCIS - lobular carcinoma *in situ*
LN - lobular neoplasia
MAPK - mitogen activated protein kinase
MAR - matrix attachment region
MENI - multiple endocrine neoplasia type I
MISS - membrane-initiated steroid signaling
MMTS - methyl methanethiosulfonate
MOPS - 3-(*N*-morpholino)propanesulfonic acid
MPP - methyl-piperidinopyrazole
MS - mass spectrometry
mTOR - mammalian target of rapamycin
NAF - nipple aspirate fluid
nano-LC-ESI-Q-TOF - nanoscale-liquid chromatography-electrospray ionization-quadrupole-time-of-flight
nano-LC-MALDI-TOF/TOF - nanoscale-liquid chromatography-matrix assisted laser desorption ionization-time of flight/time of flight
NCOR1 - nuclear receptor corepressor 1
NHS - *N*-hydroxysuccinimde
NLS - nuclear localization sequence
NM - nuclear matrix
NMP - nuclear matrix protein
Nrf2 - NF-E2 related factor 2
NuMA - nuclear mitotic apparatus
PAI-1 - plasminogen activator inhibitor
PBS - phosphate buffered saline
PDGFβ - platelet derived growth factor β
PI3K - phosphatidylinositol-3-kinase

PMSF - phenylmethanesulfonyl fluoride
PPT - propylpyrazole triol
PR - progesterone receptor
SAR - structure activity relationship
SCX - strong cation exchange chromatography
SERD - selective estrogen receptor downregulator
SERM - selective estrogen receptor modulator
SRC-1 - steroid receptor coactivator 1
St Dev - standard deviation
TCEP - tris(2-carboxyethyl)phosphine
uPA - urokinase plasminogen activator
VEGF - vascular endothelial growth factor

1.0 INTRODUCTION

1.1 THE ESTROGEN RECEPTORS

1.1.1 Overview

The steroid hormone 17β-estradiol (E2) (Figure 1) plays a major role in the growth, differentiation and function of many different target tissues, including the mammary gland, uterus, ovary, testis and prostate. Additionally, E2 functions in bone maintenance and the cardiovascular system (Clark, 1992). Estrogens are produced mainly by the testes and ovaries and then diffuse in and out of all cells (Murdoch, 1991). In a target cell, E2 exerts its effect primarily through the ER. ERα was discovered in the 1960s as a protein that specifically bound tritium-labeled E2 in the uterus (Jensen, 1962). The cDNA for ERα was cloned in 1986 (Green, 1986A; Greene, 1986). For ten years ERα was believed to be the only ER, but in 1996 a second ER was cloned from rat prostate, ERβ (Kuiper, 1996).

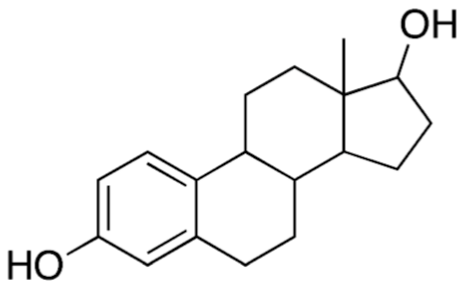

1 – 17β-Estradiol

Figure 1: The structure of E2 (1).

The structure of steroid hormone E2, which binds the ERs and plays a major role in the growth, proliferation, and/or function of many target tissues, including the male and female reproductive, cardiovascular, and skeletal systems.

The ERs belong to a superfamily of nuclear hormone receptors. ERα and ERβ are produced by distinct genes located on chromosomes 6 and 14, respectively (Green, 1986B; Kuiper, 1996). ERα is a 595 amino acid protein with a molecular weight of 66 kDa (Green, 1986A). ERβ is a 530 amino acid protein with a molecular weight of 54.2 kDa (Kuiper, 1996). In the human body, both receptors display both overlapping and tissue-specific distribution. ERα is the predominant receptor in the pituitary gland, thecal and interstitial cells in the ovaries, uterus, liver, kidneys and adrenals, while ERβ is the predominant receptor in the prostate, bone, granulosa cells of the ovaries, lung, and in the central and peripheral nervous system (Kuiper, 1997; Emmen, 2005; Harris, 2007).

1.1.2 Structure

The ER has a well-defined organization with five domains designated A/B, C, D, E, and F (Kumar, 1987). Figure 2 illustrates the domain organization of the two ERs. The A/B domain is located at the N-terminus of the protein and contains the activation function 1 (AF1). AF1 is the ligand-independent, constitutively-active activation function (Tora, 1989). The C domain contains the DNA-binding and receptor dimerization regions (Mader, 1993). The DNA-binding domain (DBD) contains two zinc-fingers responsible for specific binding to DNA (Enmark, 1997). In DNA, the ERs bind an estrogen-response element (ERE) located in the promoter of estrogen-regulated genes. An ERE has the sequence GGTCAnnnTGACC (O'Lone, 2004; Carroll, 2006). The D domain is the flexible hinge between the C and E domains and bears a nuclear localization sequence (NLS) (Picard, 1990). The E domain contains the ligand-binding domain (LBD) and a second NLS. The ligand-binding region contains twelve helices and is involved in both ligand binding and receptor dimerization. Activation function 2 (AF2) is also located in the E domain and is responsible for the ligand-dependent activation of the ER (Tora, 1989). The F domain,\ is located at the extreme C terminus of the receptor. This small domain is unnecessary for transcriptional activation but does modulate both AF1 and AF2 activity (Weatherman, 2001; Koide, 2007; Skafar 2008).

The two isoforms of the ER differ somewhat in their structures. The highest level of homology, 96%, is present in their DBDs (domain C). Their ligand binding domains (domain E) share 55% homology (Kuiper, 1996). There are only two amino acid differences in the residues within the ligand binding pockets. Met421 in ERα corresponds to Ile373 in ERβ, and Leu384 in ERα corresponds to Met336 in ERβ. These amino acid differences have an effect on the overall volume of the ligand binding pocket. ERα's binding pocket has a volume of 490 $Å^3$ and ERβ's

binding pocket has a volume of 390Å^3 (Veeneman, 2005). E2 binds to the two isoforms with similar affinity due to the similarity in their binding pockets. The K_d for E2 binding to ERα is 0.05 nM, while the K_d for E2 binding to ERβ is 0.9 nM (Kuiper, 1998). The most variable regions of the receptors are the N-terminal A/B domain and the C-terminal F domain, where the receptors share less than 20% homology. These regions likely account for some of the subtype-specific actions on target genes (McInerney, 1998).

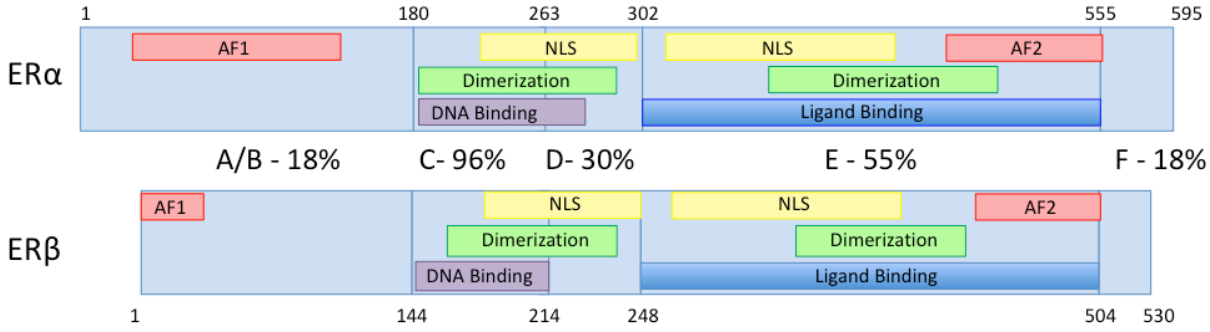

Figure 2: The domains of ERα and ERβ.

The least homology, less than 20%, is seen in domains A/B, which contains AF1, and F. Domain C contains the DNA binding domain and is the most homologous between the two isoforms, with 96% homology. Domain D is the hinge and has 30% homology between the two isoforms, while domain E is the ligand binding domain with 55% homology.

1.1.3 Mechanism of Action

The ER functions as a ligand-inducible transcription factor. When estrogen is absent from a cell, the ER exists as an inactive, monomeric protein bound to heat shock proteins (Cheung, 2000). When bound to estrogen, the ER regulates the transcription of specific target genes (Osborne, 2001; Osborne, 2005A). Estrogen binds to the LBD of the ER and induces a conformational

change, promotes phosphorylation of the receptor, leads to dissociation from heat shock chaperone proteins, and induces receptor dimerization (Osborne, 2001). The ER then functions through two different mechanisms: genomic and non-genomic.

1.1.3.1 Genomic Signaling

In the genomic signaling pathway, ligand-bound ER dimer binds to the ERE located in the promoter of estrogen-regulated genes (O'Lone, 2004; Carroll, 2006). The ER dimer then regulates expression of ERE-containing genes, which are primarily involved in cell proliferation and survival (Dobrzycka, 2003; Frasor, 2003). The perfect palindrome ERE, GGTCAnnnTGACC, is derived from highly E2-responsive genes of *Xenopus laevis* (Klein-Hitpass, 1988; Peale, 1988). Most human E2-target genes contain an imperfect palindrome sequence in their promoter. Variations in ERE sequence slightly change the confirmation of the ER and modulate gene transcription (Wood, 2001). Complement 3 and pS-2 are two example genes that contain EREs in their promoters and are regulated via this pathway, the classical pathway of ER action (Berry, 1989).

Several non-classical genomic pathways involve an interaction of the ER with another transcription factor. This interaction stabilizes the direct binding of the ER to DNA to influence the transcription of genes lacking an ERE. The first of these pathways involves the Jun/Fos transcription factors and their binding with the ER to regulate Ap-1 sites in DNA (Kushner, 2000). Another pathway involves c-Jun/ATF-2, which binds with the ER to cyclic AMP-response elements in DNA (Sabbah, 1999). One other pathway involves the Sp-1 transcription factor, which binds with the ER to Sp1 sites in DNA (Saville, 2000). Cyclin D1 and insulin-like growth factor-I receptor (IGF-IR) are two example genes that are regulated by E2 in this non-classical manner (Eeckhoute, 2006; Maor, 2006).

Once recruited to the promoter of estrogen-responsive genes through either the classical or non-classical mechanism, gene transcription is induced only if AF1 and/or AF2 are activated (Tora, 1989). AF1 activation is ligand independent and is regulated by phosphorylation at specific serine residues. These residues are phosphorylated following activation of the p42/p44 mitogen-activated protein kinase (MAPK), phosphatidylinositol-3-kinase (PI3K)/protein kinase B (AKT) and p38 MAPK pathways (Kato, 1995; Bunone, 1996; Campbell, 2001; Thomas, 2008). Phosphorylation of AF1 then stimulates ER-mediated transcription by recruiting coactivators (Webb, 1998). AF1 can also be activated in response to estrogen and interacts synergistically with AF2 to recruit coactivators that interact with both AFs to influence transcription (Hall, 2001; McInerney, 1996; Kobayashi, 2000). The activation of AF2 depends on the presence of the ligand. When estrogen binds to the ER it induces a rearrangement of several helices in the LBD. This creates a hydrophobic cleft with helix 12 enclosing the hormone in the pocket and exposing the AF2 region to the outside of the receptor. The AF2 region is where coregulatory proteins, both coactivators and corepressors containing LXXLL motifs, or NR boxes, bind and influence gene expression (Brzozowski, 1997; Shiau, 1998; McKenna, 1999). The roles of coregulatory proteins recruited to the ER are determined by both the specific ERE sequence present in the target gene and the specific ligand bound to the ER (Gruber, 2004; Yi, 2002).

1.1.3.2 Non-genomic Signaling

The ERs also influence cellular behavior through a non-genomic signaling mechanism. The non-genomic signaling pathway is also known as the membrane-initiated steroid-signaling (MISS) pathway (Razandi, 2003). A response occurs within minutes of the addition of estrogen, much faster than the genomic signaling pathway, and is mediated through membrane-bound ER,

independent of gene transcription (Evinger, 2005). This membrane bound ER is the same ER as nuclear ER (Pedram, 2006). In bone and endothelial cells, estrogen signaling occurs primarily through this pathway (Kousteni, 2002). At the membrane, the ER is associated with caveolin rafts (Marino, 2008). There are specific motifs within the E domain of the ER that are required for membrane-localization of the receptor (Pedram, 2007). When estrogen binds, the ERs dimerize and interact with adaptor proteins, such as Src, the p85 subunit of PI3K and G-proteins, and activate a variety of growth factor signaling pathways including EGFR, IGFR1, HER2, MAPKs, PI3K, AKT, and mammalian target of rapamycin (mTOR) (Marino, 2008; Evinger, 2005; Kahlert, 2000; Wong, 2002; Schiff, 2004). The cytoplasmic kinases in these growth factor signaling pathways phosphorylate the ER and its coactivators and activate nuclear ER-driven transcription as described in the genomic signaling pathway (Shou, 2004). The genomic and non-genomic activities of the ER complement each other and can even act in a synergistic manner (Zilli, 2009).

1.1.4 Ligands

One class of ligands for the ER is the selective estrogen receptor modulators (SERMs). SERMs elicit estrogenic or anti-estrogenic activity depending upon the tissue where they are located (McDonnell, 1999). SERMs act by competitively inhibiting estrogen from binding to the ERs and affect both the genomic and non-genomic signaling mechanisms of the ERs (Brzozowski, 1997). The most common SERMs are tamoxifen and raloxifene. Tamoxifen (Figure 3) is a triphenylethylene that displays a variety of estrogenic and anti-estrogenic activities. Metabolism of tamoxifen produces a highly active metabolite, 4-hydroxytamoxifen (Figure 3), that has a higher affinity for the ERs than tamoxifen. Raloxifene is a dihydroxylated nonsteroidal

compound that contains a benzothiophene core. It has high affinity for both isoforms of the ER (Kuiper, 1997). Other ER ligands are pure anti-estrogens. The most common pure antiestrogen is fulvestrant (Figure 3). This compound is a 7α-alkylamide derivative of E2 that binds both isoforms of the ER (Van Den Bemd, 1999). It binds the ER and prevents it from activating transcription. Fulvestrant is considered a selective estrogen receptor downregulator (SERD).

A variety of ligands are currently being developed in order to selectively target one isoform or the other of the ER. The first of these is propylpyrazole triol (PPT) (Figure 3), which is a 410-fold selective agonist for ERα with no ability to stimulate transcription through ERβ (Stauffer, 2000). A second pyrazole, methyl-piperidinopyrazole (MPP) (Figure 3), is an ERα-selective antagonist that binds the α isoform of the ER with about 200-fold greater affinity than it has for the β isoform of the ER, and suppresses E2-stimulation through ERα but not through ERβ (Sun, 2002). Another ligand is diarylpropionitrile (DPN) (Figure 3), a selective ERβ agonist that binds to ERβ with 70-fold selectivity compared to ERα. DPN activates transcription through ERβ with 170-fold more potency than it does through ERα (Meyers, 2001).

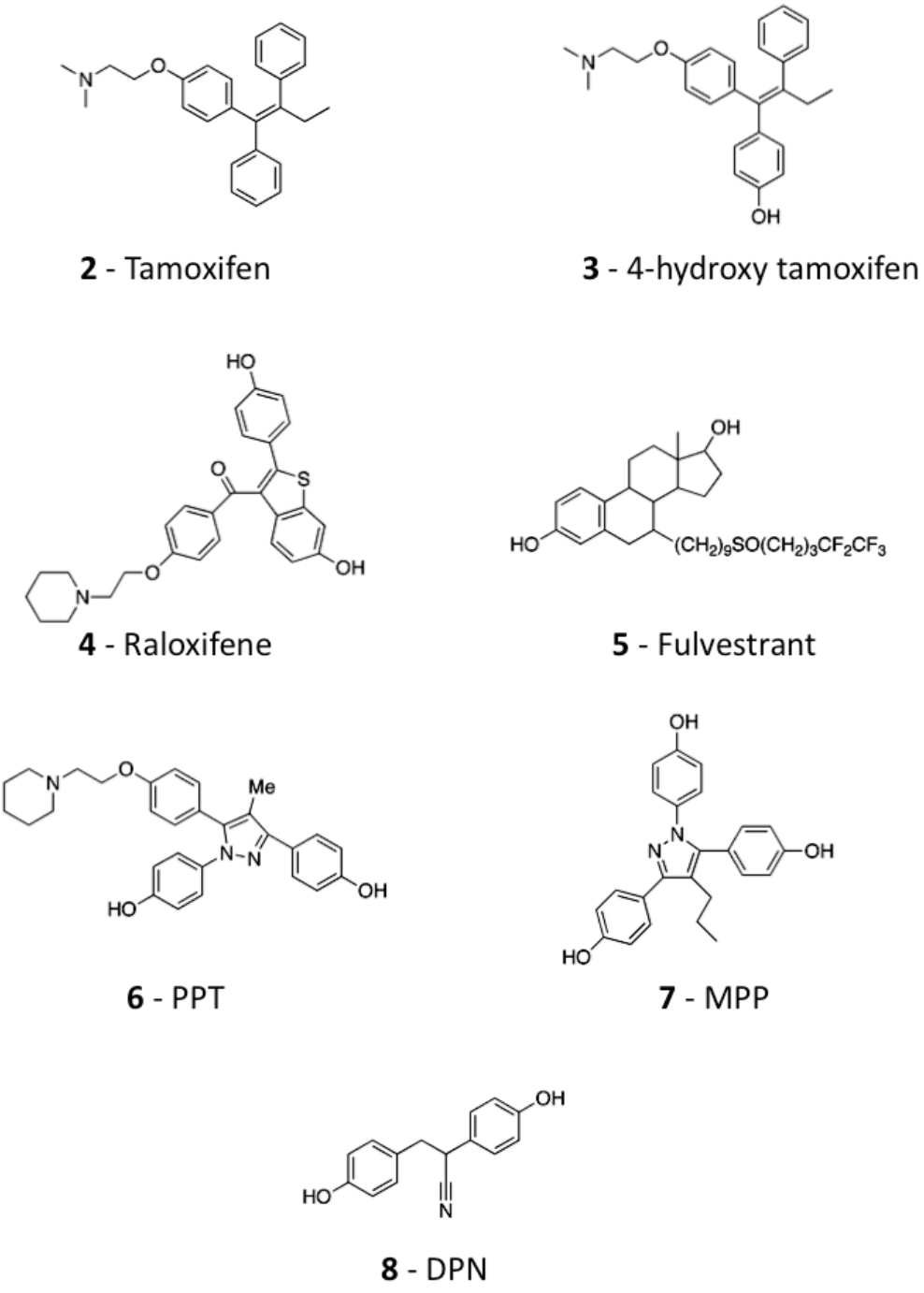

Figure 3: The structures of several ER ligands.

ER ligands include the SERM tamoxifen (**2**); its metabolite 4-hydroxy tamoxifen (**3**); the SERM, raloxifene (**4**); the SERD, fulvestrant (**5**); PPT (**6**), an ERα-selective agonist; MPP (**7**), an ERα-selective antagonist; and DPN (**8**), an ERβ-selective agonist.

1.2 BREAST CANCER

1.2.1 Overview

Breast cancer occurs when the cells in the breast grow uncontrollably because of genetic and epigenetic alterations. The breast is composed of lobules, the glands that produce milk; ducts that connect the lobules to the nipple; fatty, connective tissue; and lymphatic tissue. Breast cancer is classified as *in situ* when it remains confined within the duct (DCIS) or within the lobule (lobular carcinoma *in situ* (LCIS)). The majority of breast cancer diagnosed is classified as invasive and originated in the duct or lobule then broke through the epithelial architecture and invaded the surrounding tissue of the breast (American Cancer Society, 2007). In the United States in 2009, 192,370 women are expected to be diagnosed with invasive breast cancer, while 62,280 women are expected to be diagnosed with *in situ* disease. Of these in situ cases, 85% will be DCIS. Additionally in 2009, 40,170 women are expected to die from breast cancer, making it the second leading amongst cancer deaths to lung cancer. Mammography detects breast cancer at an early stage and on average detects 80-90% of breast cancers in women without symptoms (American Cancer Society, 2009). When a breast tumor is discovered, it is assigned a stage in order to aid in prognosis and treatment decisions. The stage is assigned based upon the size of the tumor, invasiveness, the involvement of lymph nodes and if the cancer has spread beyond the breast and metastasized to other organs (National Cancer Institute, 2009). The characteristics of each stage can be seen in Table 1.

Table 1: The staging of breast cancer.

Stage	Tumor Size	Lymph Node Status	Metastasis Status
0 (in situ)	Any	Negative	Negative
1	$\leq$ 2 cm	Negative	Negative
2A	$\leq$ 2 cm	Positive	Negative
	2-5 cm	Negative	Negative
2B	2-5 cm	Axillary Positive	Negative
	> 5 cm	Axillary Negative	Negative
3A	$\leq$ 5 cm	Ipsilateral Axillary Positive	Negative
3B	Any	Internal Mammary Positive	Negative
4	Any	Any Positive	Positive

1.2.2 The Estrogen Receptors in Breast Cancer

In breast cancer, ER status is determined as a binary factor of (+) or (−). The ER is expressed in about 70% of invasive breast cancers. ER status provides prognostic information and is a predictor of response to endocrine therapy. The current assays used to determine ER status in a patient usually detect only the α isoform (Murphy, 2006). ERβ is expressed in both normal and neoplastic breast tissue (Leygue, 1998; Jarvinen, 2000). The typical levels of the two ERs in the breast are similar. Sucrose gradient profiling demonstrates the range of ERα protein in breast tissue as 13 – 3,700 fmol/mg and 20 – 475 fmol/mg for ERβ protein (Pearce, 2004). Immunohistochemical analysis of 512 breast tumors showed 78% were ERα positive while 50% were ERβ positive and ERβ expression was positively correlated with ERα expression (Borquist, 2008). Within the breast ERβ is more broadly expressed in both epithelial and stromal cells, while ERα is primarily observed in epithelial cells (Park, 2003). Studies investigating the levels of the two ER isoforms in different stages of breast abnormalities demonstrate that the receptors function differently in the development of breast cancer. A larger ratio of ERα:ERβ is present in many breast cancer tumors compared to benign lesions and normal tissues (Roger, 2001; Shaw,

2002; Park, 2003). ERβ expression is strong in the normal mammary gland and expression is reduced during carcinogenesis (Shaaban, 2003; Skiliris, 2003). In an immunohistochemical analysis of 283 breast tissue samples ERβ expression was present in the following percentages in each class examined: 94% of normal breast lobules, 77% of ductal hyperplasia, 70% of DCIS, and 60% of invasive cancer (Shaaban, 2003). Additionally, ERβ expression is associated with a better prognosis in breast cancer patients (Sugiura, 2007). Immunohistochemical analysis of breast cancer patients receiving hormone therapy demonstrated patients with ERα positive tumors demonstrated increased disease free survival when also expressing ERβ compared to those only expressing ERα (Borgquist, 2008). Therefore the loss of ERβ expression may be involved in tumor progression (Bardin, 2004). Subtype selective ER knockout mice also demonstrate how the receptors function differently in the breast. ERα-knockout mice demonstrate very little growth of their mammary ducts, while ERβ-knockout mice develop mammary glands with normal ductal branching (Labahn, 1993; Förster, 2002).

Altering the expression of the ER isoforms in breast cancer cell lines has also added to the understanding of their roles. Overexpression of ERβ inhibits the E2-induced proliferation of ERα expressing breast cancer cells (Omoto, 2003; Ström, 2004; Paruthiyil, 2004; Williams, 2008). This ERβ overexpression represses c-myc, cyclin D1, and cyclin A1 expression; increases the expression of p21 and p27; and leads to a cell cycle arrest in the G_2 phase (Paruthiyil, 2004). ERβ expression additionally decreases the expression of positive proliferation regulators such as cyclin E, Cdc25A, and $p45^{skp2}$ (Ström, 2004). ERα positive T47D breast cancer cells altered to express ERβ show a reduced tumor size, less intratumoral blood vessels, and lower expression of proangiogenic vascular endothelial growth factor (VEGF) and platelet-derived growth factor β (PDGFβ) than the parental ERα positive T47D cells in mice

(Hartman, 2006). ERβ completely inhibits cyclin D1 gene expression while ERα induces expression (Liu, 2002). In MCF-7 breast cancer cells expressing both ERα and ERβ, shRNA knockdown of ERβ causes a significant growth increase in the cells and diminished responses to estrogen and tamoxifen with decreased protein levels of p21 (Treeck, 2009). All of these studies support the idea of ERβ as a tumor suppressor (Lazennec, 2006).

ERα and ERβ exhibit similar gene regulatory activities through the classical pathway involving ERE-containing target genes (Petterson, 2000). In the non-classical pathway involving AP-1 sites, however, ERα activates while ERβ inhibits transcription (Paech, 1997; Webb, 1993; Webb, 2003). Messenger RNA microarray studies have identified some of the genes differently regulated by the two ER isoforms. Using U20S osteosarcoma cells expressing either ERα or ERβ, 52 genes have been identified as commonly regulated by the receptors, 24 are enhanced only by ERα, and nine are induced only by ERβ (Stossi, 2004).

1.2.3 Therapy Strategies

There are currently three categories of treatment used for patients diagnosed with breast cancer. These three categories are: surgery, radiation therapy and systemic therapy. Within systemic therapy there are the three sub-categories of biological therapy, chemotherapy and hormone therapy. These different therapies are often used in combination with one another (American Cancer Society, 2007).

1.2.3.1 Surgery

Once diagnosed with breast cancer, most women undergo surgery to remove the cancer from the breast. This surgery may be a breast conserving procedure, either a lumpectomy or a partial mastectomy. A lumpectomy removes the tumor and a small amount of tissue surrounding it. A partial mastectomy removes a larger portion of the breast including the tumor and a portion of the normal tissue surrounding it. In addition to the breast conserving surgeries, another surgical procedure is a total mastectomy. This is the removal of the entire breast that contains the cancer. A modified radical mastectomy is another surgical option. This involves removal of the entire breast that contains the cancer, many of the lymph nodes under the arm, the lining over the chest muscles, and in some cases part of the chest wall muscles. The last surgery option is a radical mastectomy, which involves removal of the entire breast with the cancer, the chest wall muscles under the breast, and all of the lymph nodes under the arm. Many patients also receive radiation, chemotherapy, or hormone therapy after surgery (National Cancer Institute, 2009).

1.2.3.2 Radiation Therapy

Radiation therapy involves the use of high energy-x-rays in either an external or internal manner. External radiation involves using a machine outside of the body. Internal radiation involves the introduction of radioactive substance in a needle, seed, wire, or catheter inserted into or near the tumor. The stage of the cancer determines the specifics of the radiation therapy (National Cancer Institute, 2009). Typically with breast cancer, external radiation therapy is used. It is focused on the breast and possibly the chest wall and underarm area. The therapy is usually given for five to

seven weeks. Radiation therapy is almost always used after lumpectomy and sometimes following a mastectomy (American Cancer Society, 2007).

1.2.3.3 Systemic Therapy

There are three types of systemic therapies used to treat breast cancer: biological therapy, chemotherapy and hormone therapy.

Biological Therapy

Biological therapy works with the immune system to fight cancer. About 15-30% of breast cancers overexpress human epidermal growth factor receptor 2 (HER2/neu; a.k.a. ERBB2, CD340, and p185), a growth-promoting, membrane-bound tyrosine kinase. Tumors overexpressing HER2/neu tend to grow faster and are more likely to recur (American Cancer Society, 2007). Trastuzumab is a monoclonal antibody that directly targets HER2 and was initially used in the treatment of women with HER2 positive metastatic tumors (Cobleigh, 1999; Vogel, 2002; Slamon, 2001). Clinical trials then demonstrated adding trastuzumab to standard chemotherapy for early stage breast cancer reduces the risk of death by 33% compared to chemotherapy alone (Romond, 2005). In 2006, the FDA approved trastuzumab for the treatment of all HER2 positive breast tumors (Wolff, 2007).

Chemotherapy

Chemotherapy involves the use of drugs to stop the growth of cancer cells by either cytotoxic (killing the cells) or cytostatic (preventing the cells from dividing) mechanisms. There are two types of chemotherapy, systemic and regional. Systemic chemotherapy reaches the cancer cells through the blood stream. Regional chemotherapy involves placing the chemotherapy directly

into the organ containing the tumor. As in radiation therapy, the stage of the cancer determines the specifics of chemotherapy (National Cancer Institute, 2009). The most common chemotherapeutic agents used for the treatment of breast cancer include: cyclophosphamide, methotrexate, fluorouracil, doxorubicin, epirubicin, paclitaxel and docetaxel (American Cancer Society, 2007).

Hormone Therapy

For breast cancer, hormone therapy involves blocking the action of estrogen to stop cancer cells from growing. Hormone therapy is used when the breast cancer is ERα positive. About 70% of breast cancers diagnosed are ERα positive (Murphy, 2006). There are three different classes of agents used for hormone therapy of breast cancer. These are SERMs, aromatase inhibitors (AIs) and SERDs.

Selective Estrogen Receptor Modulators

SERMs display both estrogen agonistic and antagonistic effects, depending upon their location (McDonnell, 1999). Tamoxifen was the first SERM approved for the treatment of advanced breast cancer in the United States in 1977. In 1998, this approval was extended to reducing breast cancer development or recurrence in women who are at a high risk for the disease (Jordan, 2003). Tamoxifen functions largely through its phenolic metabolite 4-hydroxytamoxifen which competes with estrogen for binding to the ER. Tamoxifen then induces dimerization of the ERs and localization to EREs. The receptor-bound drug causes a modified positioning of helix 12 in the ER, which alters the cofactor-binding domain and inhibits AF2-dependent interactions (Brzozowski, 1997; Shiau, 1998; Privalsky, 2004; Nettles, 2005). Due to its classification as a SERM tamoxifen acts as an estrogen receptor agonist in some tissues. One of the side effects of tamoxifen is an increased risk of endometrial cancer because it acts as an agonist in this tissue.

The ability of a SERM to act as an agonist depends on the AF1 region of the ER and the cellular availability of cofactors (Lees, 1989; McDonnell, 1999; Privalsky, 2004; Smith, 2004; Jordan, 2007). Tamoxifen exhibits strong agonistic activity in endometrial cell lines where the steroid receptor coactivator-1 (SRC-1) is present in high levels. In comparison, tamoxifen exhibits antagonistic activity in mammary cells, which have low levels of SRC-1 in comparison to endometrial cells (Shang, 2002).

The second approved SERM for the treatment of breast cancer is raloxifene. Raloxifene was first investigated for its use in osteoporosis and was clinically approved for the prevention of this condition in 1998 (Jordan, 2003). Clinical trials then demonstrated in postmenopausal women tamoxifen and raloxifene are equal in their ability to reduce the risk of invasive disease, while only tamoxifen is effective for *in situ* cancer. Raloxifene, however, has a lower risk of side effects, which include uterine cancer and blood clots (Vogel, 2006). Raloxifene was approved in 2007 for the reduction of breast cancer in postmenopausal women who are at high risk for the development of invasive breast cancer (American Cancer Society, 2008).

Aromatase Inhibitors

Aromatase is a cytochrome P-450 family member and is the enzyme responsible for the production of estrogens from androgenic substances (Evans, 1986). It is highly expressed in the placenta and in the granulosa cells of the ovaries where its expression depends on cyclical gonadotropin stimulation. Aromatase is also produced in smaller amounts in the subcutaneous fat, liver, muscle, brain, normal breast and breast cancer tissue (Miller, 1982; Nelson, 2001). After menopause, the subcutaneous fat is the source of most residual estrogen production (Longcope, 1986). Plasma levels of E2 fall from 400 pM to 25 pM at menopause, yet the concentration of E2 in breast carcinoma tissue in post-menopausal women is about ten times the

level seen in plasma (Thiijssen, 1989). These levels are partly due to the aromatase enzyme located in the tumor (Smith, 2003). Therefore, AIs are of most use in postmenopausal women whose estrogen production occurs by the peripheral aromatization of androgens. The steroidal AI exemestane, which binds aromatase irreversibly, and the non-steroidal AIs, anastrozole and letrozole, are currently in clinical use (Smith, 2003). Studies have demonstrated the AIs are at least as effective as tamoxifen in the treatment of advanced breast cancer. AIs are approved for the treatment of advanced breast cancer in post-menopausal women and for the prevention of recurrence after surgery (American Cancer Society, 2008).

Selective Estrogen Receptor Downregulators

There is one clinically approved SERD, fulvestrant. Fulvestrant competes with E2 for binding to the ER LBD and its long bulky side chain alters the conformation of the binding pocket and inhibits receptor dimerization and DNA binding (Fawell, 1990; Pike, 2001). Fulvestrant is approved for the treatment of post-menopausal women whose cancer no longer responds to tamoxifen (American Cancer Society, 2008).

1.2.4 Tamoxifen Resistance

Tamoxifen has been the cornerstone of breast cancer treatment for the last thirty years; however, a major problem with tamoxifen therapy is the development of drug resistance. While there are new hormone therapies that are approved for clinical use as described above, resistance to all forms of hormone therapy remains a problem. ER transcriptional activity is a complex process and the actual binding of E2 to the ER is only a small part of this process. The growth factor signaling pathways present in a cell and the ER cofactors available make up the cellular context that determines ER-transcriptional activity. Hormone therapies are therefore influenced by a

multitude of factors. A better understanding of the mechanisms behind antiestrogen resistance will allow for the design of more effective hormonal therapies (Zilli, 2009). Many different mechanisms have been attributed to the development of tamoxifen resistance, yet the phenomenon is not fully understood.

One of the areas that has received much attention is ER status. The main predictor for a positive response to endocrine therapy is the presence of the ER, therefore a lack of ER expression is the main mechanism of *de novo* resistance. A lack of ER expression in breast cancer has been explained by several different mechanisms. The first is the aberrant methylation of CpG islands in the 5' regulatory region of the ERα gene (Ottaviano, 1994). The second is an increased deacetylation of histones, which leads to a more compact nucleosome structure and limits transcription of the ER (Yang, 2001; Parl, 2003). Finally, ER-negative breast cancers display a higher level of expression of several growth factor receptors compared to ER-positive breast cancers, suggesting that growth factor signaling may reduce ER expression (Normanno, 1994; Creighton, 2006). The loss of ER expression has also been hypothesized to be responsible for acquired resistance to tamoxifen. It has been shown, however, that only 17-28% of tumors with acquired resistance to tamoxifen have lost ER expression (Johnston, 1995; Gutierrez, 2005). Additionally, 20% of tumors that develop tamoxifen resistant still respond to another hormone therapy (Osborne, 2002; Howell, 2005). Therefore in the case of tamoxifen, loss of the ER alone does not account for drug resistance. Another explanation suggested to contribute to resistance is mutation of the ERα. Mutation of the ER occurs in less than 1% of human breast cancers, however (Herynk, 2004).

The levels of ERβ expression have also been investigated in tamoxifen resistance because of ERβ's negative influence on ERα-promoted transcription (Pettersson, 2000). High levels of

ERβ were demonstrated in tamoxifen-resistant cell lines via analysis of mRNA levels (Speirs, 1999). Overexpression of ERβ protein in MCF7 breast cancer cells confirmed by Western blot does not lead to antiestrogen resistance but is associated with an increased sensitivity to tamoxifen (Murphy, 2005). Low levels of ERβ at the protein level are predictive of tamoxifen resistance (Hopp, 2004; Esslimani-Sahla, 2004).

The intracellular environment has been investigated in relationship to acquired antiestrogen resistance. Coregulatory proteins play a major role in the impact the ER has on transcription (McKenna, 1999). Overexpression of coactivators and/or down-regulation of corepressors alter the effects of SERMs (Smith, 1997). Nuclear receptor corepressor 1 (NCOR1) is a corepressor that binds the ER and inhibits the partial agonistic activity of tamoxifen (Cottone, 2001). Low levels of NCOR1 are associated with a shorter relapse-free survival in women treated with tamoxifen (Girault, 2003). Increased growth factor signaling may also contribute to antiestrogen resistance. Estrogen is involved in cell cycle regulation as a member of a negative feedback loop that downregulates genes involved in proliferation, such as epidermal growth factor receptor (EGFR) (Yarden, 2001). When antihormonal agents bind and inhibit ER activation, the negative feedback caused by the activated ER signaling is removed. Thus, the downstream MAPK pathways from EGFR are activated. These pathways add activating phosphorylations to the ER and therefore the ER maintains nuclear activity and can influence ER-sensitive genes involved in cell proliferation (Gee, 2003; Knowlden, 2003). MCF-7 cells made resistant to tamoxifen through long-term exposure to the drug exhibit ERα redistribution with a greater number of receptors in the cytoplasm and at the plasma membrane compared to the parent MCF-7 cell line. At the plasma membrane, ERα associates with EGFR. These resistant cells present increased sensitivity to EGF and E2-stimulated activation of MAPK,

supporting the idea that enhanced non-genomic functions of the ER and its interaction with EGFR play a role in acquired tamoxifen resistance (Fan, 2007). Plasma membrane ER can activate HER2 signaling, and tamoxifen has been demonstrated to act as an agonist on the membrane ER and stimulate the ER-HER2 crosstalk. The kinase cascade downstream of HER2 adds the activating phosphorylations to the ER and its coregulators, which can then influence cell proliferation (Schiff, 2004; Shou, 2004).

Another proposed mechanism of antiestrogen resistance is the ability of breast cancer cells to become hypersensitive to estrogen. ER positive MCF-7 cells cultured in estrogen-free media for a long period of time provide one model to study this phenomenon. The MISS pathway and the rapid increase of growth factor signaling is the mechanism by which these MCF-7 cells are able to grow in very low concentrations of E2. IGF-IR and ER cross-talk is increased, leading to activation of MAPK and PI3K/AKT (Santen, 2003; Santen, 2005).

1.2.5 Biomarkers

1.2.5.1 Overview

Early detection of breast cancer not only lessens human suffering, but also reduces the burden placed on society in terms of socioeconomic resources (Levenson, 2007). Early detection allows patients to live longer, receive less treatment, and, in general, fare much better than those patients who receive a much more advanced diagnosis (Etzioni, 2003). Additionally, prognostic indicators and predictors of response to therapy during the clinical management of breast cancer have an important role in treatment decisions and may improve clinical outcome (Ravaioli, 1998). The characteristics of tumor cells are different from normal cells, biomarkers can use this difference and be developed to aid in the diagnosis and treatment of breast cancer. Different

biomarkers will be able to define risks and identify early stages of tumor development, assist in tumor detection, stratify patients for treatment, predict disease outcome, and help in monitoring for recurrence (Levenson, 2007).

The current major technique used in the diagnosis of breast cancer is mammography. While this technique is highly sensitive, 67.8%, and specific, 75%, in the diagnosis of DCIS, it does have drawbacks. The sensitivity of mammography drops to 45.8%-55% in women with dense breast tissue (Berg, 2006). Mammography depends on the presence of a certain volume of tumor cells in a specific location and may miss smaller or diffuse tumors (Levenson, 2007). The reading and assessment of mammography is also highly subjective due to the different experience levels of radiologists (Burnside, 2005). A diagnostic test for a biomarker removes the influence of the observer. Nipple aspirate fluid (NAF) has been suggested to be the source for biomarker screening in breast cancer. Screening based on NAF is, however, unlikely to be very successful, as many women do not produce NAF (Levenson, 2007). Ductal lavage is another suggested route for the detection of breast cancer biomarkers. This procedure requires the time-consuming procedure of the cannulation of each individual and only a few ducts can be successfully cannulated (Badve, 2003). The indirect analysis of diagnostic biomarkers from the blood offers the highest potential for use in population-wide screening of breast cancer. Blood interacts with every cell in the body and tumor cells, tumor-specific antigens, autoantigens and tumor RNA and DNA can be recovered from the blood (Levenson, 2007).

1.2.5.2 Breast Cancer Biomarkers in Clinical Use

The American Society of Clinical Oncology (ASCO) first published evidence-based clinical practice guidelines for the use of tumor markers in breast cancer in 1996 and last updated these guidelines in 2007. There are several breast tumor markers that demonstrate evidence of clinical

utility and are recommended for use. ASCO guidelines state ER and progesterone receptor (PR) should be measured on every primary invasive breast cancer; in DCIS, the data is, however, insufficient to recommend routine measurement of these receptors. The next biomarker recommended for clinical use by ASCO is HER2. HER2 expression and/or amplification should be evaluated in every primary invasive breast cancer at the time of diagnosis or at the time of recurrence. CA 15-3 and CA 27.29 assays detect circulating MUC-1 antigen in peripheral blood. These assays are recommended for monitoring patients with metastatic disease in conjunction with diagnostic imaging, history, and physical examination during active therapy. The guidelines do not recommend these assays to be used independently, nor for the screening, diagnosis or staging of breast cancer. The detection of carcinoembryonic antigen (CEA) is recommended along the same guidelines as CA 15-3 and CA 27.29 by ASCO. The guidelines also recommend the performance of enzyme-linked immunosorbent assays (ELISAs) on 300 mg of fresh or frozen breast cancer tissue for the detection of urokinase plasminogen activator (uPA)/plasminogen activator inhibitor (PAI-1) for the determination of prognosis in patients with newly diagnosed, lymph node-negative breast cancer. Low levels of both of these markers are associated with a sufficiently low level of recurrence, therefore chemotherapy will only contribute minimal additional benefits (Harris, 2007). Onco*type*DX is an RT-PCR assay measuring the expression of 21 genes in RNA extracted from formalin-fixed, paraffin embedded (FFPE) samples of tissue from primary breast cancer. An algorithm manipulates the levels of expression of these 21 genes and assigns a patient to a group referring to the risk of distant recurrence: low, intermediate or high (Cronin, 2004). The guidelines recommend this assay to be used in prediction of the risk of recurrence in newly diagnosed patients with lymph node-

negative, estrogen receptor-positive breast cancer who are undergoing tamoxifen treatment (Harris, 2007).

The majority of the recommended biomarkers in breast cancer involve later stage or specific treatment decisions. ER status has proven very effective for use in guiding endocrine therapy decisions (Clark, 1983). Antiestrogen resistance is, however, a problem that occurs in many patients receiving endocrine therapy (Zilli, 2009). The development of biomarkers of antiestrogen resistance will help to optimize the use of endocrine therapy. Additionally, there is no current biomarker recommended for the early detection of breast cancer.

1.2.5.3 Isobaric Tags for Relative and Absolute Quantitation

Isobaric tags for relative and absolute quantitation (iTRAQ) is a technique that can be used in the search for new biomarkers for breast cancer. iTRAQ is a proteomic technique that allows for the identification and quantification of hundreds of proteins in up to eight different biological samples in a single MS experiment. iTRAQ involves a multiplexed set of reagents, which place isobaric mass labels via amide linkage to the N terminus and lysine side chains of peptides in a protein digestion mixture. The same peptides, despite being labeled with a different reagent, are chromatographically indistinguishable. Since they are isobaric, they are also indistinguishable in a single MS experiment. The isotopically-enriched label does, however, yield unique reporter ions following collision-induced dissociation (CID), which allows for identification of the peptide from the multiplex set (Ross, 2004).

The label consists of a reporter group (based upon an *N*-methylpiperazine), a mass balance group (carbonyl), and a peptide-reactive group (*N*-hydroxysuccinimide (NHS) ester). The overall mass of the reporter and balance components are kept constant using isotopic enrichment with ^{13}C, ^{15}N, and ^{18}O. The amide linkage of the tag to the peptide fragments similar

to the peptide backbone when subjected to CID and the reporter group retains a charge and appears in the *m/z* 113 – 121 range of the mass spectrum. This region does not usually contain y and b peptide ions (Ross, 2004). The peptide backbone generates y and b ions in an MS/MS spectrum. B ions are those where the N terminus retains the charge, while y ions are those where the C terminus retains the charge (Johnson, 1987). Along with the sequence information provided by the y and b ions, the unique iTRAQ reporter ion present in the spectrum identifies the sample from which the peptide arose and provides the relative abundance of that peptide from that particular sample to be calculated amongst the other samples (Ross, 2004). Confidence in the protein identification and quantification is gained because more than one peptide from the same protein provides quantitative information (Glen, 2008).

The iTRAQ methodology has been used in many studies to identify differentially abundant proteins in cancer. One example study involved investigation of proteins associated with the progression of human prostate cancer using a poorly metastatic line along with its highly metastatic variant. Whole cell lysates made from the lines were labeled with the iTRAQ reagents followed by two-dimensional-liquid-chromatography-mass spectrometry/mass spectrometry (2D-LC-MS/MS). A large number, 280, of unique proteins were identified, and relative expression data was obtained on 176 proteins. Of the 176 proteins, ten were significantly increased (>1.5 fold) and four were significantly decreased (<1.5 fold). Tumor rejection antigen, gp96, was one of these altered proteins. Western blotting was used to confirm the levels of gp96 in the cell lines and immunohistochemistry was performed on patient samples to demonstrate its clinical relevance (Glen, 2008).

1.3 THE NUCLEAR MATRIX

1.3.1 Overview

An area that holds promise for the development of biomarkers in breast cancer is the NM. The NM, discovered in 1974, is the structural scaffolding of the nucleus. It is comprised of 98% protein, 0.1% DNA, 0.5% phospholipid and 1.2% RNA and accounts for 5-10% of the total nuclear protein (Berezney, 1974). The NM consists of the peripheral lamins and pore complexes, an internal ribonucleoprotein network, and residual nucleoli (Sjakste, 2004). A two-dimensional gel of proteins isolated from the NM demonstrates about 200 spots (Zink, 2000). Proteins found in the NM are known as nuclear matrix proteins (NMPs).

The NM is the three-dimensional support scaffold of the nucleus and, as a consequence, it is involved in many of the fundamental functions of a cell, including determining nuclear morphology, organizing DNA throughout the cell cycle, stabilizing and orienting DNA during replication, organizing gene regulatory complexes and RNA synthesis (Davido, 2000). There are many studies to support these roles for the NM. Newly replicated DNA is tightly associated with the NM (Berezney, 1975). Proteins found in the NM reach their maximum level of phosphorylation just before the onset of DNA replication in the regenerating liver, indicating the phosphorylation of NMPs regulates DNA synthesis (Allen, 1977). DNA loop domains are the sites of DNA replication, and incorporate DNA replicases and topoisomerase II into complexes that are bound to the NM (Earnshaw, 1985). These sites of attachment to the NM in the DNA are known as matrix attachment regions (MARs) (Ludérus, 1992). DNA loops on the NM can be directly visualized with fluorescent and electron microscopy (McCready, 1979; Vogelstein, 1980; Lebkowski, 1982). The NM is also the site of RNA transcription, as newly synthesized

hnRNA and its processing intermediates are associated with the NM (Jackson,1981; Ciejek, 1982).

The NM's role is its regulation of gene expression is linked to breast cancer. E2 binds the NM in an estrogen responsive tissue, chicken liver, with a K_d of 1 x 10^{-9} M (Barrack, 1980). These NM E2 binding sites have been confirmed to be the ER (Alexander, 1987). Several studies have suggested that anywhere from 46-62% of the total ER content of a nucleus is associated with the NM upon estrogen stimulation (Barrack, 1977; Barrack, 1980; Barrack, 1982). Several studies of estrogen-regulated genes demonstrate the NM plays a role in gene expression regulation. The gene for ovalbumin, a major egg white protein, associates with the NM in hen oviduct cells where it is actively transcribed, but it does not associate with the NM in hen brain cells where it is inactive. The ovalbumin gene disassociates from the NM when the hen undergoes estrogen withdrawal and reassociates when restimulated with estrogen (Robinson, 1983). DNA dot blot assays demonstrate the gene for vitellogenin II, a major egg yolk protein, associates with the NM upon E2 stimulation before its mRNA synthesis begins. When the vitellogenin gene is no longer being transcribed, it is released from the NM. Stimulation with E2 again leads to a reassociation of the gene with the NM (Jost, 1984).

The NM is a component of the tissue matrix system, which also includes the cytoskeleton and the extracellular matrix (ECM). The tissue matrix system connects the cell periphery to DNA in the nucleus in a structural and functional manner (Pienta, 1992). The cytoskeleton is composed of actin-containing microfilaments, tubulin-containing microtubules, and intermediate filaments (IFs). These IFs are made up of cytokeratins and vimentin (Ingber, 1993). These IFs maintain physical association between the NM and the cytoskeleton (Nickerson, 1990; Hendrix, 1996). The IF protein vimentin is anchored to the nuclear lamina via lamin B (Georgatos, 1987;

Djabali, 1991). Lamins are present at the nuclear periphery and in the internal NM (Hozak, 1995). This supports the notion of a molecular network that connects the plasma membrane of the cell and cytoskeleton with the nucleoskeleton. The linkage of the NM to the cytoskeleton and ECM suggests the NM may be altered by what occurs in and affects the extracellular framework (Getzenberg, 1991A).

1.3.2 Alterations to the Nuclear Matrix in Cancer

One of the hallmark events that occurs in cancer progression is that cellular structure becomes increasingly abnormal, particularly with regard to alterations of the nucleus (Zink, 2000). Nuclear alterations are commonly used as pathological indicators of malignancy. In transformed cells, the nucleus is often enlarged, has an abnormal chromatin pattern, and is irregular in shape. As the NM partly maintains the spatial arrangements of the nucleus, this suggests it has a fundamental link to the development of cancer (Replogle, 1996). Additionally, because of its role in many of the fundamental processes of a cell described earlier, disruption to the NM is a likely determinant in carcinogenesis (Davido, 2000). The NM's link to the ECM also suggests that the NM is altered in cancer, because tumor-induced changes in the surrounding ECM may alter the NM composition (Getzenberg, 1991A).

In 1979 the NM of hepatoma cells was shown to differ qualitatively from the NM of normal liver cells by microscopy. This provided the initial support for investigation into how the NM composition can provide insight into the origin of cells and how disease alters these cells (Berezney, 1979). Since the initial study, numerous investigations of the NM in cancer have been performed. Because of the potential role of the NM in cell transformation, there is much interest in finding markers for cancer screening in the NM (Davido, 2000). Further promise for

the use of NMPs for the diagnosis of cancer is supported by the detection of NMPs in the serum of cancer patients (Miller, 1992). This detection may allow for the development of a non-invasive screening procedure that could be used in the clinic.

The NM's role in cancer is supported by its binding sites for various tumor-associated proteins. The apoptotic proteins, bax and bcl-2, localize to the NM in glioblastoma (Wang, 1999). The tumor suppressor p53 binds to the NM and this binding increases in response to DNA damage (Ming, 2001). The tumor suppressor retinoblastoma (Rb) protein has also been demonstrated to be a NMP that interacts with lamin A (Mancini, 1994; Ozaki, 1994). Several inherited cancer disorders also suggests a role for the NM in cancer. For example, multiple endocrine neoplasia type I (MEN1), characterized by tumors in multiple endocrine organs, involves a defective NMP, menin (Jin, 2003).

The NM has shown some promise in terms of affording predictive biomarkers for bladder cancer. BLCA-4, a protein found only in the NM of bladder cancer samples, is being developed for use in an urine immunoassay. This protein is detectable in both tumor and normal cells from bladder cancer patients, but not in cells in bladder tissue from healthy individuals (Konety, 2000A). A clinical trial demonstrated very positive results, showing that BLCA-4 levels may be able to accurately identify individuals with bladder cancer and distinguish them from normal individuals (Konety, 2000B). Matritech, Inc. has developed an assay that measures urine levels of another NMP, NMP22. This assay is approved by the FDA for the detection of occult or rapid recurring disease after transurethral resection of bladder cancer (Sjakste, 2004). Matritech Inc. also produces an antibody to NMP 179, which has been demonstrated to be an effective marker of cervical cancer (Keesee, 1999). Further information on the NM's link to cervical cancer is revealed by the origin of the disease. Human papillomavirus (HPV) underlies 90% of all

cervical cancer cases and HPV-16 DNA binds to different NMPs in normal and cervical carcinoma cells. HPV-16 DNA has a higher affinity for the more recently expressed acidic proteins present in the transformed cells (Yang,1997). Additionally, drug treatment of cervical cancer alters the composition of the NM. Dexamethasone, which inhibits the growth of cervical cancer cells, decreases the expression of the NMP NuMa (Yam, 1998).

Dunning rat prostate tumor cell lines have significant NMP alterations compared to a normal prostate tissue line. Additionally, the NM composition is different for each of the lobes of the normal rat prostate (Getzenberg, 1991B). Matritech Inc. discovered an NMP unique to the blood of prostate cancer patients, NMP48, and developed a kit for the determination of this protein in the clinic (Sjakste, 2004). High mobility group nonhistone protein HMG1(Y), is localized to the NM in prostate cancer cells of a late stage prostate cancer mouse model (Leman, 2003). Nucleophosmin, a protein related to proliferation, is localized to the NM in prostate cancer cell lines (Subong, 1999).

NMPs in colon cancer demonstrate that throughout disease progression, the proteins localized to the NM change. In ulcerative colitis dysplasia tissue, three unique NMPs are found, while two NMPs are unique to colon cancer tissue and three NMPs are common to both ulcerative colitis dysplasia and colon cancer (Izzo, 1998). A more recent study identified four NMPs that are present in tumor samples and not in the matched normal adjacent tissue or normal colon tissue. Additionally two NMPs are found in the cancer and normal tissue, but not in the normal adjacent tissue (Brunagel, 2002A). NMPs have also been identified that are specific to colon cancer metastases to the liver (Brunagel, 2002B). In another study of the NM in colon cancer, creatine kinase B (CKB) and heterogeneous nuclear ribonucleoprotein F (hnRNP F) were demonstrated as potential biomarkers. CKB is present at higher levels in 78% of colon tumors

compared to normal colon tissues. hnRNP F is expressed in 89% of colon tumors and 100% of liver metastases and also at higher frequencies in colon polyps compared to normal donor colon (Balasubramani, 2006).

1.3.3 Alterations to the Nuclear Matrix in Breast Cancer

NMPs have also been investigated in breast cancer. An initial study investigating the NM in breast cancer involved analysis of human tumors. The NM of normal breast tissue is similar in terms of protein composition to that of breast tumor tissue. Specific differences exist though, as four NMPs are expressed in the tumor tissue but not the normal tissue. Also, two other NMPs are present in the normal breast tissue, but absent from the breast tumor sample (Khanuja, 1993). In another study, the ER+, hormone-dependent lines T47D, MCF-7 and ZR-75; the ER−, hormone-independent lines MDA-MB-231 and BT-20; the ER+, hormone-dependent line T5-PRF; and the nontumorigenic, spontaneously immortalized human breast epithelial line MCF-10A1 were examined. Five spots in a 2D gel are unique to the NM in ER+ cell lines, while one spot is associated exclusively with the NM of the ER− cell lines. The expression of these six NMPs has been examined in tumor samples from patients. The first five NMPs are found in the ER+ breast tumors, while the sixth is found in some but not all of the tissue samples. Additionally the sixth NMP is present in the ER− breast tumors, while the first five are not (Samuel, 1997).

Studies of the NM in breast cancer have also focused on the IFs and their interactions with the NM. Using the T-47D5 human breast cancer cell line, an ER+ and E2-responsive line, an estrogen-independent line, T5-PRF, was developed by chronically depleting the levels of estrogen used in the culture over a long period of time. The NM-IF isolated from the cell lines

showed three proteins as the major components; cytokeratin 8, cytokeratin 18, and cytokeratin 19. These proteins are expressed at much higher levels in the T5-PRF cell line, suggesting they are estrogen regulated (Coutts, 1996). In another study, *cis*-diamminedichloroplatinum (II) (cisplatin) was used to cross-link the nuclear proteins to nuclear DNA and determine if these IFs are bound to the nuclear DNA. Cytokeratins 8, 18, and 19 are attached to the nuclear DNA of T47D5 and T5-PRF cells, and this interaction is influenced by estrogens in the hormone dependent T-47D5 cell line, but not the hormone-independent T5-PRF line (Spencer, 1998). Differences in the nuclear proteins associated with nuclear DNA in hormone-dependent and hormone-independent breast cancer cell lines have been determined. Using two-dimensional gel electrophoresis, several proteins were found crosslinked to DNA in all cell lines investigated. These include the transcription factor hnRNP K, Lamins A and C, and cytokeratins 8, 18 and 19. Some variations was found in the levels of proteins identified amongst the lines used. Three proteins are detected only in the pseudo-normal MCF10A1 cell line, while three proteins are at significantly higher levels in the hormone-dependent, ER+ lines. Two proteins are found only in the hormone-independent, ER− lines. These proteins may serve to distinguish breast cancer epithelial cell types in breast tumors, because breast cancer cells are often very similar to their corresponding tumor. In order to verify that these cross-linked proteins are NMPs, two-dimensional gels of NM preparations from each of the cell lines was examined for the presence of the cross-linked proteins. All but two of the proteins detected only in the MCF10A1 line were present in the NMP preparations. The IF protein vimentin was also demonstrated to associate with DNA in MDA-MB231 breast cancer cells but not the other lines examined (Spencer, 2000).

NMPs also associate with DNA differently during progression of breast cancer. The parental cell line MCF-7 and the MIII, LCC1 and LCC2 derivatives of this line demonstrate this

concept (Spencer, 2001). MIII and LCC1 are ER+, invasive, metastatic, estrogen-independent, estrogen-responsive and antiestrogen-sensitive lines. LCC2 is an ER+, invasive, metastatic, estrogen-independent, estrogen-unresponsive, and tamoxifen-resistant line (Brunner, 1993). Fifteen NMPs are altered in their expression in a variety of ways over the cell lines. One particular NMP demonstrates decreased levels as the cell lines progress from MCF-7 to MIII, LCC1 and LCC2. Additionally, a general loss of the cross-linking of NMPs to nuclear DNA can be observed as samples progress to estrogen independence and antiestrogen insensitivity. This study also showed cytokeratins 8, 18 and 19 are the most abundant proteins that cross-linked to DNA. The levels of lamins A and C also progressively increase in the level of cross-linking to DNA as the cells progress from MCF-7 to LCC2. This study supports the idea that as ER positive breast cancer cells progress, there is a loss of contacts between the chromatin and NMPs (Spencer, 2001).

Matritech has evaluated an NMP, NM-200.4™, as a clinical screening assay for breast cancer. This NMP was first identified in T-47D breast cancer cells, where it is present at a high concentration. An antibody to NM-200.4 shows high reactivity to the nuclei of breast cancer cells. The NM-200.4 antibody also reacts to nuclei from lung carcinoma, papillary thyroid carcinoma, ovarian fibroma, a lymphoma and also other normal tissues, demonstrating it is not very specific. Though only one in ten benign breast biopsies show reactivity, the antibody is reactive with other normal tissues (Weidner, 1991). This antibody has therefore not been recommended for clinical use (Sjakste, 2004). This exercise does, however, provide support to continue to investigate the NM for other, more specific markers (Weidner, 1991). Matritech has also discovered a specific NMP, NMP66, in the blood of breast cancer patients that is not present in the blood of women without detectable breast cancer (Sjakste, 2004).

Heat shock protein 27 (HSP27) is known to have a role in growth and drug resistance in breast cancer cells (Oesterreich, 1993). Elevated levels of HSP27 correlate with increased invasion (Lemieux, 1996). A large study of 425 samples by immunohistochemistry and 788 samples by Western blotting revealed, however, that HSP27 is not an independent prognostic marker (Oesterreich, 1996). There is still support for HSP27's role in breast cancer development though because of its correlation with ER expression and its response to estrogen (Moretti-Rojas, 1988; Seymor, 1990). In order to try to understand more about HSP27's function in breast cancer, the promoter of HSP27 and the promoter-associated proteins have been investigated. One protein, HET (HSP27-ERE-TATA-binding protein), binds to the imperfect ERE in the promoter of HSP27 and is a NMP. Overexpression of HET decreases the activity of the HSP27 promoter (Oesterreich, 1997). HET binds the ER in its DNA-binding domain and hinge region. This interaction occurs both in the presence and absence of estrogen, and is increased when the ER is bound to tamoxifen. The protein enhances the action of tamoxifen. When HET is overexpressed, however, it represses the activity of both estrogen and tamoxifen on the ER (Oesterreich, 2000).

The levels of HET in many commonly used breast cancer cell lines have been investigated. The protein is expressed at various levels in MDA-MB468, ZR-75, MDA-MB330, T47D, MCF-7/MG and MDA-MB231 cell lines, with MDA-MB231 expressing the highest amount. HET expression appears to be inversely correlated with cell proliferation (Townson, 2000). In DNA isolated from laser capture microdissected samples of paired primary breast tumor and normal tissue, 78% of the patient tumor samples demonstrate a loss of heterozygosity in the gene locus for HET, with a microsatellite marker that colocalizes with the HET locus, 19p13.2-3. This suggests that there is a tumor suppressor gene in the area of HET (Osterreich,

2001). Results of a large study examining patient samples with long-term clinical follow-up to determine HET's potential to serve as a prognostic factor (natural progression) or a predictive factor (tamoxifen responsiveness), show that HET levels are correlated with ERα, Her-2, and bcl-2. No correlation exists, however, between HET protein levels and disease free survival. Low levels of expression in women who did not receive adjuvant therapy are, however, significantly associated with worse overall survival. Therefore HET does have some prognostic value, and women with breast cancer and low levels of HET have poorer prognoses (Hammerich-Hille, 2009).

A novel role in oxidative stress responses has been suggested for the NM in breast cancer. NF-E2-related factor 2 (Nrf2) is a basic leucine zipper transcription factor that translocates to the nucleus in response to oxidative stress and binds to genes containing the antioxidant response element (ARE) promoter sequence and up-regulates ARE-driven detoxifying and antioxidant genes (Itoh, 1999; Venugopal, 1996). These detoxifying and antioxidant genes are necessary because of the toxic by-products generated by cellular metabolism, and perhaps more so in cancer cells whose metabolic processes have become unchecked. When the detoxifying pathways are impaired, toxic free radicals and abnormal proteins accumulate and cause oxidative stress-induced damage to cells, disrupting the functions of lipids, DNA and proteins, and eventually leading to cancer progression. Analysis of the Nrf2 pathway in MDA-MB231 breast cancer cells shows that Nrf2 colocalizes with the NMP NRP/B (Seng, 2007). The NMP NRP/B is a member of the kelch-related family of actin-binding proteins (Kim, 1998). Nrf2 and NRP/B associate both *in vitro* and *in vivo*, and this association is increased in response to the oxidative stress agent, hydrogen peroxide (H_2O_2). This result was

the first demonstration of the involvement of the NM in an oxidative stress response in breast cancer cells (Seng, 2007).

As demonstrated by the examples provided, alterations to the protein composition of the NM occur in a unique and detectable fashion. These alterations demonstrate the potential for the use of NMPs as biomarkers in breast cancer. These biomarkers may provide helpful information for the diagnosis, treatment, prognosis and monitoring of disease recurrence.

1.4 HYPOTHESIS AND SPECIFIC AIMS

1.4.1 Hypothesis

The hypothesis addressed in my studies was as follows. The composition of the NM, and the influences ERα and ERβ have upon this composition, change during the progression of breast cancer and the development of antiestrogen resistance. Understanding these differences will help to unravel the underlying mechanisms of breast cancer. The differences may additionally provide biomarkers to assist in the diagnosis and prognosis of breast cancer.

1.4.2 Specific Aims

In order to address the hypothesis, three specific aims were pursued. These were:

Aim 1. Evaluate a series of biphenyl *C*-cyclopropylalkylamides to determine their potential as ERβ-selective ligands.

Aim 2. Identify and quantify the NMPs present in tamoxifen responsive and resistant breast cancer cell lines and how the levels of these NMPs change in response to ER-selective ligands.

Aim 3. Identify and quantify the NMPs differentially expressed in ductal carcinoma *in situ*.

2.0 AN ER BETA SELECTIVE BIPHENYL *C*-CYCLOPROPYLALKYLAMIDE THAT INHIBITS THE GROWTH OF BREAST CANCER CELLS *IN VITRO*

2.1 ABSTRACT

The potential benefits of selectively targeting ERβ are well documented. Previously, through the screening of a library of homoallylic amides, allylic amides and *C*-cyclopropylalkylamides, a new structural scaffold for antiestrogens was identified. A second-generation library was synthesized and screened for ERα and ERβ binding using a fluorescence polarization (FP) assay with a fluorescent derivative of E2. One compound demonstrated concentration-dependent displacement with close to 50% displacement at the highest concentration tested. Six analogues of this lead compound were synthesized in an attempt to more selectively target ERβ and improve cellular potency. These six compounds were evaluated for their ability to bind to both ERs using the FP assay. Two of the compounds demonstrated modest affinity and selectivity for ERβ. The compounds were then evaluated for their ability to inhibit estradiol-induced proliferation of MCF-7 human breast cancer cells expressing both ERα and ERβ, ATCC MCF7 breast cancer cells expressing only ERα, and ER negative MDA-MB231 human breast cancer cells. The two compounds demonstrated to be selective for ERβ had 50% growth inhibitory (GI_{50}) values of 1 and 4 μM in the MCF-7 cells, while demonstrating much less inhibition of the growth of the ATCC MCF7 or MDA-MB231 cells. Finally, the compounds did not increase

expression of the growth promoter c-Myc but did increase expression of the cyclin-dependent kinase inhibitors p21 and p27. This newly identified structural scaffold for ERβ-selective agents may be useful in understanding the differences between the two receptor isoforms, as well as provide insight into the design of other subtype selective ligands.

2.2 INTRODUCTION

The ERs are ligand-activated transcription factors. ERα and ERβ show moderate (~55%) sequence homology in their LBD, but their ligand-binding pockets differ by only two amino acids: ERα Leu^{384} versus ERβ Met^{336}, and ERα Met^{421} versus ERβ ILe^{373} (Sun, 2003). ERβ's ligand binding pocket is also about 100 $Å^3$ smaller than that of ERα (Pike, 1999). Additionally, the tissue distributions of these receptors are distinct in certain tissues (Kuiper, 1997). There is much data demonstrating the benefits of selectively targeting the ERβ. ERβ expression inhibits E2-induced proliferation in T47D and MCF-7 breast cancer cells and leads to a reduction in xenograft volume (Ström, 2004; Paruthiyil, 2004; Hartman, 2006). ERβ also has a growth inhibitory mechanism in medullary thyroid carcinoma, prostate cancer and ovarian cancer (Cho, 2007; Ji, 2005; Pravettoni, 2007; Chan, 2008). ERβ-selective agonists have also demonstrated potential as anti-inflammatory agents (Harris, 2003). Several ERβ-selective agents have been identified (Figure 4). One of these is the compound, DPN **(8)**, a 70-fold selective ERβ agonist (Meyers, 2001). DPN has been used in a variety of studies involving various tissues because of its ER binding, and a thorough search of the literature shows no off targets for DPN. Genistein (**9**) is a plant-derived ERβ-selective ligand (Kuiper, 1997). In addition to activity with ERβ, genistein has a variety of other targets. Genistein induces DNA strand breaks and cause

chromosomal aberrations (Kuiper, 1997; Boos, 2006). Genistein also specifically inhibits the activity of tyrosine-specific protein kinases such as EGFR (Akiyama, 1987). Additionally, genistein acts on DNA topoisomerase II by inhibiting ATP hydrolysis (Markovits, 1989; Robinson, 1993). Biphenyl derivatives have also been investigated for ERβ-selectivity. Simple 4-OH-biphenyls demonstrate 20-70 fold selectivity for ERβ over ERα (Edsall, 2003). In order to attempt to mimic the C-ring of genistein, an oxime moiety was incorporated into the 4-OH-biphenyl core. Altering the substitutions on the biphenyl core provided various levels of selectivity: biphenyl oximes **10** and **11** were 11-fold and 43-fold selective for ERβ, respectively (Figure 4) (Yang, 2004). No off targets were found for these biphenyl oximes after a thorough literature search.

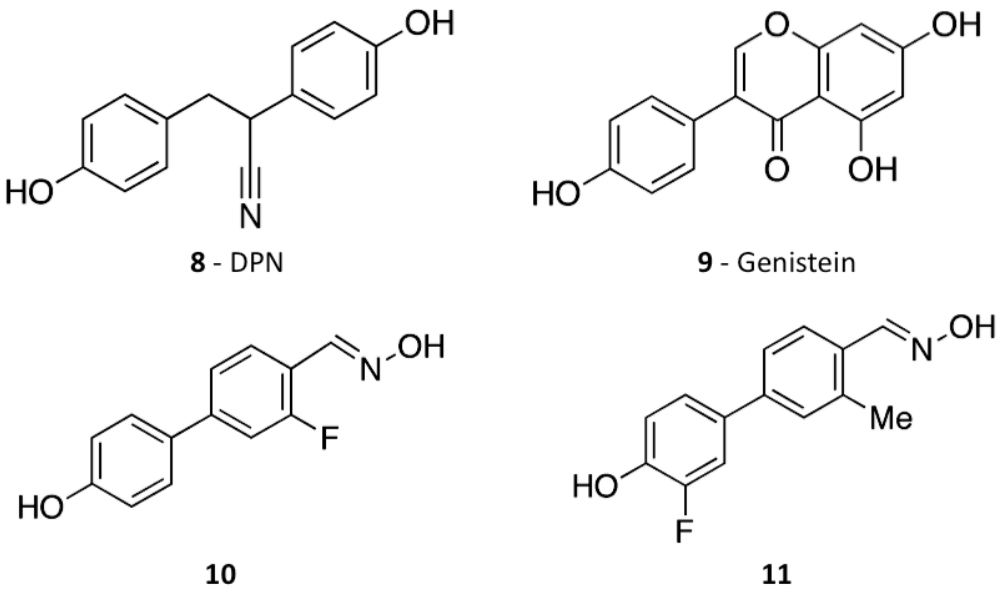

Figure 4: The structure of several ERβ-selective ligands.

DPN (**8**) is a 100-fold ERβ-selective compound. Genistein (**9**) is a plant derived compound that also possesses ERβ-selectivity. Biphenyl oximes **10** and **11** were recently synthesized in an attempt to mimic the C-ring of genistein and different substituents to the core were added to improve ERβ–selectivity.

Previously, through screening a library of homoallylic amides, allylic amides and *C*-cyclopropylalkylamides, a new structural scaffold for antiestrogens was discovered (Janjic, 2005A). Synthesis of a second generation library provided three additional agents that were found to bind strongly to ERα (Wipf, 2005). This second generation library was then screened for competing with a fluorescent E2 derivative for binding to ERβ using an FP assay. The efficiency of displacement demonstrated for ERβ by the initial screening library was significantly lower than that for ERα. One compound demonstrated a concentration-dependent displacement over the concentration range tested and almost 50% displacement at the highest concentration tested. This compound (**12**) was chosen as the lead structure for efforts to improve ERβ-selectivity (Figure 5). **12** did not quite reach 50% displacement on ERβ, so the selection criteria were modified to include structural features previously known to promote ERβ affinity (Yang, 2004). Screening results on ERα were used as co-selection criteria, and **12** was not a hit for ERα (Wipf, 2005).

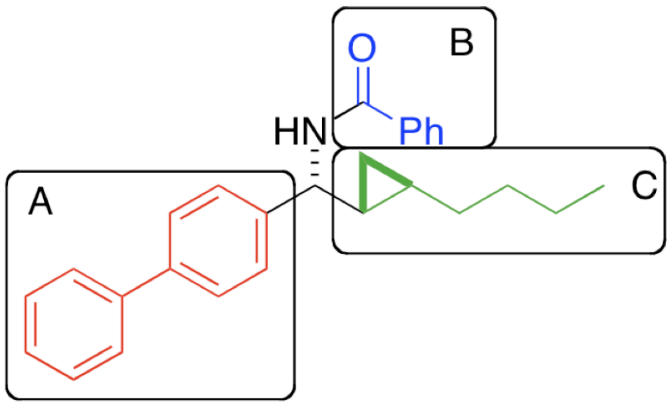

Figure 5: Lead compound for an ERβ-selective biphenyl *C*-cyclopropylalkylamide (12) and structure activity relationships.

The only compound (**12**) of the second generation library that demonstrated concentration-dependent displacement of E2 from ERβ and close to 50% displacement at the highest concentration tested. Regions A, B, and C were used for structure activity relationships.

Figure 5 demonstrates the three regions in **12** that were used for structure activity relationships (SAR). The biphenyl core is known to aid in selective targeting of ERβ (Yang, 2004). Regions A and B were chosen for further elaboration and the structures were assembled with the biphenyl core, the cyclopropane ring and the amide linkage preserved. The biphenyl group was substituted with a key 4'-OH group expected to promote hydrogen bonding with ERβ Glu^{305} and ERβ Arg^{346}. A fluorine substituent for the biphenyl core was chosen based upon published SAR for biphenyl-containing agents (Yang, 2004). The phenylamide was changed into a smaller acetylamide, or completely removed. The alkyl chain in region C was not altered because an increase in size abolished all activity. The six new compounds synthesized based on lead structure **12** can be seen in Figure 6. The synthesis of these compounds is reported in Janjic 2005B.

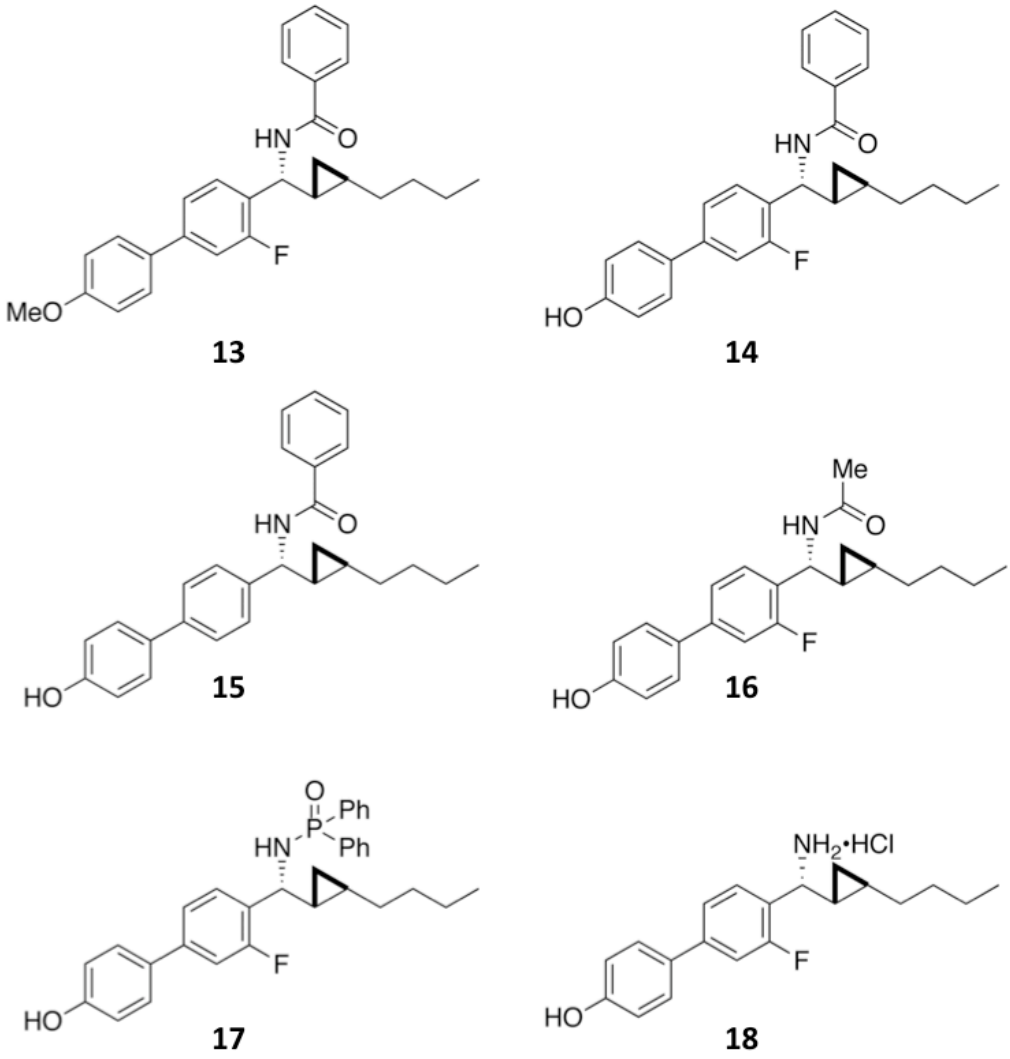

Figure 6: Library of six new compounds (13-18).

These compounds were synthesized based upon lead compound **12** in an attempt to improve selective targeting of ERβ.

The ability of these compounds to compete with E2 for binding to both ERs and inhibit the growth of breast cancer cells was investigated. Additionally, to gain some insight into the growth inhibition mechanism of these compounds, their effects on the protein levels of c-Myc, p21, and p27 were investigated.

2.3 RESULTS

2.3.1 Binding to the Estrogen Receptors

The six new compounds (**13 - 18**) and the control compound 3-fluoro-4'-hydroxy-1,1'-biphenyl-4-carbaldehyde oxime (**10**) were first evaluated for their ability to compete with the fluorescent E2 derivative (ES2) for binding to both ERs using the FP assay. The percent displacement of the E2 derivative by the test compound was evaluated from the difference in FP measured upon incubation with and without the test compound. When competition is absent, the fluorescent compound is bound to the receptor and tumbles slowly, giving a high polarization value. When the fluorescent ligand is competed out of the ER, it tumbles rapidly and gives a low polarization value. Polarization values are reported in units of mP (Parker, 2000). Figure 7 shows results for ERα and ERβ. Two compounds, **14** and **18**, significantly competed with ES2 and are presented in Figure 7. The curves in Figure 7 were constructed from one-site competition best-fit curves of mP versus concentration using Graph Pad Prism 4 software. The IC_{50} values determined from this fit are presented in Table 2. Biphenyl carbaldehyde oxime **10** and E2 were used as positive controls in this assay. ERβ/ERα selectivity ratios were calculated by dividing the IC_{50} determined for ERα by that determined for ERβ. **14** was at least 48-fold selective for ERβ with an IC_{50} value of 2.0 μM for ERβ, while **18** had an IC_{50} of 15 μM for ERβ and did not compete with ES2 for binding to ERα (Table 2).

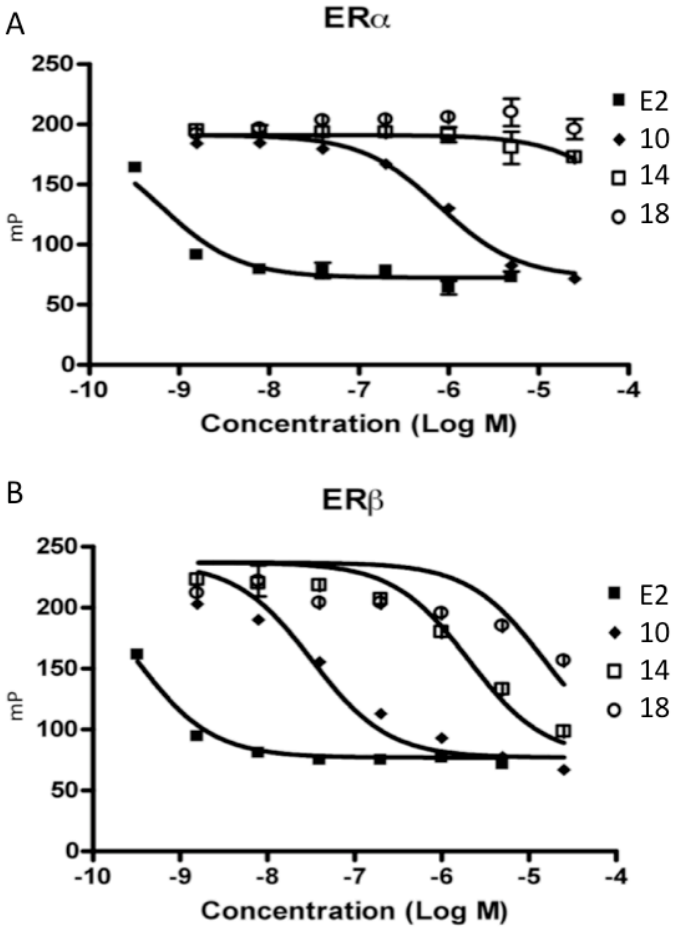

Figure 7: Competition of test compounds with ES2 for binding to ERα and ERβ in the FP assay.

The percent displacement of ES2 in ERα (A) and ERβ (B) by controls E2 and **10** and test compounds **14** and **18** was determined by the difference in FP measured upon incubation with and without the test compound. Graph Pad Prism 4 was used to construct the curves using a one-site best-fit curve of mP versus concentration (Log M).

Table 2: IC_{50} values for competition for both ERs from the FP assay.

Compound	ERα IC_{50} (nM)	ERβ IC_{50} (nM)	ER β Selectivity
E2	0.627	0.316	2.00
10	795	32.3	24.6
14	> 100,000	2048	> 48.8
18	N/A	15030	N/A

2.3.2 Inhibition of the Growth of Breast Cancer Cells

The compounds were evaluated for their ability to inhibit E2-induced proliferation of MCF-7 human breast cancer cells. This was done using two variants of the MCF-7 cell line: the later passage ATCC variant that expresses only ERα, and an earlier passage that expresses both ERα and ERβ. Additionally, to demonstrate selectivity, the compounds were also tested for their ability to inhibit the growth of the ER negative breast cancer cell line MDA-MB231 (Cailleau, 1978). The Western blot demonstrating receptor expression patterns is seen in Figure 8. Both the ATCC MCF7 and MCF-7 lines express ERα, while only the MCF-7 line expresses ERβ. The MDA-MB231 cell line was confirmed to be ER negative, as expression of neither ER isoform is seen in the Western blot.

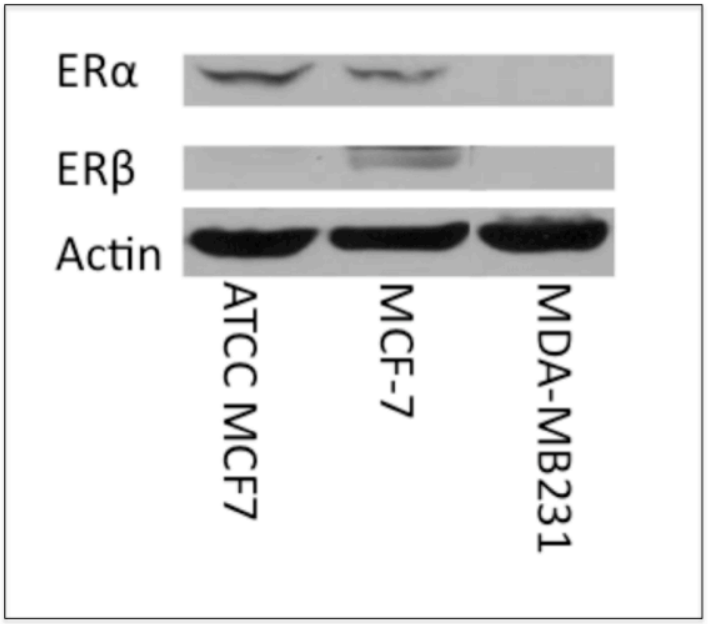

Figure 8: Western blot of ER expression in ATCC MCF7, MCF-7, and MDA-MB231 cell lines.

The expression of ERα and ERβ in the three breast cancer cell lines was determined. Actin was used to verify equal loading of the gel.

Using these ATCC MCF7, MCF-7, and MDA-MB231 cell lines, which express different isoforms of the ERs, in a cell proliferation assay helped to determine the selectivity of compounds **14** and **18**. Figure 9 shows the growth inhibition curves for all three cell lines. These curves were generated for compounds determined to be selective for ERβ using the MTS assay. Raloxifene (**4**), an antiestrogen known to inhibit the proliferation of MCF-7 cells, was included as a control (Thompson, 1988). GraphPad Prism 4 was used to estimate GI_{50} values using a non-linear best curve fit. The GI_{50} values can be seen in Table 3. In the ERα and ERβ expressing MCF-7 cells GI_{50} values of 4.1 and 1.2 μM were estimated for compounds **14** and **18**, respectively. In the ERα expressing ATCC MCF7 cells, compound **14** did not demonstrate inhibition, while a GI_{50} value of 51.7 μM was estimated for compound **18**. **14**, **18**, and raloxifene (**4**) did not demonstrate significant growth inhibitory activity against the MDA-MB231 cell line. Prior to adding the MTS reagent, cell morphology was examined by light microscopy. ATCC MCF-7 and MDA-MB-231 cells exposed to 25 μM of raloxifene (**4**), **14**, and **18** showed substantial morphological changes and appeared shrunken with many cells detached from the culture dish suggesting toxicity at this concentration.

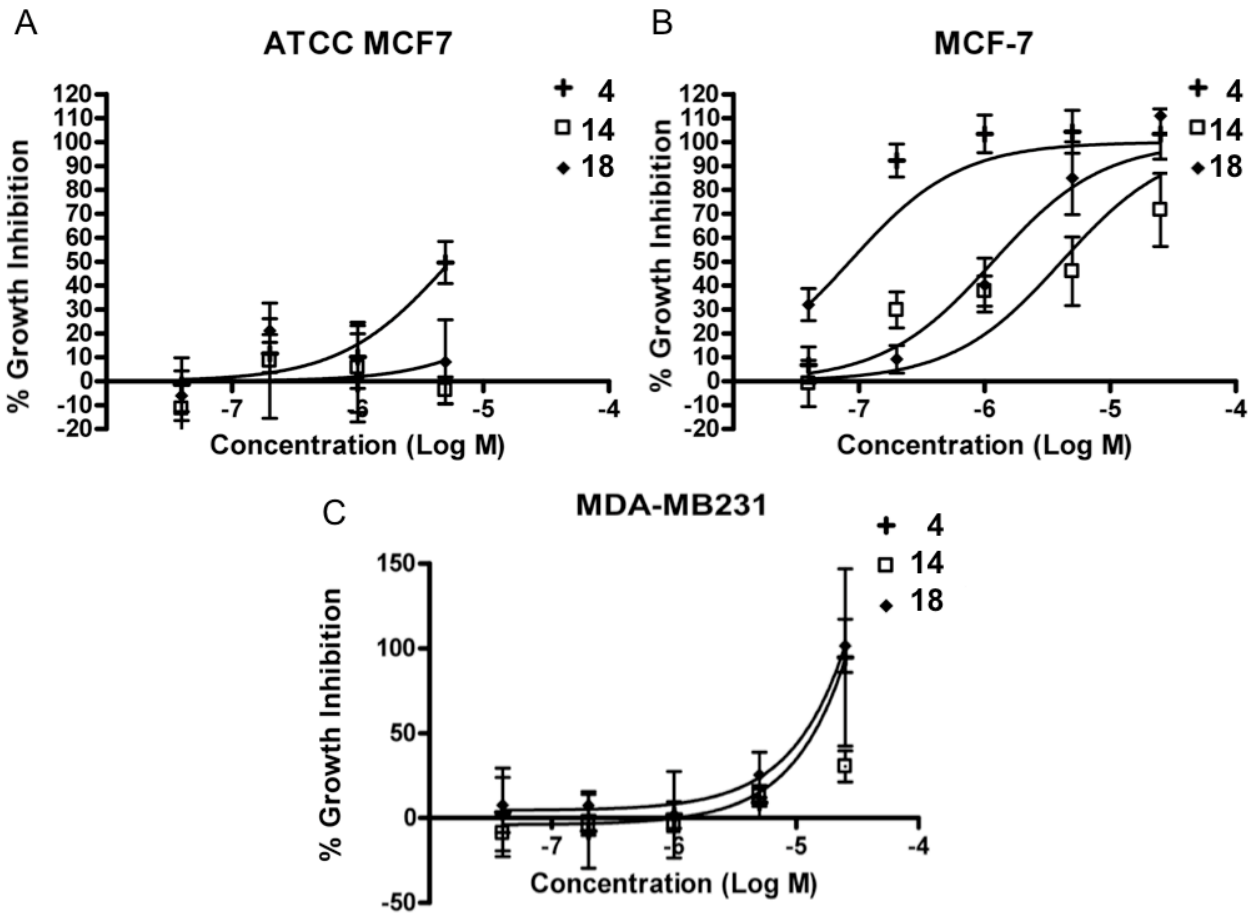

Figure 9: Growth inhibition curves of compounds 4, 14, and 18 for ATCC MCF7, MCF-7, and MDA-MB-231 cells.

The growth inhibition curves generated using control compound raloxifene (**4**) and test compounds **14** and **18** for ATCC MCF7 (A), MCF-7 (B) and MDA-MB231 (C) cell lines with the MTS assay. GraphPad Prism 4 was used for a non-linear best curve fit.

Table 3: GI_{50} values for compounds 14 and 18 in MCF-7 and ATCC MCF7 cell lines.

	GI_{50} Value (μM)	
Compound	**MCF-7**	**ATCC MCF7**
14	4.1	N/A
18	1.3	52

2.3.3 Effects on the Protein Levels of c-Myc, p21, and p27

c-Myc plays a major role in cell proliferation and malignant transformation in breast cancer (Liao, 2000). E2 treatment causes a rapid increase in the level of c-Myc expression in human breast cancer cells (Dubik, 1987). Expression of ERβ in breast cancer cells inhibits c-Myc expression at both the mRNA and protein level, while increasing the levels of its regulators, the cyclin-dependent kinase inhibitors p21(Cip1) and p27(Kip1) (Paruthiyil, 2004). The effects of **14** and **18** on the protein levels of c-Myc, p21, and p27 were determined because of their link to breast cancer and E2. Western blot analyses from whole cell lysates of MCF-7 cells treated with the indicated compounds can be seen in Figure 10. The densitometric analyses performed on these Western blots can be seen in Table 4. ImageJ was used to determine band intensity and levels were standardized to actin. The relative fold change was determined by comparison to the DMSO-treated band for each protein. Both compounds **14** and **18** decreased the levels of cMyc to 0.77 and 0.59 of control, respectively. Compound **14** increased the levels of p21 and p27 by 3.64 and 3.90 fold compared to control, respectively. Compound **18** did not have as great of an effect on p21 and p27 with relative fold changes of 1.10 and 1.51 compared to control, respectively. PPT, a 410-fold ERα-selective agonist, and DPN, a 70-fold ERβ-selective agonist, were included as controls (Stauffer, 2000; Meyers, 2001). These two compounds increased the levels of cMyc, p21 and p27.

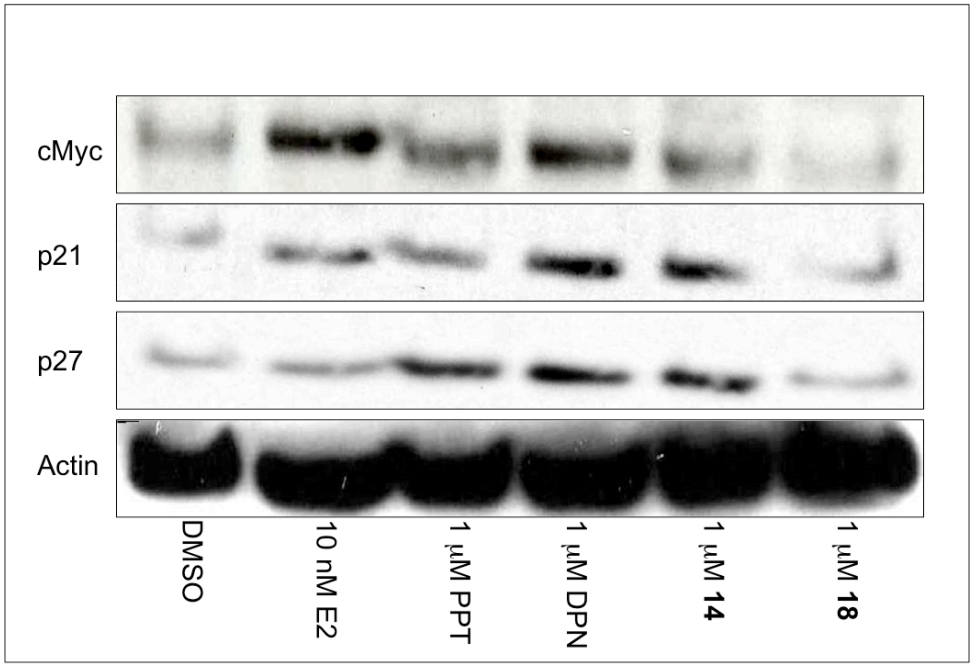

Figure 10: Western blot analysis of the levels of c-Myc, p21, p27, and actin in MCF-7 cells in response to ER ligands.

MCF-7 cells were treated with the indicated compound for 12h and whole cell lysates were prepared and then analyzed for the indicated proteins. DMSO is the vehicle control, E2 is 17β-estradiol, PPT is a 410–fold ERα-selective agonist, DPN is a 100–fold ERβ-selective agonist, and **14** and **18** are library members that demonstrated selectivity for ERβ and inhibited the growth of human breast cancer cells. Densitometry was performed using ImageJ with standardizing the levels to actin. The fold-change relative to DMSO is reported in Table 4.

Table 4: Densitometry analysis of Western blots in Figure 10.

Protein	10 nM E2	1 μM PPT	1 μM DPN	1 μM 14	1 μM 18
cMyc	3.84	2.17	2.67	0.77	0.59
p21	1.15	4.05	3.47	3.64	1.10
p27	1.76	2.47	3.32	3.90	1.51

2.4 DISCUSSION

The ongoing goal of this project is to develop new chemical tools to assist in studying the complex biology and interplay of the ERs by synthesizing and studying biphenyl *C*-cyclopropylalkylamides. The *C*-cyclopropylalkylamide core was previously identified as a scaffold for antiestrogens (Janjic, 2005A; Wipf, 2005). Modifications of this core were performed in an attempt to gain selectivity for ERβ. Six new ligands were synthesized using the one ERβ hit from the second generation library and what has been demonstrated in the literature to contribute to ERβ selectivity (Janjic, 2005B). These compounds were evaluated for their ability to selectively bind ERβ and their inhibition of the proliferation of breast cancer cell lines.

Two of the six new *C*-cyclopropylalkylamides, **14** and **18**, demonstrate selectivity for ERβ as determined by the FP assay measuring the ability of the test compound to compete with ES2 for binding to ERα and ERβ. Biphenyl carbaldehyde oxime **10**, used as a control in this assay, gave an IC_{50} comparable to that previously determined in a radioligand binding assay (Yang, 2004). These two compounds, **14** and **18**, also inhibit the E2-induced proliferation of breast cancer cells. They demonstrate greater inhibition of cells expressing both isoforms of the ER compared to those expressing only ERα. This supports the idea that the compounds are performing a specific effect through the ERβ. In breast cancer cells expressing both ERβ and ERα a significantly more potent anti-proliferative effect is demonstrated compared to breast cancer cells expressing only ERα or no ERs. It can also be concluded that the compounds are likely functioning as ERβ agonists based on what has been demonstrated for ERβ's behavior in breast cancer. ERβ inhibits the proliferation of breast cancer cells in response to E2 and represses c-Myc, cyclin D1, and cyclin A1 expression while increasing expression of the cyclin

dependent kinase inhibitors p21 and p27 (Omoto, 2003; Ström, 2004; Paruthiyil, 2004; Willams, 2008).

Compound **18** has a 4.1 μM GI_{50} against ER positive MCF-7 cells; however, its IC_{50} is 15.0 μM for binding to ERβ. Similarly, compound **14** potently inhibits MCF-7 cell growth with a GI_{50} of 1.2 μM, but its IC_{50} for binding to ERβ is 2 μM. If the growth inhibition of MCF-7 cells seen in this assay is solely through the compound binding to ERβ, a higher affinity of **14** and **18** for ERβ would be expected. The discrepancy suggests that the antiproliferative effects of these compounds are likely much more complex than a simple binding event to ERβ. One possible explanation for this discrepancy is that the activity of **18** may be derived from an active metabolite of the aliphatic primary amine that has a much higher affinity for ERβ than the parent compound. Additionally, compounds **14** or **18** may interact with the ER in a way other than via the LBD and not detected by the FP assay. It is possible that compounds **14** or **18** may interact with the coactivator domain of ERβ and alter the cofactors recruited to the receptor. Studies using the ERβ-selective compound liquiritigenin, a herb extracted from the root of *Glycyrrhizae uralensis*, supports this idea. Liquiritigenin has only 20-fold selectivity for ERβ compared to ERα as determined using the FP assay. Yet, this compound activates an ERE-luciferase reporter only in the presence of ERβ but not ERα. This was explained by a CHIP assay demonstrating that liquiritigenin causes recruitment of SRC-2 to E2-regulated genes only in cells expressing ERβ and not ERα (Mersereau, 2008). A similar mechanism could occur with compound **14** or **18**. **14** or **18** may cause recruitment of only certain cofactors when bound to ERβ but not ERα that exert an effect on the proliferation of the MCF-7 cells. The agents presented here should be explored further for their ability to target the coregulator binding domain of ERβ. Interestingly,

introducing the –OH group to the biphenyl core in **18** did not result in a significant improvement in the biological activity as well as the presence of an aliphatic alkyl chain on the compounds.

Compounds **14** or **18** may also exert an effect on the cell through ERα. While **18** did not compete with ES2 for binding to ERα, **14** did demonstrate some competition for binding ERα. The discrepancy between the binding data and the cellular data suggests the involvement of other pathways in addition to those involving the ERs.

To further understand the cellular activities of the compounds, their effects on several cell cycle proteins was determined. c-Myc has been implicated in cell proliferation, apoptosis and differentiation (Dang, 1999). It is a key player in cell cycle regulation, and can induce cell cycle progression in antiestrogen-arrested cells (Prall, 1997; Prall, 1998). Additionally, E2 is known to cause rapid increase in the level of c-Myc expressed by human breast cancer cells (Dubik, 1987). Induction of the expression of ERβ inhibits c-Myc at both the mRNA and protein level, while increasing the levels of p21 and p27 (Paruthiyil, 2004). Compounds **14** and **18**, which are selective for ERβ and inhibit the proliferation of ER positive breast cancer cells, slightly decrease c-Myc protein levels while increasing the levels of p21 and p27. The known ERβ agonist DPN increases p21 and p27 levels also, but it also increases c-Myc levels about three-fold. While the EC_{50} for DPN for ERβ is 0.85 nM, it also has an EC_{50} for ERα of 66 nM as determined by a luciferase reporter transcription assay (Meyers 2001). In another luciferase reporter transcription assay, DPN produces a 20-fold increase in transcription in the presence of ERα and a 75-fold increase in the presence of ERβ compared to vehicle control (Mersereau, 2008). **14** and **18** are targeting cell cycle regulators that are influenced by ERβ. Additionally, compounds **14** and **18** hold promise because of their ability to cause increased levels of cyclin-dependent kinase inhibitors, likely inhibiting cell cycle progression.

In conclusion, compounds **14** and **18** demonstrate selectivity for ERβ as well as promising antiproliferative effects in breast cancer cells. The compounds are likely acting as agonists for ERβ based on what has been shown about ERβ's activity in breast cancer, and this encourages future investigation (Ström, 2004; Parythiyil, 2004; Hartman, 2006). Luciferase reporter assays should be conducted with compounds **14** and **18** in order to verify their activity as ERβ agonists. Compared to the lead compounds **10** and **11**, **14** and **18** show no affinity for ERα and moderate affinity for ERβ. This initial investigation into the biphenyl *C*-cyclopropylalkylamide pharmacophore demonstrates the potential of this scaffold to deliver ER-selective antiestrogens. Furthermore, the preliminary SAR provides clues for improving selectivity for ERβ. A subtype-selective antiestrogen will help to understand the complex biology of the ERs and their interplay. The arrival of new ER ligands with differential subtype selectivity ratios enables the tailoring of antiestrogenic or estrogenic therapy according to the condition and level of receptor isoforms present in patients.

2.5 MATERIALS AND METHODS

2.5.1 Fluorescence Polarization Assay

The ERα and ERβ FP competitor assays were performed according to the manufacturer's (Invitrogen, Carlsbad, CA) recommendations with some modifications. Human recombinant ER was used at the recommended concentration of 15 nM and the Fluormone™ ES2 was used at a concentration of 1 nM in the final mixture. Aliquots (20 μL) of the mixture of ER and Fluormone™ ES2 were distributed in 384-well, black flat-bottom plates and serial dilutions of

test compounds prepared in DMSO were then added. Each compound was tested in duplicate, and 1 μM E2 was used as a positive control. The DMSO concentration was kept at 1% (*v*/*v*) throughout the experiment. After 2 h, FP was measured using an Analyst™ AD & HT Assay Detection Systems reader (Molecular Devices, Sunnyvale, CA) equipped with 485 nm excitation and 530 nm emission filters with the appropriate FL505 dichroic mirror. The instrument was validated using serial dilutions of methylfluorescein in the screening buffer. FP was determined after background subtraction from perpendicular and horizontal fluorescence measurements by the Analyst™ AD & HT Assay Detection Systems integrated software. mP was determined by the equation: mP = 1000 x (S-(G*P))/(S+(G*P)), where S and P are the background-subtracted intensity measurements for the parallel and perpendicular components respectively and G is a constant of the instrument. Data was then analyzed using GraphPad Prism's one site competition method. The fit was constrained by the high polarization control, which was the ER/ES2 complex with no competition, and the low polarization control, which was the ER/ES2 complex with 1 μM E2 for 100% competition.

2.5.2 Cell Proliferation Assay

MCF-7 and ATCC MCF7 breast cancer cells were seeded in 96-well plates at a density of 4 x 10^3 cells per well in phenol red free RPMI-1640 medium containing 10% charcoal-dextran stripped fetal bovine serum (FBS) (to remove estrogens) and allowed to adhere overnight. Test compounds were then added (concentrations ranging from 25 pM to 50 μM) along with 1 nM E2, and cells were incubated for 6 days. Effect of the test compounds on growth was determined using the CellTiter Aqueous One assay system (Promega, Madison, WI), which utilizes the MTS dye reduction assay with phenazine methanesulfonate as the electron acceptor. Absorbance was

measured at 490 nm using an M5 plate reader (Perkin Elmer, Boston, MA) and the background absorbance at 630 nm was subtracted after 2 h incubation with the reagents. Data represents the average of at least two independent experiments done in quadruplicate. A plate of control cells (16 wells) was measured at day 0 to establish 0% growth. E2-stimulated growth at day 6 was set to 100% growth. GraphPad Prism 4 (GraphPad Software Inc, La Jolla, CA) software was used for constructing dose-response curves and calculating GI_{50} values.

MDA-MB231 cells were plated in 96-well plates at 1 x 10^3 cells/well and allowed to adhere for 72 h in phenol red-free RPMI-1640 containing 10% FBS. Test agents were added (concentrations ranging from 3.2 nM to 50 μM) and cells were incubated for 72 h. Cell density was determined using the MTS assay as described above.

2.5.3 Western Blots

Cells were plated in 25-cm^2 flasks in RPMI-1640 with 10% FBS and allowed to attach for 48 h. Media was then changed to RPMI-1640 with charcoal-dextran stripped FBS. After 48 h, cells were incubated with test agent at the given concentration or with vehicle (DMSO) for 12h. Cells were washed in cold phosphate buffered saline (PBS) and lysed in RIPA buffer with phenylmethanesulphonyl fluoride (PMSF), sodium orthovanadate, and protease inhibitors according to the manufacturer's protocol (Santa Cruz Biotechnology, Santa Cruz, CA). Lysates were centrifuged at 10,000xg for 10 min at 4°C. Concentration of protein in the supernatant was determined using the bicinchoninic acid (BCA) Protein Assay (Thermo Fisher Scientific, Rockford, IL). Equal amounts of protein were loaded into wells of 4-12% Bis/Tris gels (Invitrogen, Carlsbad, CA) with 3-(*N*-morpholino)propanesulfonic acid (MOPS) buffer and separated by SDS-PAGE. Proteins were transferred onto nitrocellulose membranes using a Bio-

Rad (Hercules, CA) Trans-Blot Semi Dry transfer system. The Amersham ECL™ Western Blotting Detection Reagents (GE Healthcare, Piscataway, NJ) were used to detect protein bands. Band quantitation was performed using the ImageJ program (National Institutes of Health, Bethesda, MD).

3.0 SPECIFIC ALTERATIONS TO THE NUCLEAR MATRIX IN A TAMOXIFEN RESISTANT CELL LINE

3.1 ABSTRACT

Tamoxifen has long been the standard of treatment in women with ER+ breast cancer. One of the major problems with tamoxifen is drug resistance. Only about half of ER+ breast cancers respond to tamoxifen initially, and those that do respond eventually develop resistance over the course of treatment. The mechanism behind this resistance is not completely understood. Several mechanisms have been proposed, such as alterations to cofactors, loss of ER expression, and compensation by growth factor signaling pathways. In order to investigate the alterations to the proteins of the NM, the NMPs from MCF-7 breast cancer cells, and their antiestrogen resistance derivative, MCF-7/LY2, were isolated and examined. These two cell lines were also exposed to several ER isoform-selective ligands in order to discern how the two receptor isoforms may alter NMP composition of tamoxifen responsive and resistant cell lines. The 8-plex iTRAQ method was used in order to identify and quantify the NMPs present in these cell lines. A total of 148 NMPs were identified, and several interesting changes between the resistant and responsive line and in response to the subtype selective ligands were found. These proteins may shed some light on the mechanism behind antiestrogen resistance and eventually serve as biomarkers to help customize breast cancer treatment.

3.2 INTRODUCTION

Tamoxifen was developed in the 1970's as an antiestrogen (Jensen, 2003). Tamoxifen has been a major component used for the treatment and prevention of breast cancer for the past thirty years through its role as a SERM and the blocking of the action of estrogen in the breast (Jordan, 2007). Tamoxifen functions by competing with E2 for binding to the ER and repositioning helix 12 in the receptor, so coactivators can no longer bind and corepressors are recruited (Brzozowkski, 1997; Shiau, 1998; Nettles, 2005). Adjuvant treatment for five years with tamoxifen has been shown to reduce the annual risk of recurrence and death from the disease by 47% and 26% respectively (Early Breast Cancer Trialists' Collaborative Group, 2005).

One of the major problems in tamoxifen therapy is *de novo* or acquired drug resistance. Only about half of ER+ tumors respond to the drug initially and those that do respond eventually develop resistance over the course of treatment (Osborne, 1998). An explanation for acquired resistance to tamoxifen is the loss of ER expression; however, only about 17-28% of tumors with acquired resistance lose ER expression (Johnston, 1995; Gutierrez, 2005). 20% of tamoxifen-resistant tumors respond to another therapy that involves targeting the ER (Howell, 2005; Osborne, 2002). This suggests that the cell has altered the way it handles the ER-tamoxifen complex when it has developed resistance (Clarke, 1996). There are two similar isoforms of the ER, ERα and ERβ. While structurally similar, there are some differences in their N- and C-terminal domains, which contribute to their subtype specific actions (McInerney, 1998). ERβ has a negative influence on ERα-mediated transcription (Sugiura, 2007). Alteration of the expression level of ERβ has also been shown in tamoxifen resistant cell lines. There is controversial as both low and high levels of ERβ expression have been associated with tamoxifen resistance (Hopp, 2004; Esslimani-Sahla, 2004; Speirs, 1999). Altered expression of coregulators that significantly

influence ER-mediated transcription may also play a part in tamoxifen resistance (McKenna, 1999). Overexpression of coactivators and down-regulation of corepressors can inhibit the effects of SERMs (Smith, 1997). The ER lies in a complex system of interlocking signal transduction pathways that may also play a role in the development of resistance (Zilli, 2009).

A particular area of the cell that may hold important clues to understand how the ERs influence the behavior of a breast cancer cell in its response to antiestrogens is the NM. The shape of the nucleus, commonly used as a pathological marker in cancer, is partially determined by the NM (Replogle-Schwab, 1996; Samuel, 1997). The NM is the structural scaffolding of the nucleus and is a dynamic structure involved in DNA replication, transcription, repair, RNA processing, and a modulator of hormone action (Getzenberg, 1990). Specific binding sites for E2 have been demonstrated in the NM and the structure plays a role in regulating hormone action (Barrack, 1980). The ER localizes to the NM in response to E2 (Alexander, 1987). NMPs specific to several types of cancer have been identified and used as specific biomarkers for several types of malignancies (Leman, 2008). Adding to their potential as biomarkers is the fact that NMPs can be identified in the serum of patients (Miller, 1992). This detection may allow for the development of a non-invasive screening procedure that could be used in the clinic to detect the development of resistance to tamoxifen.

This study was performed in order to examine how the protein content of the NM changes in a cell that progressed to antiestrogen resistance in the constant presence of an antiestrogen in culture. These alterations to the NM may aid in the development of biomarkers for tamoxifen resistance that may be used to more effectively treat breast cancer. This study was performed by using the MCF-7 ER+ breast cancer cell line and its ER+ antiestrogen resistant derivative, MCF-7/LY2 (Bronzert, 1985). Additionally, by using ligands that are ER isoform-

selective antagonists or agonists, the effect of specific targeting of the ER isoforms on the proteins in the NM was also determined.

The 8-plex iTRAQ method was used to identify changes on NMP levels between the two different cell lines and four treatments investigated. The iTRAQ method employs amine-specific isobaric tags that allow for the multiplexed relative quantitation of proteins by MS (Ross, 2004). In this study, two sets of iTRAQ labeling were performed in which the order of the labels was reversed to account for any label specific effects. Two separate methods, strong cation exchange chromatography (SCX) and OFFGEL electrophoresis, were then used to fractionate the iTRAQ-labeled peptides generated by trypsin digestion. Nanoscale-liquid chromatography-matrix assisted laser desorption ionization-time of flight/time of flight (Nano-LC-MALDI-TOF/TOF) or nanoscale-liquid chromatography-electrospray ionization-quadrupole-time-of-flight (nano-LC-ESI-Q-TOF) MS were then performed for protein identification and quantification. Figure 11 shows the three different workflows used. In addition to understanding the changes in the abundances of NMPs in the samples, comparisons can also be made between the different fractionation and MS techniques employed by each of three different workflows to aid in future iTRAQ experiments.

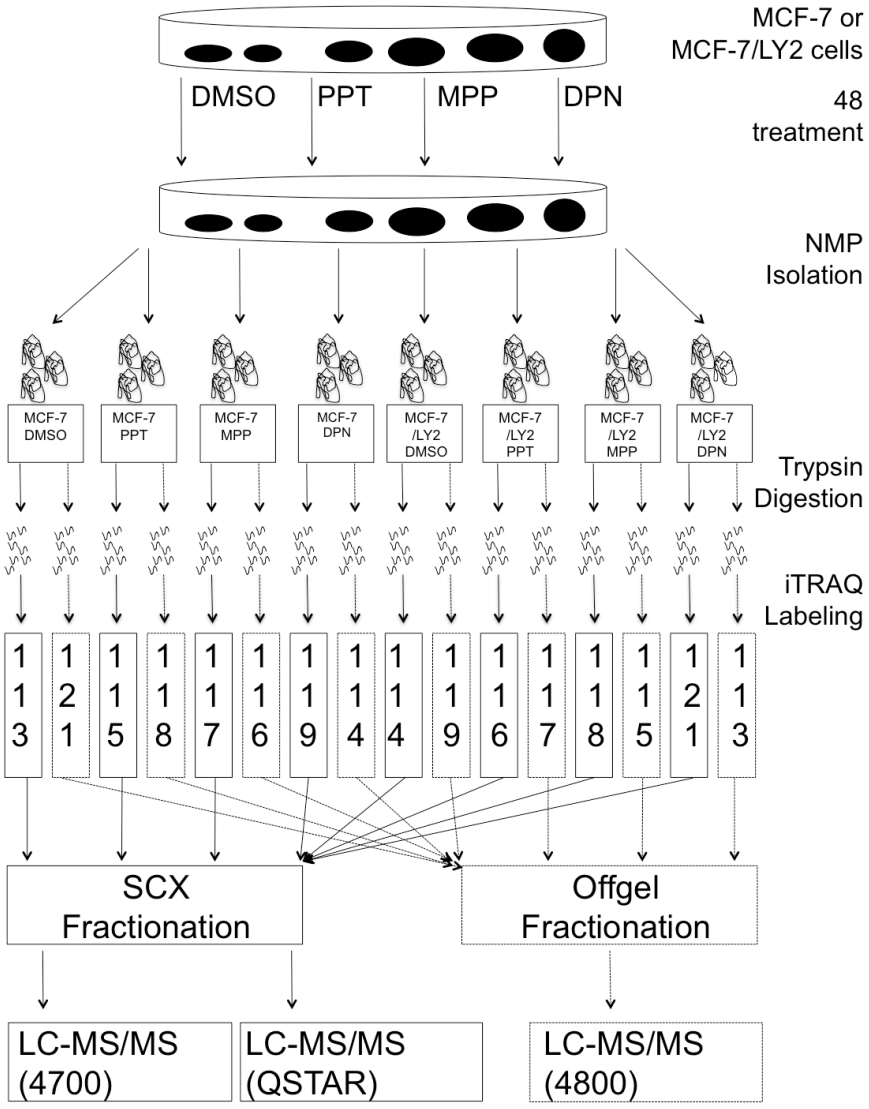

Figure 11: The three proteomic workflows used in this study.

MCF-7 and MCF-7/LY2 were treated with 5 μM PPT, 5 μM MPP, 5 μM DPN, or DMSO control for 48h and NMPs were isolated. Overnight trypsin digestion was performed and iTRAQ labeling was done as seen. One set of labeling follows solid arrows and the second set follows dashed arrows. The first workflow fractionated using SCX spin columns and then LC-MS/MS analysis using the ABI 4700 Proteomics analyzer. The second workflow used the same set of labeled samples as the first workflow and also separated by SCX spin columns; however, LC-MS/MS analysis was done using the ABI QSTAR. The third workflow changed the label each sample was tagged with and separated by OFFGEL fractionation. These samples were then analyzed by the ABI 4800 Proteomics Analyzer.

3.3 RESULTS

3.3.1 Estrogen Receptor Expression in MCF-7/LY2 Breast Cancer Cells

The early passage MCF-7 line and the MCF-7/LY2 derivative of this line, which has developed antiestrogen resistance in culture, were used. This MCF-7 cell line is different from the later passage ATCC MCF7 commonly used. Expression of the ER isoforms in these lines was determined by Western blotting (Figure 12). The ATCC MCF7 line expressed primarily ERα, while the early passage MCF-7 cells expressed similar levels of both ERα and ERβ. The MCF-7/LY2 cell line maintained expression of ERα but has lost expression of ERβ.

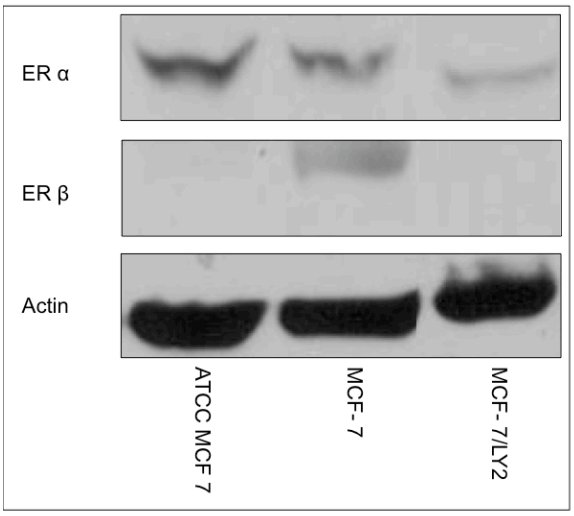

Figure 12: ER expression in the ATCC MCF 7, MCF-7, and MCF-7/LY2 breast cancer cell lines.

Whole cell lysates were prepared from ATCC MCF7, MCF-7, and MCF-7/LY2 cell lines, and these lysates were investigated for the expression of ERα and ERβ by Western blotting. Actin was used as a loading control for the gel.

3.3.2 Nuclear Matrix Proteins Identified in MCF-7 Cells

The first aspect of this study is the determination of what proteins are located in the NM of the MCF-7 breast cancer cell line. In order to verify the integrity of NMP preparations from these cells, Western blotting was performed using the fractions generated during the preparation. Figure 13 shows a schematic of how the NM is isolated from cells in culture and the different protein fractions generated throughout the isolation.

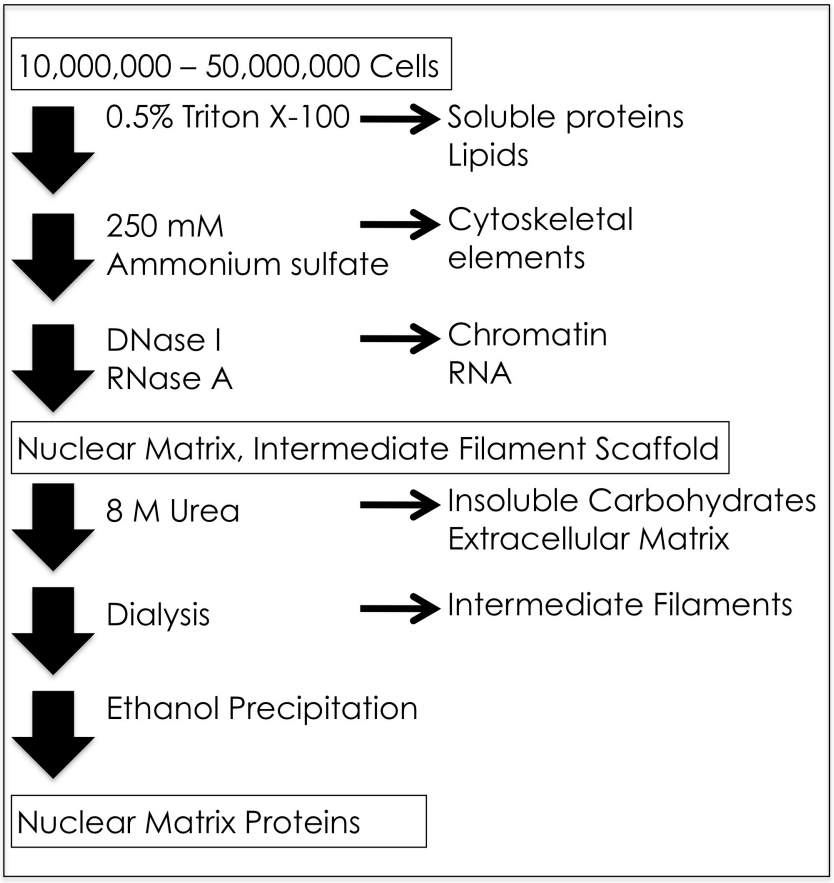

Figure 13: The isolation procedure for NMPs from cells in culture.

The NMP preparation involves a series of buffer changes and centrifugations. Different cellular fractions are generated through the procedure, including soluble protein, cytoskeletal elements, chromatin, and finally, the nuclear matrix.

Figure 14 shows an example Western blot of the fractions isolated during the NM preparation. Actin is present in the soluble, cytoskeletal and chromatin fractions generated during the isolation procedure but absent in the final NMP isolation. The NM marker, Lamin B1, is specific to the NM fraction (Fey, 1988).

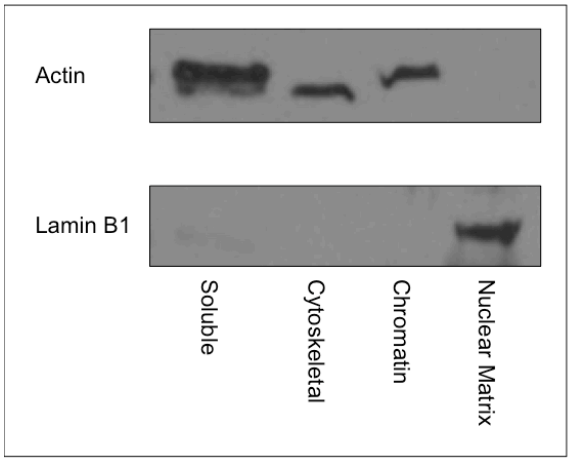

Figure 14: Western blot verification of a NMP preparation.

The proteins generated during each step of the NMP preparation were precipitated and a Western blot was performed to show the lack of actin in the final NM fractions, but presence of the specific NM marker Lamin B1.

After isolation the NMPs underwent the iTRAQ labeling procedure. The NM isolations were separated and two separate labeling schemes were followed. These labeling schemes can be seen in Figure 11. After labeling, three different workflows were followed for protein identification and quantitation. These workflows can also be seen in Figure 11. Combining the confident protein identifications made from all of the workflows used a total of 148 NMPs with a ProtScore $\geq$ 1.3 were identified using ProteinPilot analysis software. A ProtScore of 1.3 corresponds to an identification with 95% confidence. Eighty-six of these proteins were identified from at least two distinct peptides with 95% confidence for each peptide identification. A complete list of these proteins is presented in Table 14 (Appendix A). The table lists all of the

NMPs that were identified with 95% confidence from any of the three workflows used from the NMP preparation.

An example of the protein coverage for one of the proteins identified can be seen in Figure 15. This is the amino acid sequence of hNRNP R and the peptides that were identified following workflow 3, offgel fractionation and the ABI 4800 Proteomics Analyzer, in Figure 11. This protein was identified with a ProtScore of 4.28 and 46.7% coverage.

MANQVNGNAVQLKEEEEPMDTSSVTHTEHYKTLIEAGLPQK*VAERLDEIFQTGLV*
*AYVDLDER*AIDALREFNEEGALSVLQQFKESDLSHVQNKSAFLCGVMKTYRQREKQGSK
VQESTKGPDEAKIKALLERTGYTLDVTTGQRKYGGPPPDSVYSGVQPGIGTEVFVGKIPR
DLYEDELVPLFEKAGPIWDLR*LMMDPLSGQNRGYAFITFCGKEAAQEAVK*LCDSYEIRPGK
HLGVCISVANNR*LFVGSIPK*NKTENILEEFSKVTGLTEGLVDVILYHQPDDKKK*NRGFCFL*
*EYEDHKSAAQAR*RRLMSGKVKVWGNVVTVEWADPVEEPDPEVMAKVKVLFVR**NLATT**
VTEEILEKSFS*EFGK*LERVKKLK*DYAFVHFEDR*GAAVKAMDEMNGKEIEGEEIEIVLAKP
PDKKRKER*QAARQASR***STAYEDYYYHPPPR***MPPPIRGRGRGGGRGGYGYPPDYYGYEDY*
*YDDY*YGYDYHDYP*GGYEDPYYGYDDGYAVRGRGGGR*GGRGAPPPPRGR*GAPPPRGRAGY*
*SQRGAPLGPPRGSRGGRGGPAQQQRGRGSRGSRGNRGGNVGGK*R*KADGYNQPDSK*RR*QT*
*NNQQNWGSQPIAQQP*LQQGGDYSGNYGYNNDNQEFYQDTYGQQWK

Figure 15: The amino acid coverage of hnRNP R as determined by workflow 3 using offgel fractionation and the ABI 4800 Proteomics Analyzer.

This is the amino acid sequence of hnRNP R. Peptides that were identified with ≥ 95% confidence are bold. Peptides that were identified with ≥ 50% but < 95% confidence are underlined. Peptides that were identified with > 0% but < 50% confidence are italic. These are the peptide identifications made using workflow 3, which involved fractionation using OFFGEL electrophoresis and nano-LC-MALDI-TOF/TOF with the ABI 4800 Proteomics Analyzer.

An example spectrum of one of the peptides identified by workflow 3 from hnRNP is shown in Figure 16. Table 5 shows the predicted y and b ions for this peptide and indicates which of these ions were found in this spectrum. The matched ions are shown in bold. This peptide was identified with 99% confidence.

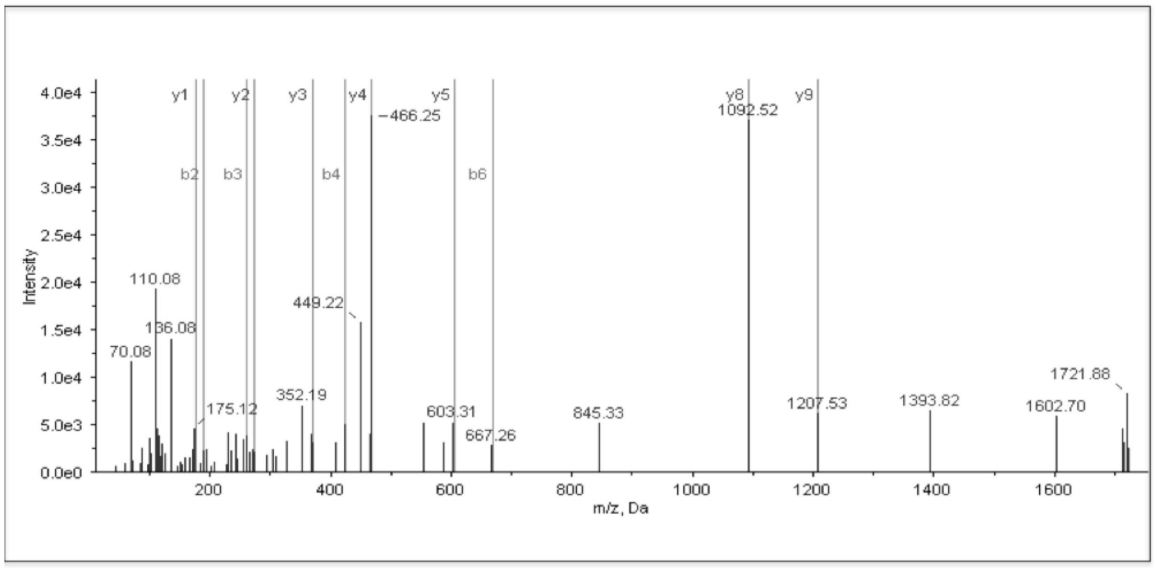

Figure 16: The mass spectrum of an example peptide from hnRNP R.

An example mass spectrum of one of the peptides of hnRNP R. This spectrum was generated on the ABI 4800 Proteomics Analyzer. Assignment of the y and b ions can be seen in Table 5.

Table 5: The y and b ions identified for the peptide seen in Figure 16.

Residue	b	y
S	88.0393	1758.7758
T	**189.0870**	1671.7438
A	**260.1241**	1570.6590
Y	**423.1874**	1499.6590
E	552.2300	1336.5957
D	**667.2570**	**1207.5531**
Y	830.3203	**1092.5261**
Y	993.3836	929.4628
Y	1156.4469	766.3995
H	1293.5059	**603.3362**
P	1390.5586	**466.2772**
P	1487.6114	**369.2245**
P	1584.6642	**272.1717**
R	1740.7653	**175.1190**

3.3.3 Nuclear Matrix Protein Abundance Levels Altered in MCF-7/LY2 Cells

Of the 148 NMPs identified in the MCF-7 cells, abundance was determined for 131 using the iTRAQ labels. This represents 88% of the total proteins identified. 70% of these 131 proteins were quantified based on at least two peptides. The first comparison that can be made using the iTRAQ ratios from the three different sets of data is to compare levels of the different NMPs between the parental MCF-7 cell line and its antiestrogen resistant derivative MCF-7/LY2. Of the 131 proteins quantified, 52 provided a MCF-7/LY2:MCF-7 ratio with a p-value less than 0.05 indicating that the levels of expression were different between the cell lines. In every case except one where quantification of a protein was determined by more than one of the workflows, the increase or decrease in abundance of the protein was consistent between the different workflows. Table 15 in Appendix B presents these 52 proteins and the ratio of expression between the resistant (MCF-7/LY2) and responsive (MCF-7) line. Cut-off values for statistically significantly altered proteins were determined by taking the mean value of all protein ratios obtained and moving out two standard deviations from this mean. These values were 0.451 and 1.63. Table 6 presents the seventeen proteins that fell outside of these limits when comparing abundance in MCF-7/LY2 to that in MCF-7 cells. A standard deviation for the ratio is provided in the table for those proteins where more than one workflow provided a ratio. Ten proteins were more abundant and seven proteins were less abundant in the MCF-7/LY2 cells. One protein, represented by a ratio of 9999, was found in the MCF-7/LY2 cells but not the MCF-7 cells. Three proteins, represented by a ratio of 0, were found in the MCF-7 cells but not in the MCF-7/LY2 cells.

Table 6: Statistically significantly alterations to NMP abundance in MCF-7/LY2 cells compared to MCF-7 cells.

Protein Name	Accession Number (IPI)	Gene Symbol	MCF-7/ LY2: MCF-7	Std Dev
NUMA1 variant protein	00872028.2	NUMA1	9999	
Histone H3.1	00902514.1	HIST1H2AD	3.439	2.114
ATP synthase subunit alpha	00440493.2	ATP5A1	2.537	
Histone H2B	00646240.3	HIST2H2BA	2.301	
Small nuclear ribonucleoprotein Sm D3	00017964.1	SNRNPD3	2.191	0.5964
P37 AUF1	00903278.1	HNRNPD	2.178	
60S acidic ribosomal protein P1	00008527.3	RPLP1	1.813	
Lamin-B2	00009771.6	LMNB2	1.766	0.5235
Fus-like protein	00260715.5	FUS	1.728	
40S ribosomal protein S19	00215780.5	RPS19	1.693	
Keratin, type II Cytoskeletal 8	00554648.3	KRT8	0.4466	0.08853
Splicing factor, proline- and glutamine-rich	00010740.1	SFPQ	0.3955	
Desmoplakin, isoform DPI	00013933.2	DSP	0.3705	0.2411
Keratin, type II cytoskeletal 1	00220327.3	KRT1	0.2214	
Dynein heavy chain 5, axonemal	00152653.3	DNAH5	0	
hnRNP R, isoform 1	00644055.3	HNRNPR	0	
Serpin H1	00032140.4	SERPINH1	0	

An example of the reporter region of an MS/MS spectrum of a peptide from hnRNP R isoform 1 obtained on the ABI 4800 Proteomics Analyzer can be seen in Figure 17. The lack of a signal from the 119 reporter ion in this spectrum demonstrates this peptide is not present in the NMP isolation from MCF-7/LY2 cells. This is represented by the ratio of 0 seen in Table 6 for MCF-7/LY2:MCF-7.

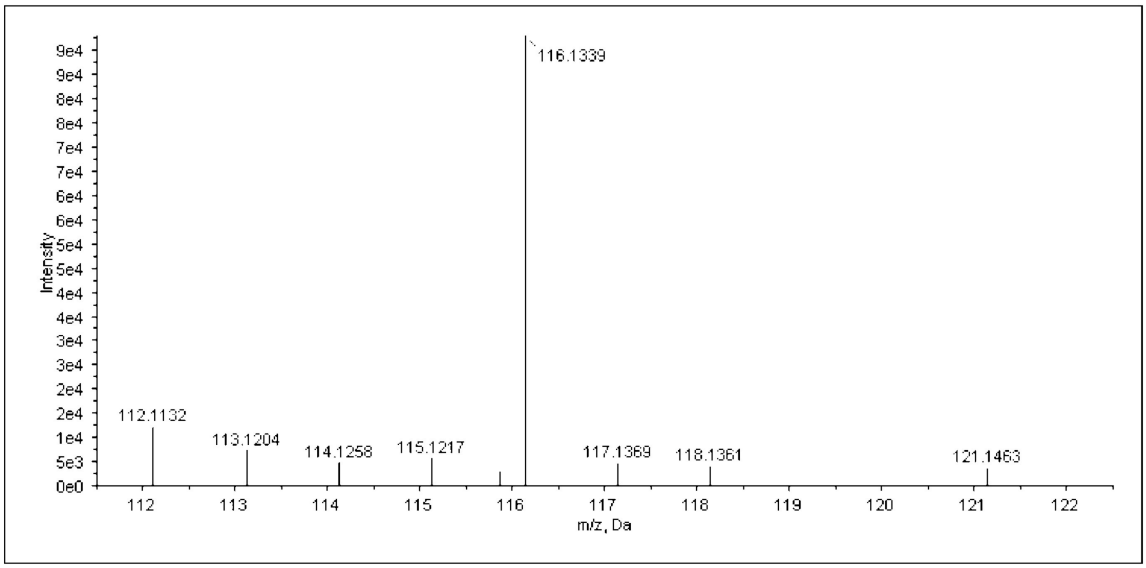

Figure 17: iTRAQ reporter region of an MS/MS spectrum from a peptide identified as hnRNP R.

There is no peak present at 119, which corresponds to the isolation from MCF-7/LY2 cells. This spectrum was obtained on the ABI 4800 Proteomics Analyzer.

3.3.4 Nuclear Matrix Protein Abundance Levels Altered in MCF-7 and MCF-7/LY2 Cells in Response to PPT

In addition to understanding how the protein composition of the NM changes with antiestrogen resistance, it was also of interest to determine how the two isoforms of the ER differently influence the protein composition of the NM. In order to do this, the MCF-7 and MCF-7/LY2 cells were treated with one of three ER-subtype selective ligands at a concentration of 5 μM for 48 h or the DMSO vehicle control, followed by NM isolation. The first ligand, PPT, is a 410-fold selective agonist for ERα and does not stimulate transcription through ERβ (Stauffer, 2000).

Table 16 in Appendix C presents 30 NMPs with altered levels of abundance in MCF-7 cells in response to PPT. Table 7 presents the proteins that were significantly altered when comparing abundance of NMPs in MCF-7 cells treated with PPT to those treated with the vehicle

control. Three proteins demonstrate a significantly increased abundance in MCF-7 cells in response to PPT.

Table 7: Statistically significant alterations to NMP abundance in MCF-7 cells in response to PPT.

Protein Name	Accession Number (IPI)	Gene Symbol	PPT : DMSO
Histone H3.1	00902514.1	HIST1H2AD	2.196
60S acidic ribosomal protein P1	00008527.3	RPLP1	2.100
TUBA1B protein	00793930.1	TUBA1B	1.739

Table 17 in Appendix C presents the eleven NMPs with altered levels of abundance in response to PPT in MCF-7/LY2 cells. No proteins in the NM of MCF-7/LY2 cells were significantly altered in response to PPT.

3.3.5 Nuclear Matrix Protein Abundance Levels Altered in MCF-7 and MCF-7/LY2 Cells in Response to MPP

MPP is an ERα-selective antagonist that binds ERα with about 200-fold more affinity than ERβ and suppresses E2-stimulation through ERα but not through ERβ (Sun, 2002). Table 18 in Appendix D presents forty-six NMPs with altered levels of abundance in MCF-7 cells in response to MPP. Table 8 presents the proteins that were significantly altered when comparing abundance of NMPs in MCF-7 cells treated with MPP to those treated with vehicle control. Fourteen proteins demonstrate an increased abundance and five proteins demonstrate a decreased abundance in the NM of MCF-7 cells in response to MPP. One of these proteins is NuMA, which with a ratio of 9999 was present in the NM of MCF-7 cells in response to MPP but absent in the vehicle-treated cells.

Table 8: Statistically significant alterations to NMP abundance in MCF-7 cells in response to MPP.

Protein Name	Accession Number (IPI)	Gene Symbol	MPP : DMSO	Std Dev
NUMA1 variant protein	00872028.2	NUMA1	9999	
Keratin, type I cytoskeletal 15	00290077.1	KRT15	141.5	
Dynein heavy chain 5, axonemal	00152653.3	DNAH5	49.53	
48 kDa protein	00879060.1	GCAT	47.36	
Epiplakin	00010951.2	EPPK1	42.24	
hnRNP R, isoform 1	00644055.3	HNRNPR	32.83	
Interferon-induced guanylate-binding protein 2	00848358.1	GBP2	27.45	
Cingulin-like protein 1, isoform 1	00307829.7	CGNL1	25.9	
Highly similar to AF4/FRM2 family member 1, CDNA FLJ61397	00396310.5	AFF1	21.10	
Tau-tubulin kinase	00217437.6	TTBK2	15.68	
Keratin 7	00847342.1	KRT7	10.86	
60S acidic ribosomal protein P1	00008527.3	RPLP1	4.651	
ATP synthase subunit alpha	00440493.2	ATP5A1	2.032	0.7981
40S ribosomal protein s20	00012493.1	RPS20	1.749	
Zinc finger protein 595	00478170.1	ZNF595	0.487	
hnRNPQ, isoform 2	00402182.2	SYNCRIP	0.4418	
hnRNP F	00003881.5	HNRNPF	0.4017	
Keratin, type I cytoskeletal 24	00004550.5	KRT24	0.2323	
Keratin, type I cytoskeletal 16	00217963.3	KRT16	0.1578	

Table 19 in Appendix D presents twenty-nine NMPs with altered levels of abundance in MCF-7/LY2 cells in response to MPP. Table 9 presents the proteins that were significantly altered when comparing abundance of NMPs in MCF-7/LY2 cells treated with MPP to those treated with vehicle control. Ten proteins demonstrate an increased abundance and one protein demonstrate a decreased abundance in the NM of MCF-7/LY2 cells in response to MPP. NuMA and dynein heavy chain 5 have ratios of 9999 meaning they were present in the NM of MCF-7/LY2 cells in response to MPP but absent in the vehicle treated cells.

Table 9: Statistically significant alterations to NMP abundance in MCF-7/LY2 cells in response to MPP.

Protein Name	Accession Number (IPI)	Gene Symbol	MPP : DMSO
Dynein heavy chain 5, axonemal	00152653.3	DNAH5	9999
hnRNP R, isoform 1	00644055.3	HNRNPR	9999
Zinc finger protein 595	00478170.1	ZNF595	2.988
60S acidic ribosomal protein P2	00008529.1	RPLP2	2.855
hnRNPA3, isoform 1	00419373.1	HNRNPA3	2.401
hnRNP A1, isoform A1-A	00215965.4	HNRNPA1	2.15
hnRNP A2/B1, Isoform B1	00396378.3	HNRNPA2B1	1.95
60S ribosomal protein L12, isoform 1	00024933.3	RPL12	1.846
hnRNPL, isoform a	00027834.3	HNRNPL	1.812
hnRNPQ, isoform 2	00402182.2	SYNCRIP	1.671
Interferon-induced guanylate-binding protein 2	00848358.1	GBP2	0.3863

3.3.6 Nuclear Matrix Protein Abundance Levels Altered in MCF-7 and MCF-7/LY2 Cells in Response to DPN

DPN is a selective ERβ agonist that binds to ERβ with 70-fold selectivity compared to ERα and it activates transcription through ERβ with 170-fold more potency than through ERα (Meyers, 2001). Table 20 in Appendix E presents forty NMPs with altered levels of abundance in the NM of MCF-7 cells in response to DPN. Table 10 presents the proteins that were significantly altered when comparing abundance of NMPs in the NM of MCF-7 cells treated with DPN to those treated with vehicle control. Eleven proteins demonstrate an increased abundance and two proteins demonstrate a decreased abundance in the NM of MCF-7 cells in response to DPN. One of these proteins is NuMA; with a ratio of 9999 NuMA is present in the NM of MCF-7 cells in response to DPN but not in the vehicle treated cells. Histone H2A type 1A with a ratio of 0 is no longer found in the NM of MCF-7 cells when treated with DPN.

Table 10: Statistically significant alterations to NMP abundance in MCF-7 cells in response to DPN.

Protein Name	Accession Number (IPI)	Gene Symbol	DPN : DMSO
NUMA1 variant protein	00872028.2	NUMA1	9999
48 kDa protein	00879060.1	GCAT	5.748
Cingulin-like protein 1, isoform 1	00307829.7	CGNL1	3.542
60S ribosomal protein L12, isoform 1	00024933.3	RPL12	3.531
Interferon-induced guanylate-binding protein 2	00848358.1	GBP2	2.909
Keratin 7	00847342.1	KRT7	2.507
Highly similar to AF4/FRM2 family member 1, CDNA FLJ61397	00396310.5	AFF1	2.002
Histone H2B	00646240.3	HIST2H2BA	1.995
Putative Histone H2B type 2-C	00454695.4	HIST2H2BC	1.765
P37 AUF1	00903278.1	HNRNPD	1.748
51 kDa protein	00479191.2	HNRNPH1	1.707
hnRNP F	00003881.5	HNRNPF	0.4783
Enhancer of rudimentary homolog	00029631.1	ERH	0.343
Histone H2A type 1-A	00045109.3	HIST1H2AA	0

Table 21 in Appendix E presents forty-one NMPs with altered levels of abundance in MCF-7/LY2 cells in response to DPN. Table 11 presents the eight proteins that were significantly altered when comparing abundance of NMPs in the NM of MCF-7/LY2 cells treated with DPN to those treated with vehicle control. Six proteins demonstrate an increased abundance and two protein demonstrate a decreased abundance in the NM of MCF-7/LY2 cells in response to DPN. hnRNP R and dynein heavy chain 5 have ratios of 9999 meaning they were found in the NM of MCF-7/LY2 cells in response to DPN, while histone H2A type 1-A has a ratio of 0 meaning it was no longer found in the NM of MCF-7/LY2 cells in response to DPN.

Table 11: Statistically significant alterations to NMPs in MCF-7/LY2 cells in response to DPN.

Name	Accession Number (IPI)	Gene Symbol	DPN : DMSO	Std Dev
Dynein heavy chain 5, axonemal	00152653.3	DNAH5	9999	
hnRNP R, isoform 1	00644055.3	HNRNPR	9999	
Keratin, type II cytoskeletal 1	00220327.3	KRT1	4.0085	
Interferon-induced guanylate-binding protein 2	00848358.1	GBP2	1.843	
Keratin, Type II Cytoskeletal 19	00479145.2	KRT19	1.842	1.937
Putative elongation factor 1-alpha-like 3	00472724.1	EEF1A1	1.769	
Histone H2B	00646240.3	HIST2H2BA	0.4359	
Histone H2A type 1-A	00045109.3	HIST1H2AA	0	

3.3.7 Western Blot Validation

In order to validate the data obtained using the iTRAQ methodology, a second NM isolation was performed on MCF-7 and MCF-7/LY2 cells creating a biological replicate. Western blotting was then performed using antibodies for several of the proteins quantification was obtained for in Table 6. The Western blots for these proteins are shown in Figure 18. Additionally the ratios provided by iTRAQ for these proteins is seen below in Table 12.

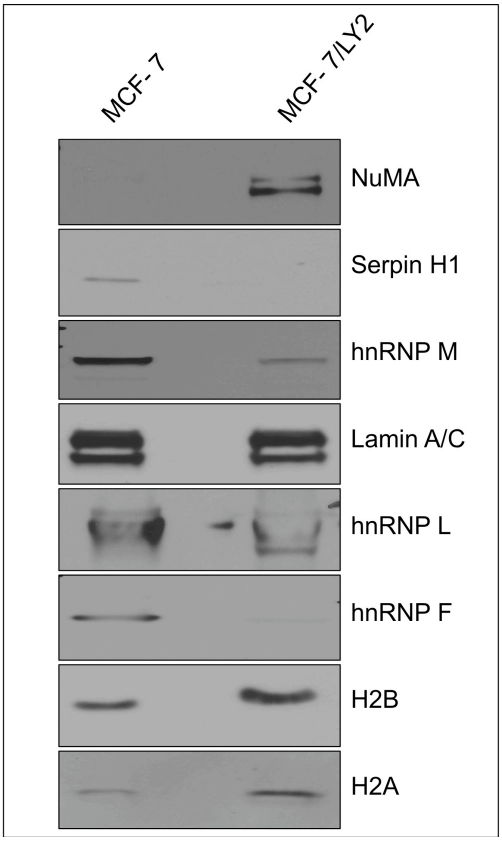

Figure 18: Western blot validation of NMPs quantified by iTRAQ.

Several of the proteins quantified in NMP preparations from MCF-7 and MCF-7/LY2 cells were verified using Western blot analysis. A second NMP isolation was performed to generate a biological replicate and Western blot analysis with the appropriate antibody was performed. Table 12 gives the iTRAQ ratios obtained for these proteins.

Table 12: iTRAQ ratios obtained for NMPs validated by Western blotting in Figure 18.

Protein	MCF-7/LY2 :MCF7
NuMA	9999
Serpin H1	0
hnRNP M	0.7657
Lamin A/C	1.203
hnRNP L	0.7024
hnRNP F	0.5719
H2B	2.301
H2A	1.595

3.3.8 Comparison of the Different Workflows

Figure 11 shows the three different workflows used in this study. Within these three workflows, there were two separate labelings performed, in which a different label was used on each sample to account for any label specific effects. For the first set of labeling, the peptides were fractionated using SCX. The first workflow involved analysis by nano-LC-MALDI-TOF/TOF with the ABI 4700 mass spectrometer. The second workflow involved the same SCX fractionation, but then nano-LC ESI Q-TOF was performed with the ABI QSTAR Elite mass spectrometer. The third workflow used the second set of labeled samples and fractionated using OFFGEL electrophoresis followed by nano-LC-MALDI-TOF/TOF with the ABI 4800 mass spectrometer.

The first workflow using SCX spin column fractionation and the ABI 4700 gave a total of thirty proteins with a ProtScore > 1.3 (95% confidence). Of these NMPs, thirteen were identified from at least two distinct peptides with 95% confidence. A total of 16,130 MS/MS spectra were searched and quantified in this workflow. In the second workflow, using the SCX spin column fractionation and the QSTAR, sixty-nine NMPs with a ProtScore > 1.3 (95% confidence) were identified. Of these NMPs, twenty-two were identified from at least two distinct peptides with 95% confidence. A total of 69,094 MS/MS spectra were searched and quantified in this workflow. With the third workflow, using the OFFGEL electrophoresis and 4800, 99 NMPs with a ProtScore > 1.3 (95% confidence) were identified. Of these NMPs, forty-eight were identified from at least two distinct peptides with 95% confidence. A total of 63,049 MS/MS spectra were searched and quantified in this workflow.

Eleven NMPs were identified by all three workflows with a ProtScore $\geq$ 1.3. Thirty-nine NMPs were identified in at least two workflows with a ProtScore $\geq$ 1.3, and 109 NMPs were identified by only one workflow. A Venn diagram demonstrating the number of NMPs identified in each of the workflows can be seen in Figure 19.

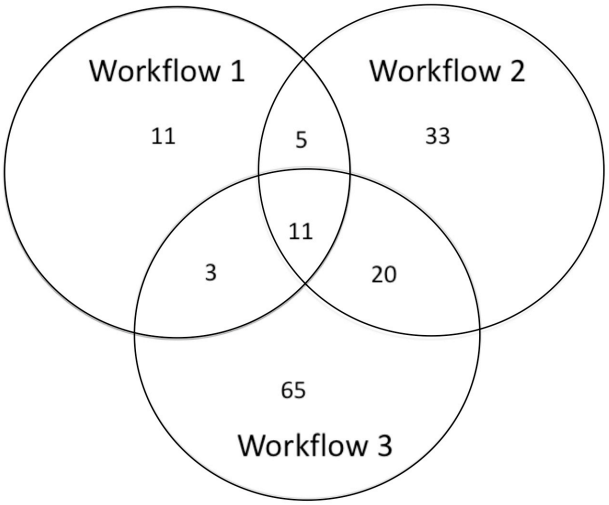

Figure 19: Protein identifications corresponding to the three different workflows used.

This Venn diagram demonstrates how the 148 NMPs were identified by each of the three different workflows. Workflow 1 involved the SCX spin column fractionation and analysis with the ABI 4700 Proteomics Analyzer. Workflow 2 involved the SCX spin column fractionation and analysis with the ABI QSTAR Elite. Workflow 3 involved the OFFGEL fractionation and analysis with the ABI 4800 Proteomics Analyzer.

3.4 DISCUSSION

The antiestrogen resistant cell line, MCF-7/LY2, maintains expression of ERα but does not express significant levels of ERβ compared to the parental MCF-7 cells (Figure 12). The loss of ERβ expression in MCF-7/LY2 corroborates studies suggesting that low levels of ERβ are predictive of antiestrogen resistance (Hopp, 2004; Esslimani-Sahla, 2004). Since ERβ has a

negative influence on the transcription of ERα-regulated genes, the loss of ERβ expression in tamoxifen resistance allows ERα to overcome this repression (Sugiura, 2007).

This study is the most comprehensive examination to date of the NM proteome in breast cancer. Most studies of the NM in breast cancer describe differences between spots on two-dimensional gels, but the identification of these spots is lacking. In one study that examined the NM in breast cancer, a two-dimensional gel of NMPs isolated from MCF7 breast cancer cells revealed fifty-six protein spots. Three of these spots were identified as Lamins A, B, and C, and many of the RNP complex proteins were present on the gel. Despite attempts to remove the IFs from the preparation, cytokeratins 8, 18 and 19 were the top identifications. Actin was also seen in the gel (Fey, 1988). The iTRAQ analysis of the NM in MCF-7 cells agrees with this study, as cytokeratins 8, 18, and 19 were the top hits. Actin was also observed. Cytokeratins 8, 18 and 19 were also previously demonstrated to be expressed at higher levels in an estrogen-independent breast cancer cell line compared to an estrogen-dependent line. These three cytokeratins were shown to be estrogen regulated (Coutts, 1996). Of these three cytokeratins, cytokeratin 8 is significantly less abundant in the NM of MCF-7/LY2 resistant cells compared to MCF-7 responsive cells. This cytokeratin may play a role in the ability of an antiestrogen to act on a breast cancer cell and warrants further investigation.

Many other proteins that have never before been detected in the NM of MCF-7 cells were identified. ProteinCenter software was used to classify the NMPs identified into the gene ontology (GO) categories of cellular component and molecular function. Within cellular component, proteins from many different organelles were present in the NM. Nucleus was the most abundant category, but cytoplasm, membrane, cytoskeleton, and organelle lumen were also strongly represented. It is likely that in these MCF-7 breast cancer cells, proteins that are not

normally found in the NM are being retained by the structure. If one of these proteins is specific to breast cancer it may be very useful as a biomarker. Protein binding, nucleotide binding, DNA binding, and RNA binding were the top molecular functions assigned to the NMPs identified in MCF-7 cells. This reinforces the idea that the proteins of the NM interact with DNA, RNA, and transcription factors to regulate gene expression.

The proteins that have the potential to serve as biomarkers for tamoxifen resistance are those with significant alterations in antiestrogen resistant cells. There are several of these proteins in MCF-7/LY2 cells and they should be investigated in other antiestrogen resistant cell lines and tissue samples. NuMA (nuclear mitotic apparatus) is not found in the NM of MCF-7 cells, but it is present in the NM of resistant MCF-7/LY2 cells. NuMA was identified in 1980 and determined to function as an NMP in interphase that plays a role in microtubule organization around centrosomes during mitosis (Lyderson, 1980). NuMA moves from the nucleus of interphase poles to the spindle poles of mitotic cells (Saredi, 1997). NuMA is bound to small nuclear ribonucleoprotein particles and may connect RNA metabolism to the NM (Zeng, 1994). NuMa's localization patterns differ from diffuse nuclear staining to punctate staining, and this staining pattern has been attributed to different functions of the protein depending upon cell type (Zeng, 2000). The NuMA region on chromosome 11q13 is a candidate for breast cancer susceptibility (Kammerer, 2005). When confluent MCF-7 cells are cultured long-term, they no longer express NuMA in the nucleus (Taimen, 2000). NuMA associates with the NM in estrogen-responsive MCF-7 cells and disperses into the cytoplasm during the onset of mitosis (Gobert, 2001). NuMA is an interesting protein because its ability to control the proliferation of cancer cells is influenced by environmental factors and depending on external stimuli NuMA may participate in cell division or apoptosis. Relevant to breast cancer is the fact that NuMA

expression is regulated by hormones (Yam, 1998). The NM of antiestrogen resistant MCF-7/LY2 cells contains NuMA while the NM of antiestrogen responsive MCF-7 cells lacks this protein. This is worth further investigation as it provides insight into the mechanism of antiestrogen resistance, and the difference seen between responsive and resistant cells may mean NuMA is a biomarker for determining when to stop tamoxifen treatment. NuMA abundance in the other protein fractions generated during NM preparation should be determined in order to confirm that NuMA is altered specifically in the NM or whether it is a global change in the cell.

Three proteins are present in the NM of MCF-7 cells, but absent in the NM of antiestrogen resistant MCF-7/LY2 cells. These proteins are dynein heavy chain 5, serpin H1, and hnRNP R. Dynein is a cytoskeletal motor protein consisting of several different components, and the movement of this protein is produced by the heavy chain component of the protein (Asai, 2001). Dynein heavy chain 5 is an axonemal dynein, and is a component of the axoneme, or central cytoskeletal core of a cilium. This particular isoform of dynein has only been studied in primary ciliary dyskinesia, which is a disease characterized by dysfunctioning motile cilia and flagella. Recurrent respiratory infections and reduced fertility in males are often observed with the disease. One of the major causes of this disease is mutations in the dynein heavy chain 5 (Hornef, 2006). Therefore it is very novel to find this axonemal dynein in the NM of breast cancer cells. Specific loss of dynein heavy chain 5 in tamoxifen resistant cells demonstrates its potential as a biomarker. Other components of the dynein complex have been investigated in breast cancer. Dynein light chain 1 is known to promote the growth of breast cancer cells and plays a role in estrogen receptor signaling (Rayala, 2005).

Serpin H1 is also known as HSP47. HSP47 is associated with the binding and processing of collagens in the endoplasmic reticulum (Sauk, 2005). This protein is overexpressed in

pancreatic cancer, osetosarcomas and squamous cell carcinoma of the head and neck (Maitra, 2002; Uozaki, 2000; Poschmann, 2009). This is the first report of any alteration to the protein in breast cancer. Further investigation into HSP47's role in breast cancer is necessary, as it may play an important role based on its specific expression loss in the NM of antiestrogen resistant cells.

hnRNP proteins are RNA-binding proteins. They were first described as a family of proteins that bind RNA polymerase II transcripts to form hnRNP particles. Originally it was thought the complex consisted of only six proteins, but additional factors have since been identified (Choi, 1984; Carpenter, 2006). Thirty spots are observed on a two dimensional gel when the immunopurified complex is run (Pinol-Roma, 1988). A variety of functions have been attributed to the hnRNP proteins, including roles in both DNA and RNA regulation. Because of their involvement in these fundamental cell processes, several of these proteins have been proposed to play roles in tumor development (Carpenter, 2006). hnRNP R is one of the least studied members of the family. Recently, hnRNP R was demonstrated to enhance transcription of the proto-oncogene c-fos. This supports the emerging view that transcription is tightly coupled to subsequent RNA metabolism (Fukuda, 2009). There is still much to determine about hnRNP R's role, but its absence in the NM of antiestrogen resistant breast cancer cells suggests it may play a role in ER signaling.

PPT, the ERα-selective agonist, has very little effect on the composition of the NM of either of the cell lines. In MCF-7 calls, PPT significantly increased the abundance of three proteins in the NM, but no NMPs were effected in MCF-7/LY2 cells. PPT has a very strong affinity for ERα with a K_i of 0.54 nM (Stauffer, 2000). It may be that when activated by PPT, ERα does not interact strongly with the NM. Other ERα-selective agonists should be used in

order to determine if this is a compound or receptor specific phenomenon. MPP demonstrates the largest effect of the subtype selective ligands on the NMPs in both MCF-7 and MCF-7/LY2 cells. MPP has a K_i of 2.7 nM for ERα. MPP does not bind to ERα as strongly as PPT, but it functions as an antagonist and alters the confirmation of the receptor in a different way. The compound also does have some affinity for ERβ with a K_i of 1800 nM (Sun, 2002). It may be that MPP has a greater effect on the composition of the NM in MCF-7 cells compared to MCF-7/LY2 cells, because this cell line retains expression of both ER isoforms. In MCF-7 cells, NuMA is present in the NM upon treatment with MPP. This supports the idea that NuMA's interactions with the NM are hormone-regulated. Further investigation should be done to understand how the different ER isoforms influence NuMA to determine its function in breast cancer and possible role as a biomarker. Dynein heavy chain 5 and hnRNP R were not present in the NM of MCF-7/LY2 cells until the cells were treated with MPP. Since these cells do not express ERβ, this response is likely a result of MPP's interaction with ERα. These proteins warrant further investigation as they may be specifically regulated in the NM by ERα.

DPN, the ERβ-selective agonist, impacted the NM composition of both cell lines somewhat. Since it is an ERβ-selective ligand, it is interesting to see it exerting an effect in MCF-7/LY2 cells, which lack this isoform of the receptor. DPN does have considerable activity on ERα though, demonstrating an EC_{50} of 66 nM for ERα in a luciferase reporter assay (Meyers, 2001). As MPP did in MCF-7/LY2 cells, DPN also lead to the retention of dynein heavy chain 5 and hnRNP R in the NM. This further supports the localization of these proteins to the NM is effected by ER signaling. NuMA was found in the NM of the MCF-7 cells when they were treated with DPN, similar to what is seen with MPP. It is possible that MPP and DPN both interact with the NM in a similar way as they are sharing several effects in the cell lines

investigated. Further investigation into these mechanisms may help in tailoring antiestrogen therapies.

3.5 MATERIALS AND METHODS

3.5.1 Cell Culture

MCF-7 and MCF-7/LY2 breast cancer cells were obtained from Dr. Marc E. Lippman. The generation of the MCF-7/LY2 cell line can be seen in Bronzert DA *et al*. (Bronzert, 1985). The cells were maintained in phenol red-free RPMI-1640 with 10% charcoal-dextran stripped FBS. 2,3-bis(4-hydroxyphenyl)propionitrile (DPN) and propylpyrazole (PPT) were obtained from Tocris Bioscience. Methyl-piperidinopyrazole (MPP) was obtained from Sigma Aldrich. Stock solutions (10 mM) of each compound were made in DMSO. Cells were treated with the appropriate compound at a concentration of 5 μM for 48 hours.

3.5.2 Nuclear Matrix Isolation

The NM was isolated according to the method of Fey and Penman (Fey, 1988). Briefly, 10,000,000 to 50,000,000 cells were incubated in 0.5% Triton X-100 in a buffered solution with 2 mM vanadyl ribonucleoside, an RNase inhibitor, for 10 min on ice to release lipids and soluble proteins. Remaining sample was then pelleted at 1800 rpm at 4°C for 10 min and incubated in ammonium sulfate (0.25 M) with 2 mM vanadyl ribonucleoside for 10 min on ice. This step was performed as a salt extraction to release soluble cytoskeletal elements. The remaining sample

was then pelleted at 1800 rpm at 4°C for 10 min. Dnase I treatment was then added to remove soluble chromatin for 30 min at room temperature and then the sample was pelleted at 2200 rpm at 4°C for 10 min. RNase A was then added to remove RNA with a 10 min incubation at room temperature and then the sample was pelleted at 2200 rpm at 4°C for 10 min. The intermediate filaments and NMPs were then disassembled with 8 M urea and the insoluble carbohydrates and extracellular matrix components were pelleted with ultracentrifugation at 50,000 rpm for 1 h at 15°C. Dialysis was performed overnight in an assembly buffer containing KCl and imidazole-HCl to remove the urea and reassemble the intermediate filaments. Ultracentrifugation at 45,000 rpm for 90 min at 20°C is then done to pellet out the intermediate filaments. The NMPs were precipitated with ethanol then quantified using the Coomassie (Bradford) Protein Assay (Thermo Scientific, Waltham, MA). All solutions contained 1 mM phenylmethylsulfonyl fluoride to inhibit serine proteases.

3.5.3 iTRAQ Labeling

The manufacturer's protocol for iTRAQ was followed (Applied Biosystems, Foster City, CA). Briefly, 60 μg of precipitated NMPs from the 8 different samples were each resuspended in 20 μL of Dissolution Buffer (0.5 M triethylammonium bicarbonate) with 1 μL of Denaturant (0.1% SDS). 2 μL of the Reducing Reagent, 5 mM tris(2-carboxyethyl) phosphine (TCEP), was then added to each sample and incubated at 60°C for 1 h. They were then alkylated with 1 μL of the Cysteine Blocking Reagent, 10 mM methyl methanethiosulfonate (MMTS), at room temperature for 10 min. Trypsin (10 μg) was then added to each sample and they were digested at 37°C overnight. The eight iTRAQ reagents were then added to the appropriate sample and incubated at room temperature for 2 h. After labeling, the eight samples were then pooled. Using the same

NM preparations, two aliquots of the NMPs were taken through the iTRAQ procedure with the only difference being the label that was used for each sample. The first set of labeling used was: 113 – MCF-7, DMSO; 114 – MCF-7/LY2, DMSO; 115 – MCF-7, PPT; 116 - MCF-7/LY2, PPT; 117 – MCF-7, MPP; 118 – MCF-7/LY2, MPP; 119 – MCF-7, DPN; 121 – MCF-7/LY2, DPN. The second set of labeling used was: 113 - MCF-7/LY2, DPN; 114 – MCF-7, DPN; 115 – MCF-7/LY2, MPP; 116 – MCF-7, MPP; 117 – MCF-7/LY2, PPT; 118 – MCF-7, PPT; 119 - MCF-7/LY2, DMSO; 121 – MCF-7, DMSO.

3.5.4 SCX Fractionation

The first set of the pooled iTRAQ samples was speed vacuumed dry, resuspended in 10 mM potassium phosphate, 20% ACN, pH 2.7, and fractionated using PolySULFOETHYL A macro spin columns (PolyLC, Columbia, MD). The column was first pre-conditioned with 10 mM potassium phosphate, 20% ACN, pH 2.7. The sample was then applied and washed. Increasing concentrations of KCl (20, 40, 60, 80, 100, 120, 140, 160, 180, 200, 225, 250, 275, 300, 350, 400, 450, and 500 mM) in 10 mM potassium phosphate with 20% ACN at pH 2.7 were then used to elute off the peptides. Each fraction was then desalted using a PepClean C-18 Spin Column (Pierce) according to the manufacturer's protocol. They were then resuspended in 0.1% TFA for nanoLC.

3.5.5 OFFGEL Fractionation

The second set of pooled iTRAQ samples was desalted using a SepPak and then speed vacuumed dry for OFFGEL fractionation. OFFGEL fractionation was performed according to the

manufacturer's guidelines with minor modifications as described. The 3100 OFFGEL Fractionater and the OFFGEL Kit pH 3-10 (Agilent Technologies, Santa Clara, CA) was used following a 24-well set up. An Immobiline DryStrip pH 3-10, 24 cm (GE Healthcare Bio-Sciences, Piscataway, NJ) was used instead of the strip provided in the kit. Fifteen minutes before sample loading, the gel strip was rehydrated in the assembled device with 40 µL OFFGEL Rehydration solution per well. The iTRAQ peptides were resuspended in the Peptide OFFGEL solution to a final volume of 3.6 mL. 150 µL of the diluted sample was distributed into the 24 wells. The default OFFGEL peptide 24 cm strip program on the instrument was used with a max current of 50 µA until 50 kVh was reached. The fractions were then recovered from each well. 150 µL of 50% MeOH, 0.1% TFA was then added back to each well and left on the benchtop for 20 min. This solution was then recovered and added back to the appropriate fraction and the entire sample was speed vacuumed dry and resuspended in 0.1% TFA for nanoLC.

3.5.6 Nano-LC-MALDI-TOF-TOF-MS with the ABI 4700 Proteomics Analyzer

The SCX-fractionated samples were loaded onto a RP LC-Packing Ultimate system (Dionex, Sunnyvale, CA). Samples were loaded onto a trap column (300 µm i.d. x 5 mm, PepMap 100 C_{18} material 5 µm, 100 Å) (Dionex, Sunnyvale, CA) and washed for 5 min with 2% ACN, 0.1% FA at a flow of 30 µL/min. They were then loaded onto an analytical column (75 µm i.d. x 100 mm, ProtePep II C_{18} material 5 µm, 300 Å) (New Objective, Woburn, MA) and fractionated using a gradient of 5-30% B in 95 minutes, 30-60% B in 50 minutes, and 60-100% B in 10 minutes at a flow rate of 300 nL/min. Solution A was 2% ACN, 0.1% TFA, and solution B was 80% ACN, 0.1% TFA with a flow rate of 300 nL/min. The Probot™ Micro Fraction Collector was used to collect 50 sec spots on the 192 well ABI 4700 metal target off-line. 5 min after

sample injection, the Probot™ was signaled to begin spotting. One target was used for each fraction from SCX. Once the LC run was complete, 10 mg/mL α-cyano-4-hydroxy cinnamic acid (CHCA) with 5 fmol of a 3 peptide calibration mix was spotted on top of each sample spot. For 4700 (Applied Biosystems, Foster City, CA) analysis, MS spectra were acquired from 900 to 4000 Da with a focus mass of 2500 Da. MS Processing was done using 2 of the 3 internal standards spiked into the matrix with a 5 ppm max outlier error. Up to 15 peaks with a S/N filter of 20 were selected for MS/MS. Peptide CID (air) was performed at 1 kV. The MS/MS default calibration was updated before each target was run by using a peptide in the calibration mix spots.

3.5.7 Nano-LC-ESI-Qq-TOF-MS with the ABI QSTAR Elite

The Ultimate 3000 RP-LC system (Dionex, Sunnyvale, CA) interfaced with the QSTAR Elite (Applied Biosystems, Foster City, CA) consisted of a trap column (300 μm i.d. x 5 mm, PepMap C_{18} 100 material 5 μm, 100 Å) (Dionex, Sunnyvale, CA) and an analytical column (75 μm i.d. x 100 mm, ProteoPep II C_{18} material 5 μm, 300 Å) (New Objective, Woburn, MA). Samples were loaded onto the trap column at 20 μL/min and washed for 10 min in 0.1% FA. They were then loaded onto the analytical column and resolved using a gradient of 5-30% B in 95 min, 30-60% B in 50 min, and 60-100% B in 10 min with a flow rate of 200 nL/min. Solution A was 2% ACN, 0.3% FA, and solution B was 80% ACN, 0.3% FA. The mass spectrometer was set up for information-dependent acquisition (IDA) mode with the scan cycles set up to perform a 1 s MS scan in the mass range of 300 – 1500 Da, followed by three MS/MS scans in the mass range of 100 – 1800 Da of the 3 most abundant ions with a +2 to +4 charge and above a 10 count

threshold for 2 s each. Dynamic exclusion was performed for 30 s with a ±50 amu mass tolerance.

3.5.8 Nano-LC-MALDI-TOF-TOF-MS with the ABI 4800 Proteomics Analyzer

For the samples fractionated by OFFGEL fractionation, they were further fractionated on an RP-LC Ultimate system (Dionex, Sunnyvale, CA). They were first loaded onto a trap column (300 μm i.d. x 5 mm, PepMap C_{18} 100 material 5 μm, 100 Å) (Dionex, Sunnyvale, CA) and washed for 10 min with 2% ACN, 0.1% TFA at a flow of 30 μL/min. They were then loaded onto an analytical column (75 μm i.d. x 150 mm, Pep Map C_{18} 100 material 3 μm, 100 Å) (Dionex, Sunnyvale, CA) and fractionated using a gradient of 5-30% B in 110 minutes, 30-60% B in 60 minutes, and 60-100% B in 10 minutes with a flow rate of 250 nL/min. Solution A was 5% ACN, 0.1% TFA, and solution B was 85% ACN, 5% IPA, and 0.1% TFA. 5 minutes after the sample injection, the Probot was signaled to start spotting. The Probot™ Micro Fraction Collector was used to collect 15 second spots on the ABI 4800 LC-MALDI (ABI, Foster City, CA) metal target in a 16 x 48 array. 5 min after the sample injection, the Probot™ was signaled to begin spotting. 768 spots were collected for each OFFGEL fraction, and 2 LC runs were done on each target. This resulted in a total of 12 plates. The μTee mixer was used to co-spot matrix (7 mg CHCA in 1 mL of 50% ACN, 0.1% TFA, with mM ammonium citrate and 10 fmol of angiotensin II), delivered at a flow rate of 1.577 μL/min. For 4800 (ABI, Foster City, CA) analysis, MS spectra were acquired from 900 to 4000 Da with a focus mass of 2000 Da. MS processing was done using the Angiotensin II internal standard with a 250 ppm max outlier error. Up to 10 peaks were selected for MS/MS. Peptide CID (air) was performed at 2 kV.

3.5.9 Protein Identification and Quantification

The Paragon algorithm in ProteinPilot™ Software 2.0 (Applied Biosystems, Foster City, CA) was used for protein identification for all three of the workflows followed. Proteins were identified by searching against the IPI database. For the 4700 Proteomics Analyzer, v 3.49 was used. For the QSTAR Elite, v 3.58 was used. For the 4800 Proteomics Analyzer, v 3.46 was used. Searched results were processed by the Pro Group algorithm. Search parameters included iTRAQ labeling of the N-terminus and lysine residues, cysteine modification by MMTS, and digestion by trypsin. Isoform specific identification and quantification was done by excluding all shared peptides and including only unique peptides. Proteins identified with >95% confidence or ProtScore $\geq$ 1.3 were used for further analysis. The p-value calculated by the software was used to determine if the change in protein expression was real or not. This p-value tests the null hypothesis, the actual protein ratio is 1 and the observed protein ratio is different than 1 only by chance. Cut-off values for statistically significant alterations were determined by calculating the mean of all ratios obtained and moving two standard deviations away from this mean. Proteins that met these two stipulations were analyzed using ProteinCenter (Proxeon, Cambridge, MA).

4.0 ALTERATIONS TO THE NUCLEAR MATRIX IN DUCTAL CARCINOMA *IN SITU*

4.1 ABSTRACT

DCIS is the earliest identifiable breast cancer lesion. It is a pre-invasive malignancy that may or may not progress to invasive disease. There is no true understanding as to why and what cases of DCIS will progress to invasive breast cancer. DCIS is not easy to study, as there are no commercial cell lines available. The Latimer lab at the University of Pittsburgh Cancer Institute has recently developed a novel tissue engineering system that allows for the culture of both normal breast cells and early stage breast tumor cells, including DCIS, in an environment that is more similar to the *in vivo* environment than most tissue culture systems. The normal cells are able to form organotypic three-dimensional structures in the system. Using two of the normal breast reduction lines and one set of the DCIS lines, consisting of the tumor, the margin adjacent to the tumor, and the non-diseased contralateral lines the NM was investigated. NMPs are specifically altered in cancer and can be detected in the blood and urine of patients. Therefore identifying a NMP specifically altered in DCIS may help to create an early detection assay. Two NMPs, HSP90 and EEF1D, were altered in the DCIS series and warrant further investigation.

4.2 INTRODUCTION

In order to better understand the origins of breast cancer and work towards prevention, one must study the earliest stages of the disease. DCIS is the earliest identifiable breast cancer lesion. It is a pre-invasive malignancy that may or may not progress to an invasive disease. Around 53,000 women are expected to be diagnosed with DCIS in 2009. This represents 20-25% of breast cancer cases currently being diagnosed (American Cancer Society, 2009). It is the fourth leading cause of cancer in women in the United States. The detection of the disease has improved dramatically since the introduction of screening mammography. Treatment, which includes surgery and often radiation and/or tamoxifen therapy, is aimed at preventing the development of invasive disease. There is, however, no true understanding of the mechanisms that will cause DCIS progression to invasive disease (Kuerer, 2009). The University of Pittsburgh Medical Center reports a 20-25% ten year recurrence rate of breast CIS, both ductal and lobular. Therefore, the majority of patients diagnosed with DCIS are probably overtreated. An understanding of the basis of the disease and ways to identify those with the more aggressive form that will progress to invasive disease would be of great benefit to tailor treatment and avoid overtreating women who do not need it.

One of the major issues in studying DCIS is that there are currently no cell lines that represent this early form of breast cancer. The majority of breast cancer cell lines used in research are late stage tumors that have metastasized to the pleural sack around the lung. The most frequently studied breast cancer cell lines is MCF-7, originally developed by Dr. Herbert Soule at the Michigan Cancer Foundation in 1973 from a pleural effusion in a postmenopausal woman with metastatic breast cancer treated with hormones (steroids) and radiation (Soule, 1973). A problem using cell lines is that cell lines are prone to genotypic and phenotypic drift

during long-term culture, and this has been demonstrated to occur in the MCF-7 cell line. MCF-7 lines demonstrate different degrees of amplification of the oncogene N-*ras* (Graham, 1985). Karyotyping and restriction fragment length polymorphism analyses show an early passage MCF-7 from the Michigan Cancer Foundation and a later passage MCF-7 from the American Type Culture Collection (ATCC) likely came from different individuals (Graham, 1986). More MCF-7 lines were then analyzed, including several that were obtained from the Michigan Cancer Foundation at different time periods and one from the ATCC. The lines from the Michigan Cancer Foundation had similar chromosomal alterations and marker chromosomes; however, the ATCC line shares almost no chromosomal alterations with the other lines. In spite of the karyotypic differences these lines did appear morphologically similar. The ATCC line grows much slower than the other lines and it is not responsive to estrogen or antiestrogen treatment. Even the lines obtained from the same place, Michigan Cancer Foundation, but cultured in different labs, demonstrate unique biological properties, such as ER level, cell proliferation rates, and cloning efficiency despite having similar karyotypes (Osborne, 1987). More recent studies using comparative genomic hybridization (CGH) and fluorescent *in situ* hybridization have demonstrated that MCF-7 lines from different labs have undergone unique changes (Jones, 2000; Wenger, 2004; Bahia, 2002). These changes could have resulted from clonal evolution under different culture conditions, inherent genetic instability of cells in long-term culture, or contamination with another cell line (Osborne, 1987). Therefore it is hard to compare the results different labs obtain using different variants of the MCF-7 cells. Additionally, this line came from a pleural effusion in a late stage case, therefore it is likely very different from the original cells in the early primary tumor. Lines more representative of what occurs in the breast *in vivo* and representative of the earlier stages of the disease are needed.

The recently developed tissue engineering system for culture of human mammary epithelial cells (HMEC) generated by Dr. Jean Latimer's laboratory allows for the culture of both normal breast cells and early breast tumor cells in an environment more representative of the human breast. A schematic of this method for non-diseased breast can be seen in Figure 20. It involves the disaggregation of the tissue in a medium that is adapted from media used in stem cell culture (Latimer, 2002). A diluted form (1:1) of Matrigel is used to create a substratum for the tissue. Initially, the system contains cell types from the stroma, epithelial, myoepithelial cells and adipose compartments of the breast. This maintains the paracrine and juxtacrine factors the cells see *in vivo*. The minced tissue adheres to the substratum within 24 to 48 hours. Within three days, the living cells appear as monolayer outgrowths of multiple cell types, epithelial and fibroblastic. After 10-11 days, there is a marked increase in the proliferation and migration of both cell populations. The first recognizable three-dimensional structure the cells form is an episphere. This is a cluster of 20-100 epithelial cells in which only the bottom of layer of cells is in contact with the Matrigel. These epispheres then differentiate into complex organotypic branching ducts and lobules. These structures demonstrate Epithelial Specific Antigen (ESA) staining, cytokeratin (CK)-18 and -19 staining, lumen, polarized nuclei, desmosomes along lateral cell surfaces, microvilli on apical surfaces and β-casein secretion into the lumen. The system allows normal cells to form organotypic structures (Johnson, 2006). 39 out of 39 primary HMEC cultures have been established by the Latimer lab including tissue from European derived white women, African American women, Middle Eastern women and one Native American woman.

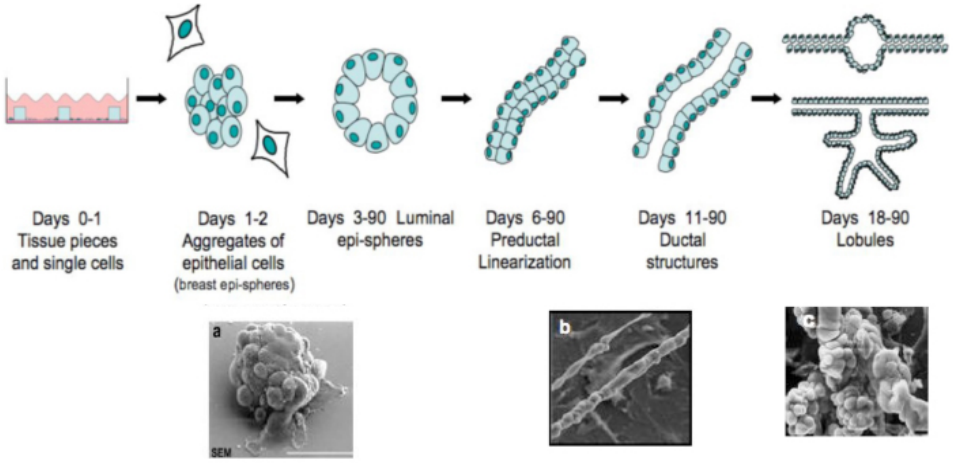

Figure 20: The Latimer tissue engineering system for the culture of Human Mammary Epithelial Cells.

The cells begin by forming epispheres (a) and then proceed to form organotypic ducts (b) and lobules (c). The flasks used are coated with a thin layer of Matrigel.

Cell lines have been established from this tissue engineering system. Using conservative trypsinization, the primary cell cultures of breast reduction epithelium were passaged out to passage thirty and beyond without the use of any transformation agents. Figure 21 shows the generation of a cell line using the Latimer system. The primary explant culture is trypsinized off of the chamber slide into a flask where it is considered an extended explant culture up to thirteen passages, at which point it is now considered a cell line. These cell lines are more heterogeneous than the commercial lines that are available. Some of the non-diseased cell lines are able to reiterate the ductal structure seen in the breast (Johnson, 2006).

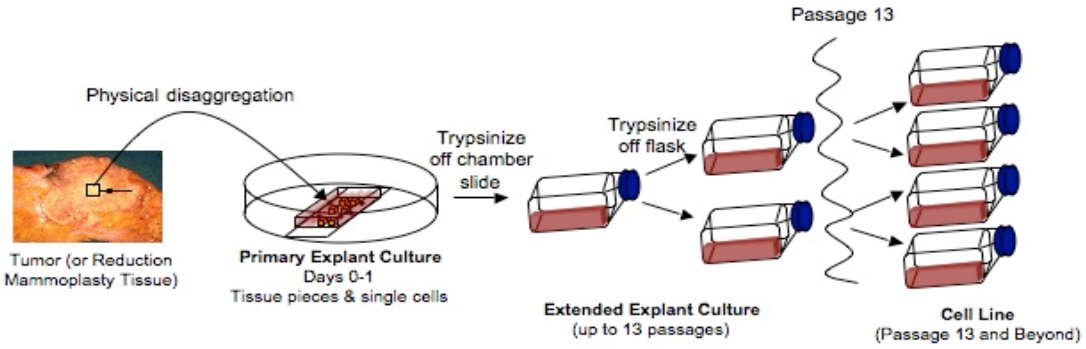

Figure 21: Generation of cell lines using the Latimer tissue engineering system.

Cell lines are generated by performing conservative trypsinization. The primary explant is made on a chamber slide and is then trypsinized into a flask where it is considered an extended explant up to thirteen passages. After passage thirteen it is then considered a cell line.

Cell lines are advantageous because they are renewable resources and provide fresh, intact samples for proteins and nucleic acids for research. They can also be experimentally manipulated. The Latimer lab offers these lines that provide access to samples from breast tissue that were never available before. Additionally the cells behave more like they would *in vivo* in this system.

All thirty-nine of the primary HMEC cultures have originated cell lines. Many of these breast reduction cell lines maintain a normal karyotype. The karyotype of JLBRL- (breast reduction line) 14, one of the normal lines used in this study, is shown in Figure 22. Karyotyping was performed by Suzanne Gollin and Sharon Wenger.

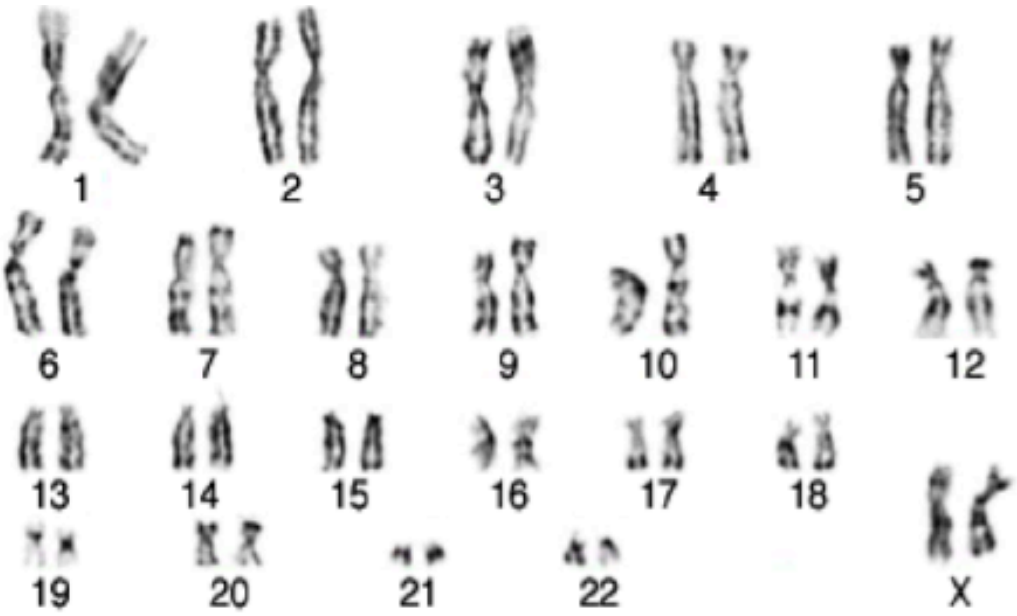

Figure 22: The karyotype of JLBRL-14.

This is one of the normal breast reduction lines generated using the Latimer tissue engineering system. It displays a normal 46, XX karyotype.

The Latimer tissue engineering system also allows for the development of tumor lines, including DCIS. Currently, the Latimer lab has established 45 tumor lines ranging from stage 1 to 4 and six DCIS-derived cell lines along with their matching isogenic normal counterparts. These tumor cell lines do not demonstrate the structures formed by the normal breast reduction lines but rather a distinct tumor phenotype. These cultures do not contain the stromal elements but come from within the tumor where there is no possibility of stromal contamination. The culture system can culture both normal and tumor cell lines, which makes it an ideal experimental model for the study of transformation (Johnson, 2006). A table demonstrating what is known about several of the Latimer lines available for study compared to the commonly used commercial lines can be seen in Table 22 in Appendix F.

In this study, three different DCIS lines that came from one woman were investigated. The patient was a 39-year old woman with widespread ER+ DCIS and an 8 cm mass. The tumor line is designated JLDCIS-1A. A second line designated JLNTALDCIS-1 was derived from the margin adjacent to the tumor. The non-diseased contralateral (unaffected) breast line is designated JLDCIS-1Contra. The karyotypes of these three lines can be seen in Figures 23, 24, and 25, respectively. JLDCIS-1Contra displays a normal karyotype. JLNTALDCIS-1 has an extra copy of chromosome 17. JLDCIS-1A has an extra copy of 5q on chromosome 14. Two normal breast reduction lines were also used, JLBRL-14 and JLBRL-24. These lines were derived from breast reduction mammoplasties performed on pre-menopausal women. The normal karyotype of JLBRL-14 was discussed earlier and can be seen in Figure 22.

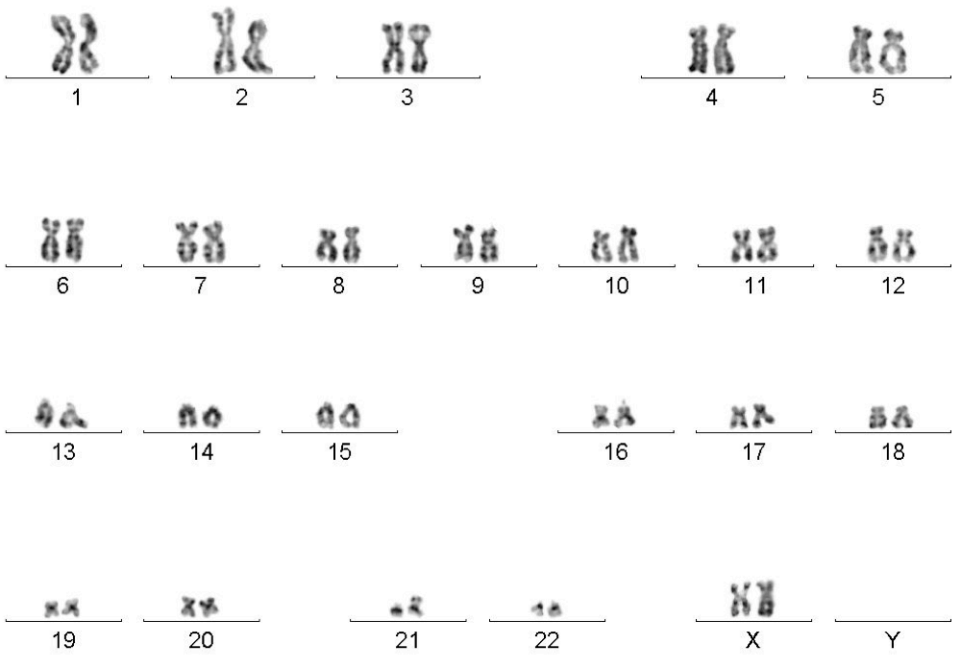

Figure 23: The karyotype of JLDCIS-1Contra.

This is the cell line developed from the contralateral, unaffected breast in a woman who had widespread ER+ DCIS. It displays a normal 46, XX karyotype.

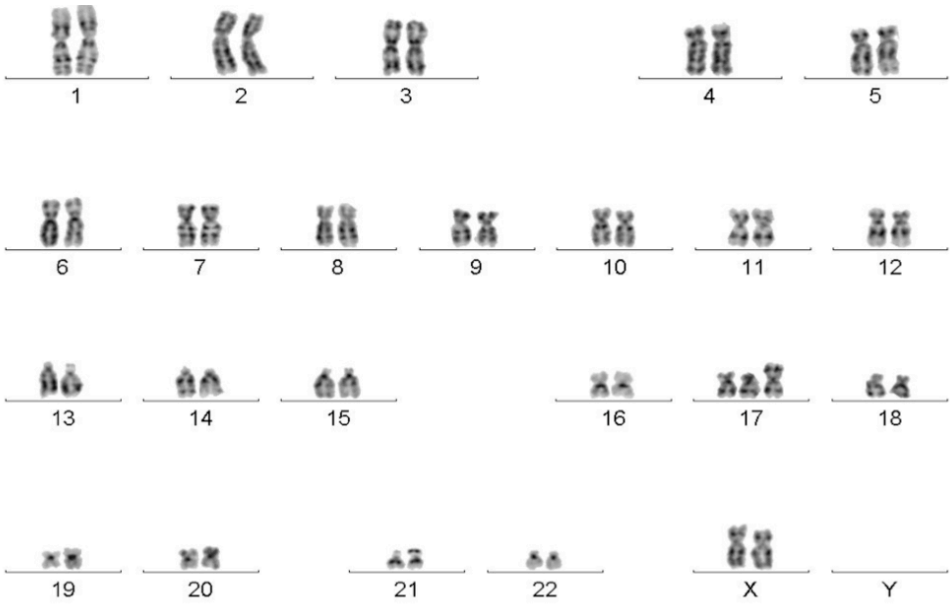

Figure 24: The karyotype of JLNTALDCIS-1.

This is the karyotype derived from the non-tumor adjacent tissue in the woman with widespread DCIS. The karyotype is: 47,XX,i(17)(q10)[3]/46.

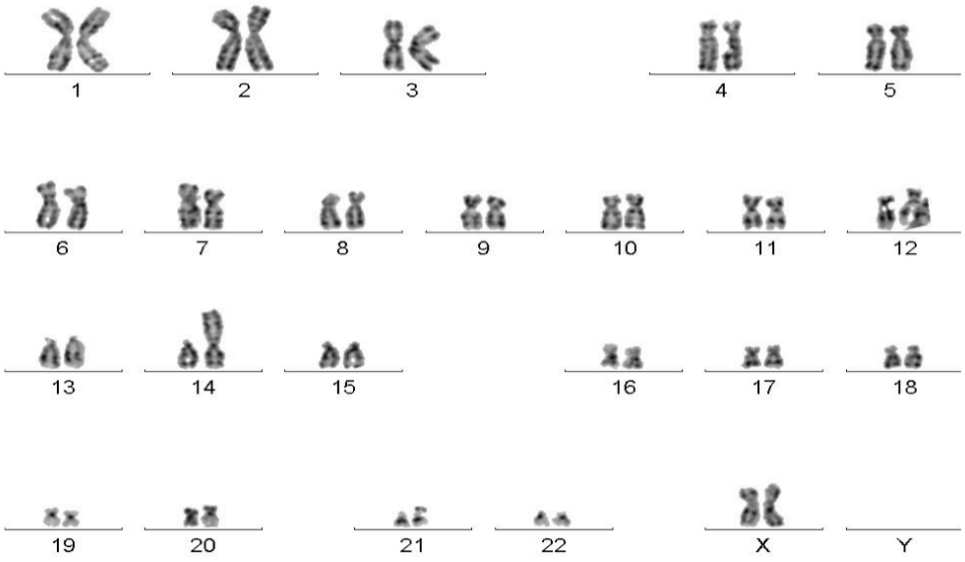

Figure 25: The karyotype of JLDCIS-1A.

This is the karyotype generated from the actual DCIS tumor. The karyotype is: 45, X, -X, der(14)t(5;14)(q11.2;p11.2)[3]/46,X,-X,der(14)t(5;14)(q11.2;p11.2)[3]/46, XX [10].

Expression microarray and supervised hierarchical clustering have been performed on many of the Latimer lab lines to compare them with the commonly used, commercial cell lines. Expression microarray was performed by the University of Pittsburgh Genomics core and analysis was performed by Dr. Stephen Grant and Tim Furphee. Clustering based on a set of 521 genes/probe sets based on replication can be seen in Figure 26. This clustering generates three major groups. The cluster on the far left contains eight distinct BRLs, some of which replicate runs were performed on, generated by the Latimer lab and includes the karyotypically normal contralateral line from the woman with DCIS, JLDCIS-1Contra, and the non-tumor adjacent line, JLNTALDCIS-1. The next closet cell lines are derived from stage I tumors, JLBTL (breast tumor line) -4 and -8, which flank the JLDCIS-1A line. Then finally is MCF-10A, an established, originally normal cell line (Soule, 1990). This line now has an abnormal karyotype (45-48,XX,i(1)(q10),-3,del(3)(p13),+4,der(9),der(9),+19 (Latimer, personal communication). This is the most abnormal line of this first cluster. The middle cluster contains three stage II derived cell lines, JLBTL-34, -7, and -10. These lines flank JLDCIS-4, which is a DCIS line with an invasive component. This patient had a palpable DCIS mass surrounding a 0.4 mm internal focus of microinvasion. The third cluster shows the commercially available stage IV pleural effusion cell lines along with JLBTL-12, which is a stage III cell line derived from the primary tumor site. Clustering based on a set of 811 genes/probe sets based on invasiveness can be seen in Figure 27. There are more clusters than there were in Figure 26, but the lines follow generally the same order as they did when clustered based upon replication. It is interesting to see just how different the Latimer lab lines are from the commercially available later-stage lines. These lines offer the opportunity to access cells in culture from normal breast tissue and early stage breast cancers.

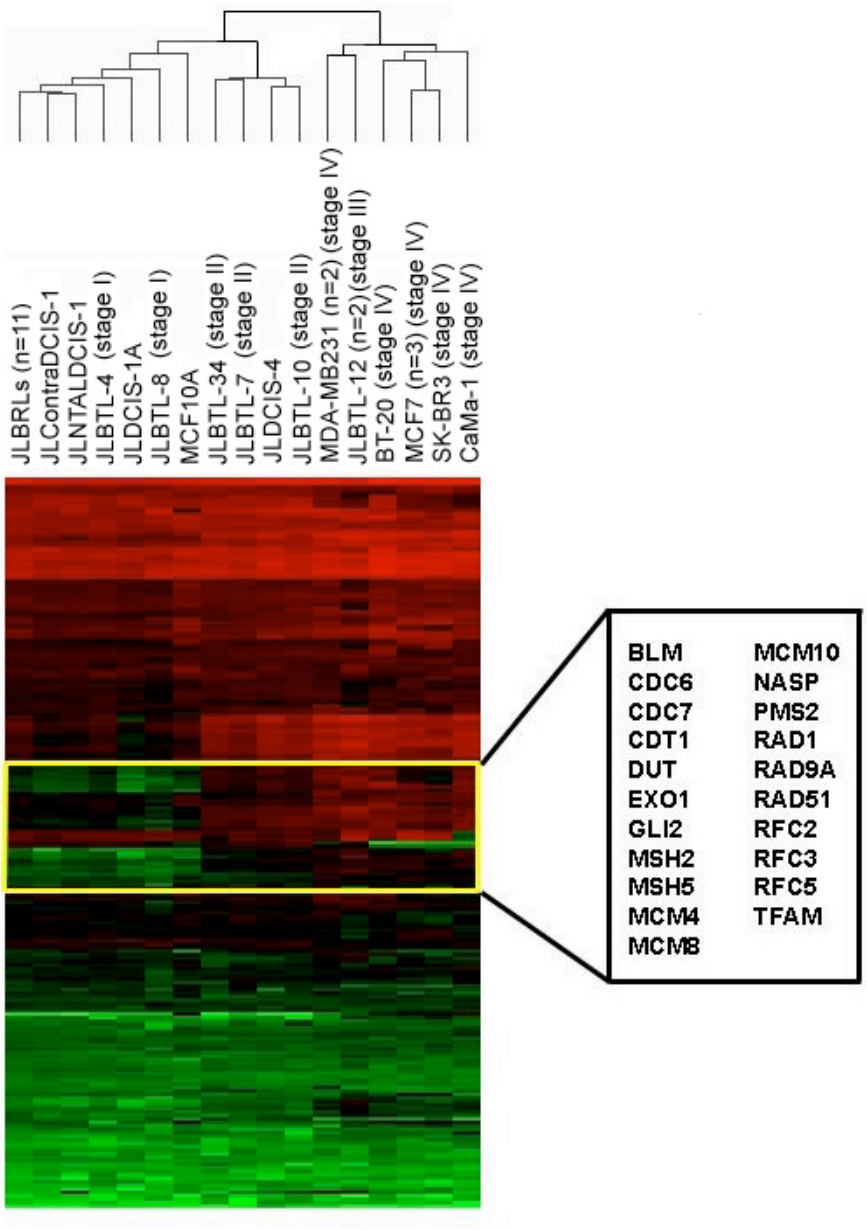

Figure 26: Latimer lines and commercial lines investigated by replication-based genes.

Supervised expression microarray with a probe set of 521 replication-based genes. The color bars are set so that the <5 percentile of expression are the brightest green and the >95 percentile of expression is the brightest red. The Affymeterix HGU133 Plus 2.0 Array is comprised of 51,000 probe sets.

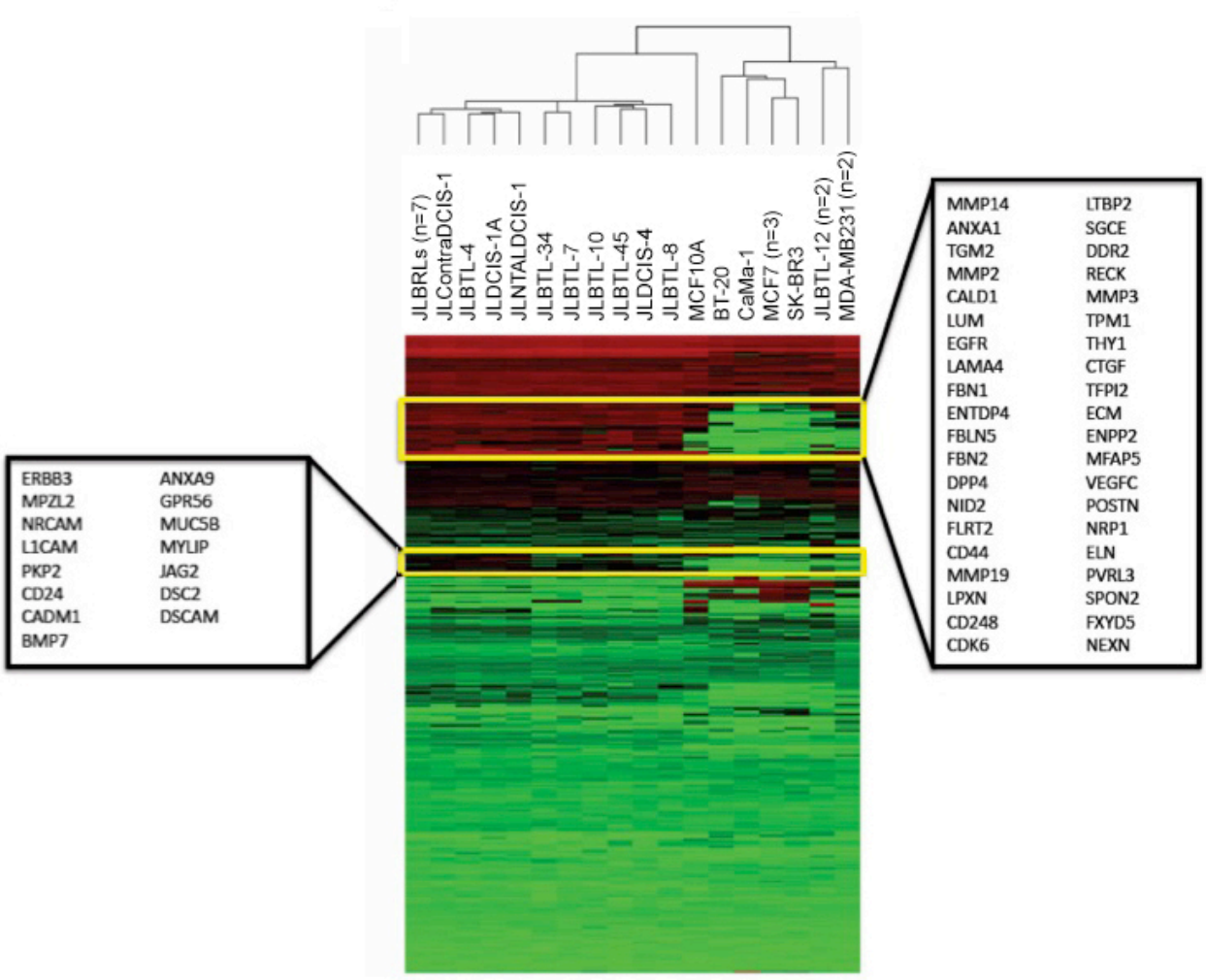

Figure 27: Latimer lines and commercial lines investigated by invasion-based genes.

Supervised expression microarray with a probe set of 811 invasion-based genes. The color bars are set so that the <5 percentile of expression are the brightest green and the >95 percentile of expression is the brightest red. The Affymeterix HGU133 Plus 2.0 Array is comprised of 51,000 probe sets.

In this study, the NM proteome of some of the Latimer lines was studied. Alterations to the NM have been examined before in breast cancer cell lines, however most of these studies were performed on late stage tumor samples or breast cancer cell lines (Samuel, 1997; Khanuja, 1993; Spencer, 2000; Spencer, 2001). Therefore many of the changes that occur in the NM during the early stages of tumor formation may have been missed. Investigating this early stage of the disease may allow for the identification of potential biomarkers and new tools for prevention of disease progression.

Characterization of the novel lines compared to traditional commercial lines was first done using the Transwell invasion assay. The JLDCIS-1 cell line series was used along with HT-1080, MCF-7, and MDA-MB231 cell lines. HT-1080 cells are a commonly used as a control in the assay. NMPs were then isolated from the JLDCIS-1 series along with JLBRL-14 and -24, MCF-7, and MDA-MB231 cells. The 8-plex iTRAQ proteomics technology was then used to identify and quantify the NMPs in these cell lines. Based upon how the JLDCIS-1 series behaved in the invasion assay and specific alterations seen in the NM of the cell lines compared to normal BRL lines, some understanding of the changes that occur in a cell to induce DCIS has been made. These specifically altered NMPs may serve as biomarkers of the disease or potential new therapeutic targets to treat breast cancer in its earliest stages.

4.3 RESULTS

4.3.1 Transwell Invasion Assay

The BD BioCoat Matrigel Invasion Assay studies the cellular invasion of both malignant and normal cells (Albini, 2004). The assay uses an 8-micron pore size PET membrane, which is covered in a thin layer of Matrigel basement membrane matrix to occlude the pores and block the non-invasive cells from migrating through the membrane. Invasive cells enzymatically digest the Matrigel matrix and, in addition, migrate through the pores. The assay has been used to develop an orthotypic model for human bladder cancer (Dinney, 1995). It has also been used to investigate a series of breast cancer cell lines and demonstrated that MDA-MB231 cells were much more invasive than MCF-7 cells (Hughes, 2008).

The behavior of the isogenic JLDCIS-1 cell lines in this assay was determined. This includes the tumor line, JLDCIS-1A, the non-tumor adjacent line, JLNTALDCIS-1, and the contralateral, normal line, JLDCIS-1Contra. As a control for this assay a highly invasive human fibrosarcoma line, HT-1080, was used. The commonly used commercial breast cancer cell lines, MCF-7 and MDA-MB231, were also used. Migration was measured by the cells ability to move through the uncoated membrane, and invasion was measured by the cells ability to move through the membrane coated with matrigel. All cell counts were standardized to the average number of HT-1080 cells that migrated. Figure 28A contains the graph demonstrating the migration and invasion ability of each cell line expressed as a ratio to HT-1080 migration. The number of cells per 200x field were counted with three 200x fields taken for each filter. A total of three filters were counted for each line. Figure 28B shows the JLDCIS-1 series. MCF-7 cells, previously reported to scarcely migrate or invade, did not move much in this assay. MDA-MB231 cells did

migrate and were invasive, although slightly less than what has been reported in previous studies relative to HT-1080 (Hughes, 2008). MDA-MB231 migrates and invades similarly to JLDCIS-1A but more than JLNTALDCIS-1 ($p<0.01$), derived from the breast tissue adjacent to the tumor (though not proven to be tumor free) and JLDCIS-1Contra ($p<0.01$) (which was karotypically normal). JLDCIS-1A demonstrates migration and invasion that are significantly greater than JLNTALDCIS-1 and JLDCIS-1Contra. The migration and invasion of JLDCIS1-Contra and JLNTALDCIS-1 are not statistically significantly different from each other.

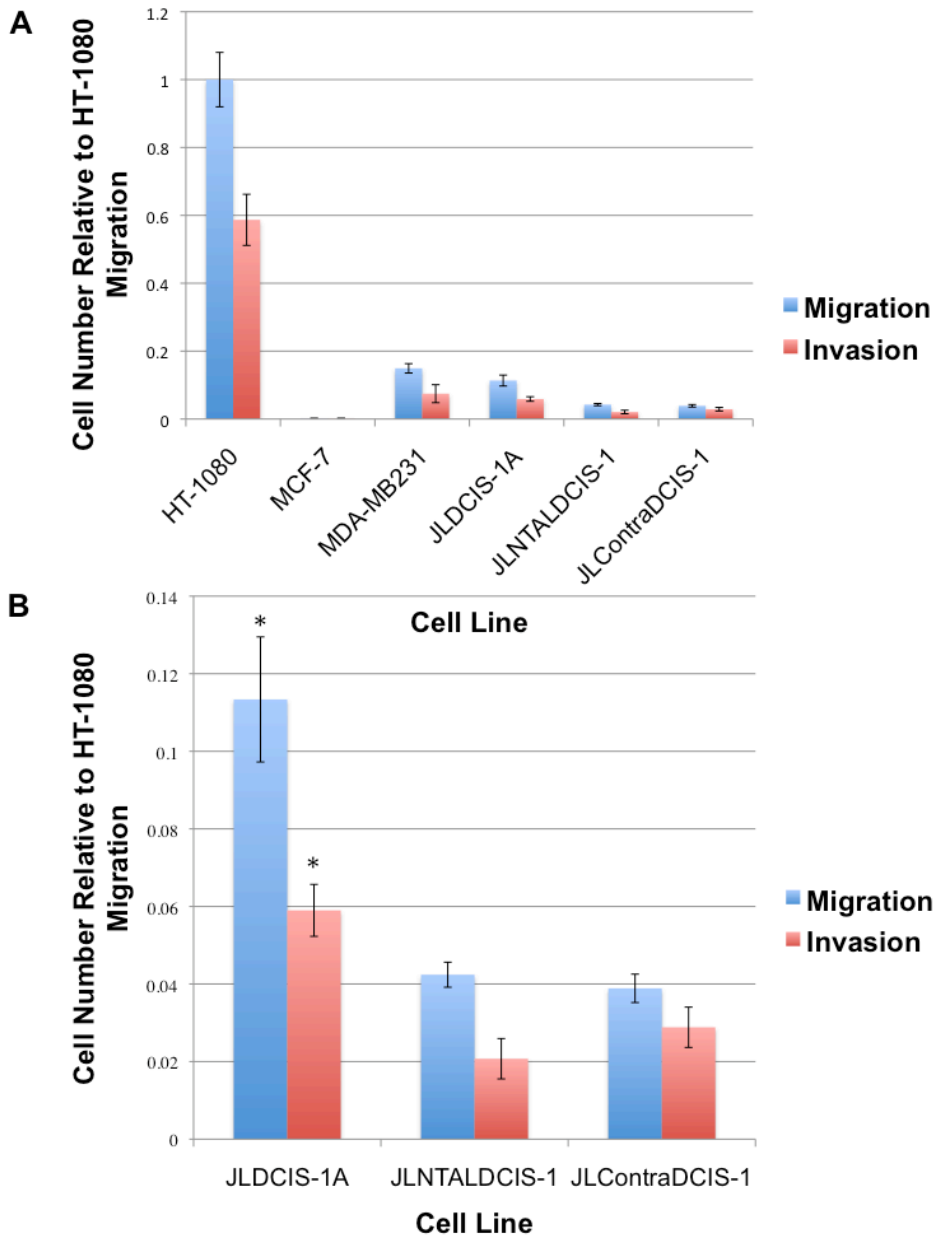

Figure 28: Migration and invasion data of DCIS1 series and HT-1080, MCF-7, MDA-MB-231 cell lines.

Migration was measured using uncoated control filters, while invasion was measured using Matrigel-coated filters. The average number of cells was determined using at least three filters with three fields of 200x counted per filter. All values are normalized to the number of migratory HT-1080 cells as an experimental standard. Error bars represent standard error of the mean. * denotes statistically significant difference from JLContraDCIS-1 and JLNTALDCIS-1 values with p-value < 0.01 using a Student's T-Test.

4.3.2 Protein Identification in the Nuclear Matrix of DCIS

Using iTRAQ with NMPs isolated from MDA-MB231, MCF-7, two breast reduction lines (JLBRL-14 and JLBRL-24), and the JLDCIS-1 series (JLDCIS-1A, JLNTALDCIS-1, and JLDCIS-1Contra), the proteins present in the NM of these cell lines were determined. The OFFGEL fractionation technique and 4800 MALDI-TOF/TOF analysis developed in Section 3 was used for this analysis. A total of 270 NMPs were identified with a ProtScore $\geq$ 1.3 (95% confidence). The entire list of these NMPs along with their unused ProtScore and percent coverage can be seen in Table 23 in Appendix G.

4.3.3 Alterations to the Nuclear Matrix in DCIS

iTRAQ allowed for quantification of the levels of each of these NMPs in the lines analyzed. In the search for a biomarker to allow for the early detection of DCIS and a better understanding of the alterations to the NM that play a role in breast cancer development, NMPs that were present at similar levels in the two normal breast reduction lines and the DCIS contralateral line but altered in the DCIS tumor line were of interest. Assessment of the trends shown by these markers against the most well known breast cancer tumor cell lines was also performed. Table 13 demonstrates the two proteins that fit this criteria. The p-value determined by the ProteinPilot software for the ratio is given in parentheses below the fold increase. Both eukaryotic translation elongation factor 1 delta (EEF1D) and HSP90 were identified by at least two peptides that were sequenced with 95% confidence. Both of these proteins are present at similar levels in JLDCIS-1Contra, JLBRL-14, and JLBRL-24. EEF1D abundance is decreased almost six-fold in the non-tumor adjacent JLNTALDCIS-1 line and decreased eighteen-fold in the tumor JLDCIS-1A line

compared to the normal JLDCIS-1Contra line. EEF1D abundance is also decreased about four and three fold in the MCF-7 and MDA-MB231 commercial lines, respectively, showing a consistent trend among tumor cell lines but not a specificity to early stage disease. HSP90 is less abundant in the non-tumor adjacent JLNTALDCIS-1 line, 8.1 fold, than in the tumor JLDCIS-1A line, 3.0 fold. HSP90 abundance is increased in MCF-7 and MDA-MB231 by 3.5 and 1.9 fold, respectively.

Table 13: Fold alterations to NMP levels in several cell lines in comparison to JLDCIS-1Contra line.

Protein Name	(Normal) JLBRL-14	(Normal) JLBRL-24	JLNTAL DCIS-1	JLDCIS-1A	MCF-7	MDA-MB231
Eukaryotic translation elongation factor 1 delta, isoform 3	1.4↑ (0.34)	1.3↓ (0.51)	5.7↓ (0.090)	18↓ (0.016)	4.1↓ (0.026)	2.9↓ (0.056)
Heat shock 90 kDa protein 1, alpha isoform 1	1.4↑ (0.29)	1.1↓ (0.48)	8.1↓ (0.12)	3.0↓ (0.01)	3.5↑ (0.02)	1.9↑ (0.04)

4.4 DISCUSSION

Through the use of the novel DCIS cell lines described in this study new knowledge about the earliest stages of breast cancer has been obtained. Tissue classified as normal because it is located adjacent to the tumor, such as JLNTALDCIS-1, is not necessarily normal. The karyotype, seen in Figure 24, demonstrates an abnormality with chromosome 17. In the invasion and migration assay, the non-tumor adjacent line behaves very similar to the contralateral, normal line, while the tumor line is significantly more invasive and migratory than both lines. Thus, these non-tumor adjacent cells, while harboring changes in karyotype, did not behave as

aggressively as the tumor line. Therefore the tumor line is likely further transformed or mutated differently, which allows it to be more invasive. The non-tumor adjacent line does harbor alterations to its karyotpe, and is not normal tissue, therefore it should also be removed with the tumor during surgery. This is true particularly in a case of widespread disease, which is manifested outside the rather significant DCIS mass, as was the case in this patient. The presence of widespread disease is often the case in DCIS patients. Non-tumor adjacent tissue harbors changes even though pathologically it may be morphologically considered to be "normal" and if left behind may lead to recurrence.

This invasion and migration assay should be used on DCIS lines in the future in order to characterize their behavior. Knowledge can be gained by comparing recurrence in these women with DCIS and how invasive and migratory the cell line generated from their DCIS is when using this assay. Recurrence rates are rather low since DCIS is treated by removal of a large portion of the breast plus radiation and tamoxifen treatment. The fact that treatment works underscores the need for cell lines derived from DCIS to be utilized in functional assays such as invasion. Additionally, the migration and invasion assay allows for isolation of the cells that are more invasive than the others. Iteratively investigating these cells for unique alterations compared to the others in the DCIS may help to identify a biomarker that could be of great use in determining how aggressively to treat a woman who presents with DCIS. Currently, women who are diagnosed with DCIS undergo surgery, radiation and often tamoxifen treatment. For women who have DCIS that will never become invasive (i.e. indolent), removing the DCIS lesion would be proper treatment compared to those women who have DCIS that may become invasive who should have the more aggressive treatment (radiation and hormone treatment).

In the search for biomarkers to diagnose DCIS and understand the origins of the disease, the NM was investigated. Two proteins with altered abundance in DCIS compared to contralateral normal breast and two normal breast reduction lines from other women demonstrated promise. The first of these proteins is EEF1D. EEF1D is a subunit of elongation factor-1 complex that is responsible for delivering aminoacyl tRNAs to the ribosome and plays a role in the elongation step of protein synthesis (Proud, 1994). Until now, EEF1D overexpression has been studied exclusively in the context of advanced tumor stage in various organs. EEF1D overexpression is associated with advanced tumor stage in gastrointestinal carcinomas (Joseph, 2004). Additionally, mRNA expression of EEF1D is higher in esophageal carcinomas compared to normal tissue, and the higher the expression, the more advanced the disease is (Ogawa, 2004). Additionally, in medulloblastoma, the most common malignant brain tumor of childhood, EEF1D gain of expression is associated with adverse outcome (De Bortoli, 2006). In a proteomics investigation of adriamycin-resistant squamous cell lung cancer, EEF1D is correlated with invasion (Keenan, 2009). Other groups have demonstrated this protein to have transcriptional repressor activities (Sekido, 1997). In breast cancer, EEF1D has been mainly studied for its role in invasive and metastatic breast cancer. One study examined the EpFosER mouse mammary epithelial cells as an inducible tumor model system. These cells constitutively express a fusion protein of c-Fos and the LBD of the ER. Upon stimulation with E2, the cells undergo epithelial-mesenchymal transition (Eger, 2000). When the cells are treated with E2 and undergo this transition, an increase in the expression of EEF1D is seen. This increased expression of EEF1D coincides with transcriptional repression of E-cadherin, and EEF1D was directly represses transcription of E-cadherin (Eger, 2005). E-cadherin is a major component of the epithelial to mesenchymal transition, and down-regulation of this protein plays a role in the

progression of breast cancer (Berx, 2001). Therefore, EEF1D is a key player in late stage carcinogenesis (Eger, 2005). EEF1D mRNA levels were also investigated in several commercially available breast cancer cell lines, and higher levels of EEF1D mRNA are seen in MDA-MB231 cells compared to MCF-7 cells. The levels of EEF1D mRNA in MDA-MB231 are slightly increased compared to normal HMEC-184B5 cells established from normal mammary gland (Eger, 2005). Most consistent with the present findings, bone morphogenetic protein-6 (BMP-6) down-regulates EEF1D, which leads to an up-regulation of E-cadherin in MDA-MB-231 cells transfected with E-cadherin and EEF1D (Yang, 2007). EEF1D acts as a transcriptional activator of the ovalbumin gene when estrogen is added to chick oviduct tubular gland cells (Dillner, 2002; Dillner, 2004).

EEF1D is downregulated six-fold in the non-tumor adjacent DCIS and eighteen-fold in the DCIS tumor compared to the contralateral DCIS line. Since both of these cell lines are abnormal karyotypically and the DCIS in this woman was widespread and heterogeneous, this result is not surprising. EEF1D is also down-regulated in MCF-7 and MDA-MB231 compared to the contralateral DCIS line, though not as much as it was in DCIS. This is contrary to the study that showed higher levels of EEF1D mRNA in MDA-MB231 cells compared to normal breast cells (Eger, 2005). A possible explanation is that this study examined global mRNA expression, while the current study is examining protein abundance in the NM. More EEF1D was found in the NM of MDA-MB231 cells than MCF-7 cells, which corroborates what was found at the global mRNA level (Eger, 2005). Support for the specific modulation of EEF1D in DCIS is also demonstrated by expression microarray analysis that has been done by the Latimer lab. BMP-6 is modulated in JLDCIS-1A where it is turned on and expression increases 2-fold compared to normal control lines. BMP-6 is known to repress EEF1D (Yang, 2007), so it is

interesting to see levels of BMP-6 increased in the microarray. BMP-6 may likely be playing a role in DCIS and modulating the expression of EEF1D. The expression of BMP-6 and related pathways should be investigated in the DCIS cell lines in future studies.

EEF1D has previously not been shown to associate with the NM. This study shows EEF1D is associated with the NM and this interaction is altered when DCIS develops. A more dramatic alteration in EEF1D expression is seen in the early DCIS lines compared to the late stage commercial lines. Perhaps this down-regulation of EEF1D is something that occurs very early in the development of breast cancer, making it both a promising target to prevent the progression of breast cancer and a potential biomarker of early stage disease.

The second protein demonstrated to be present at different levels in DCIS is HSP90. HSP90 is an important molecular chaperone in cells (Welch, 1982). It functions as part of a multi-chaperone complex and associates with cochaperones and client proteins. In breast cancer, HSP90 chaperones several proteins known to play a role in the disease, such as hormone receptors, protein kinases, and proteins regulating the cell cycle and apoptosis. HSP90 levels are increased in late stage breast cancer cell lines and patient samples and high expression is associated with decreased survival when examining patient specimens (Yano, 1999; Pick, 2007). HSP90 is also known to be a part of the chaperone complex that binds the unstimulated ER in a cell, and when MCF-7 cells were treated with HSP-90 drugs, the ERs are destabilized and their levels decreased (Bagatell, 2001). Like with most biomarker discovery work, all of these studies have focused on HSP90 in the traditionally used late stage commercial breast cancer lines or late stage patient samples.

In this work, HSP-90 is increased almost four-fold in MCF-7 cells and almost two-fold in MDA-MB231 cells. These findings are consistent with what has been shown about HSP-90

expression in late stage breast cancer. HSP-90 levels are, however, eight-fold less in the DCIS non-tumor adjacent line and decreased by about three-fold in the DCIS tumor line compared to the contralateral DCIS cell line. Again, this is not unexpected, as both of these cell lines are abnormal karyotypically and the DCIS was widespread. This may indicate that decreased expression of HSP90 is associated more with early stage DCIS. More work is required to ascertain whether this early stage specificity is real. It is likely HSP90 has a different role in the development of breast cancer than it does in later stages of the disease. HSP90 levels in lobular hyperplasia and lobular carcinoma *in situ* are decreased (Zagouri, 2008). This is similar to the results reported in this study.

This is the first report of the association of HSP90 with the NM. Other HSPs are known to associate with the NM. A recent study on the NM in rat liver carcinogenesis identified HSP70 and HSP60 in the NM (Barboro, 2009). The specificity of HSP90 to associate with the NM in breast cancer demonstrates that this protein may be a useful biomarker or drug target. It is possible that HSP90 may play a role in the progression of *in situ* diseases to invasive disease, as a dramatic change in the levels of this protein in the NM of DCIS samples compared to late stage breast cancer cell lines occurs. Further investigation into HSP90 levels in the NM of other cases of DCIS should be performed.

4.5 MATERIALS AND METHODS

4.5.1 Cell Culture

JLBRL-14, JLBRL-24, JLDCIS-1Contra, JLDCIS-1A, and JLNTALDCIS-1 were established by and obtained from the laboratory of Dr. Jean Latimer. These lines were maintained on Matrigel-coated flasks in MWRIα media (Latimer, 2002). MCF-7, MDA-MB231, and HT-1080 were maintained on plastic flasks with DMEM with 10% FBS.

4.5.2 Transwell Invasion Assay

The BD BioCoat Matrigel Invasion Assay (24-well format) was used according to the manufacturer's protocol. JLDCIS-1Contra, JLDCIS-1A, and JLNTALDCIS-1 were cultured in MWRIα on Matrigel-coated flasks. To set up the assay, cells were pelleted and plated with 25,000 cells per chamber in MWRI in 2.5% FBS and 2.5% CFBS (colostrum free bovine serum). The chambers were placed into wells that contained MWRI with 20% FBS. The Matrigel coated invasion filters were used to measure invasion, along with the control, uncoated membranes to measure migration. Cells were plated and incubated for 22 h. A cotton tipped swab was used to remove non-invading cells from the upper surface of the membrane. The filters were then stained using the Fisher Hema 3 manual staining system according to the protocol. The filters were mounted on slides and three images captured at 200x magnification for counting.

4.5.3 Nuclear Matrix Isolation

The NM was isolated according to the method of Fey and Penman (Fey, 1988). Briefly, 10,000,000 to 50,000,000 cells were incubated in 0.5% Triton X-100 in a buffered solution with 2 mM vanadyl ribonucleoside, an RNase inhibitor, for 10 min on ice to release lipids and soluble proteins. The remaining sample was then pelleted at 1800 rpm at 4°C for 10 min and incubated in ammonium sulfate (0.25 M) with 2 mM vanadyl ribonucleoside for 10 min on ice. This step was performed as a salt extraction to release soluble cytoskeletal elements. The remaining sample was then pelleted at 1800 rpm at 4°C for 10 min. Dnase I treatment was added to remove soluble chromatin for 30 min at room temperature and then the sample was pelleted at 2200 rpm at 4°C for 10 min. RNase A was then added to remove RNA with a 10 min incubation at room temperature and then the sample was pelleted at 2200 rpm at 4°C for 10 min. The intermediate filaments and NMPs were then disassembled with 8 M urea and the insoluble carbohydrates and extracellular matrix components were pelleted with ultracentrifugation at 50,000 rpm for 1 h at 15°C. Dialysis was performed overnight in an assembly buffer containing KCl and Imidazole-HCl to remove the urea and reassemble the intermediate filaments. Ultracentrifugation at 45,000 rpm for 90 min at 20°C was then done to pellet out the intermediate filaments. The NMPs were precipitated with ethanol then quantified using the Coomassie (Bradford) Protein Assay (Thermo Scientific, Waltham, MA). All solutions contained 1 mM phenylmethylsulfonyl fluoride to inhibit serine proteases.

4.5.4 iTRAQ Labeling

The manufacturer's protocol for iTRAQ was followed. Briefly, 50 μg of precipitated NMPs from the 8 different cell lines were each resuspended in 20 μL of Dissolution Buffer (0.5 M triethylammonium bicarbonate) with 1 μL of Denaturant (0.1% SDS). 2 μL of the Reducing Reagent, 5 mM TCEP, was then added to each sample and incubated at 60°C for 1 h. They were then alkylated with 1 μL of the Cysteine Blocking Reagent, 10 mM MMTS, at room temperature for 10 min. 10 μg trypsin was then added to each sample and they were digested at 37°C overnight. The eight iTRAQ reagents were then added to the appropriate sample and incubated at room temperature for 2 h. After labeling, the 5 samples were then pooled. The samples were labeled as follows: 113 - MCF-7; 114 – MDA-MB231; 116 – JLBRL-14; 117 – JLBRL-24; 118 – JLDCIS-1Contra; 119 – JLDCIS-1A; 121 – JLNTALDCIS-1.

4.5.5 OFFGEL Fractionation

The pooled iTRAQ sample was desalted using a SepPak and then speed vacuumed dry for OFFGEL fractionation. OFFGEL fractionation was performed according to the manufacturer's guidelines with minor modifications as described. The 3100 OFFGEL Fractionater and the OFFGEL Kit pH 3-10 (Agilent Technologies, Santa Clara, CA) was used following a 24-well set up. An Immobiline DryStrip pH 3-10, 24 cm (GE Healthcare Bio-Sciences, Piscataway, NJ) was used instead of the strip provided in the kit. Fifteen minutes before sample loading, the gel strip was rehydrated in the assembled device with 40 μL OFFGEL Rehydration solution per well. The iTRAQ peptides were resuspended in the Peptide OFFGEL solution to a final volume of 3.6 mL. 150 μL of the diluted sample was distributed into the 24 wells. The default OFFGEL

peptide 24 cm strip program on the instrument was used with a max current of 50 μA until 50 kVh was reached. The fractions were then recovered from each well. 150 μL of 50% MeOH, 0.1% TFA was then added back to each well and left on the benchtop for 20 min. This solution was then recovered and added back to the appropriate fraction and the entire sample was speed vacuumed dry and resuspended in 0.1% TFA for nanoLC.

4.5.6 Nano-LC-MALDI-TOF/TOF with the ABI 4800 Proteomics Analyzer

The OFFGEL- fractionated samples were further fractionated on an RP-LC Ultimate system (Dionex, Sunnyvale, CA). They were first loaded onto a trap column (300 μm i.d. x 5 mm, PepMap C18 100 material 5 μm, 100 Å) and washed for 10 min with 2% ACN, 0.1% TFA at a flow of 30 μL/min. They were then loaded onto an analytical column (75 μm i.d. x 150 mm, Pep Map C18 100 material 3 μm, 100 Å) and fractionated using a gradient of 5-30% B in 110 minutes, 30-60% B in 60 minutes, and 60-100% B in 10 minutes with a flow rate of 250 nL/min. Solution A was 5% ACN, 0.1% TFA, and solution B was 85% ACN, 5% IPA, and 0.1% TFA. 5 minutes after the sample injection, the Probot was signaled to start spotting. The Probot™ Micro Fraction Collector was used to collect 15 second spots on the ABI 4800 LC-MALDI metal target in a 16 x 48 array. 5 minutes after the sample injection, the Probot™ was signaled to begin spotting. 768 spots were collected for each OFFGEL fraction, and 2 LC runs were done on each target. This resulted in a total of 12 plates. The μTee mixer was used to co-spot matrix (7 mg CHCA in 1 mL of 50% ACN, 0.1% TFA, with mM ammonium citrate and 10 fmol Angiotensin II), delivered at a flow rate of 1.577 μL/min. For 4800 analysis, MS spectra were acquired from 900 to 4000 Da with a focus mass of 2000 Da. MS processing was done using the Angiotensin II

internal standard with a 250 ppm max outlier error. Up to 10 peaks were selected for MS/MS. Peptide CID (air) was performed at 2 kV.

4.5.7 Protein Identification and Quantification

The Paragon algorithm in ProteinPilot™ Software 2.0 was used for protein identification. Proteins were identified by searching against the IPI database v 3.46. Searched results were processed by the Pro Group algorithm. Search parameters included iTRAQ labeling of the N-terminus and lysine residues, cysteine modification by MMTS, and digestion by trypsin. Isoform specific identification and quantification was done by excluding all shared peptides and including only unique peptides. The p-value calculated by the software was used to determine if the change in protein expression was real or not. This p-value tests the null hypothesis that the actual protein ratio is 1 and the observed protein ratio is different than 1 only by chance. Proteins identified with >95% confidence or ProtScore > 1.3 were used for further analysis.

5.0 OVERALL DISCUSSION

5.1 SUMMARY OF FINDINGS AND SIGNIFICANCE

This study was undertaken in order to obtain a better understanding of how the NM is altered in breast cancer. The NM was studied at several different stages of the disease. Using the MCF-7 commercial, late stage breast cancer cell line and an antiestrogen resistant version of this cell line (MCF-7/LY2), an exploration into how the NM is specifically altered in antiestrogen resistance was made. Additionally, using the novel tissue engineering system created by the Latimer lab, it was possible to investigate the earliest, pre-invasive stage of breast cancer, DCIS.

The first aim in this study was to search for an ERβ-selective ligand. Previous work had focused on the development of new ER ligands and identified the *C*-cyclopropylalkylamide structure as a pharmacophore for the ER. Efforts were then undertaken to optimize this pharmacophore for subtype selectivity. There is much interest to create a ligand selective for ERβ, based upon its protective role in breast cancer and role in other diseases such as prostate cancer, medullary thyroid carcinoma, ovarian cancer, and inflammatory diseases (Ström, 2004; Paruthyiyil, 2004; Hartman, 2006; Cho, 2007; Ji, 2005; Pravettoni, 2007; Chan, 2008; Harris, 2003). This ERβ-selective ligand could also be used in the investigation of ER subtype specific interactions with the NM. Two compounds that demonstrated selectivity for ERβ and promising anti-proliferative effects in breast cancer cell lines were identified. Compared to other ERβ

selective compounds in the literature, these compounds demonstrated no affinity for ERα and modest affinity for ERβ. While the compounds were not more selective than the commercially available ERβ-selective ligand, DPN, they do provide some insight into further modifying the biphenyl *C*-cyclopropylalkylamide core to improve selectivity. Therefore DPN was used in the next aim to selectively target ERβ. The biphenyl *C*-cyclopropylalkylamide scaffold does have the capability to deliver ER-selective antiestrogens. Development of subtype-selective ER ligands will help to further understand the complex biology of the two isoforms and their different roles. Additionally, in the clinical setting, ER-subtype selective ligands may allow for the customization of antiestrogen treatments and eliminate some of the current negative side effects associated with the therapy.

The NM in breast cancer was next examined. The first objective was to investigate alterations to the NM in an antiestrogen-resistant derivative of the commonly studied MCF-7 breast cancer cell line, MCF-7/LY2. In addition, subtype selective ER ligands were used to examine how selective agonism or antagonism of the different isoforms alters the composition of the NM. The NM in breast cancer has been studied before, but the majority of studies were done using two-dimensional electrophoresis and noted protein spots that were changed from one sample to the next, but did not identify these proteins (Khanuja, 1993; Samuel, 1997). One hundred forty eight NMPs were identified in this analysis, giving the most complete understanding of the proteins found in the NM in breast cancer. Quantification was obtained on many of these NMPs, and some very interesting changes were demonstrated to occur. The most promising proteins are those that showed dramatic alterations. There were four such proteins. Dynein heavy chain 5, hnRNP R, and Serpin H1 were not present at detectable levels in the resistant cell line, while NuMA 1 was present in the resistant line but not detected in the

responsive line. All of these proteins should be investigated in patient samples in order to determine their potential as biomarkers to be used during tamoxifen treatment. If these proteins play a role in the development of resistance to tamoxifen, monitoring them when a woman is receiving tamoxifen will help to customize the treatment and knowing when to change. As tamoxifen is currently the most used therapy for breast cancer, an assay such as this may have a significant impact in the management of breast cancer. Additionally, seeing how NMPs have been developed for the use in other cancer-related assays and that they can be detected in the blood and urine, these altered NMPs in antiestrogen resistant may be developed as biomarkers for antiestrogen resistance (Miller, 1992; Replogle-Schwab, 1998). Specific alterations were also seen to the levels of NMPs present when the cells were treated with ER-selective ligands. Therefore the two isoforms seem to influence the composition of the NM in different ways. These alterations will help to understand the complex biology of the ERs, and perhaps help guide therapy.

In this second aim a workflow was optimized for the identification and quantification of proteins in up to eight samples simultaneously. This workflow involved using the iTRAQ methodology to label samples, fractionation using the OFFGEL technique, and mass spectrometry using the ABI 4800 Proteomics Analyzer for nano-LC-MALDI-TOF-TOF-MS and –MS/MS analyses. This optimized workflow will be useful for future proteomic studies aimed at identifying and quantifying proteins from complex biological samples. This workflow was used in the subsequent third aim.

The third aim shifted to the investigation of the earliest, pre-invasive stage of breast cancer, DCIS, using the novel Latimer tissue engineering system. Here, the workflow developed in aim 2 was used to identify 270 NMPs present in DCIS and breast reduction cell lines. Two

proteins, HSP90 and EEF1D, were present at similar levels in the two normal breast reduction lines and the contralateral, normal line examined. EEF1D was, however, strongly down-regulated in the DCIS samples and somewhat downregulated in the late stage commercial breast cancer cell lines that were included for comparison. HSP90 is strongly decreased in the DCIS lines, including the non-tumor adjacent tissue, but it is increased in the late stage commercial lines. Both of these proteins may serve as the basis for future assays to improve the diagnosis of DCIS and diagnose breast cancer in its earliest stage. Additionally, these proteins demonstrate some of the earliest changes that occur in the development of breast cancer and may allow for the design of new targeted therapies that improve treatment.

5.2 FUTURE DIRECTIONS

The compounds developed in aim 1 demonstrate the potential of the biphenyl *C*-cyclopropylalkylamide pharmacophore for the development of ERβ-selective ligands. While a compound was developed that was somewhat selective for ERβ and demonstrated promising effects in the inhibition of the proliferation of breast cancer cell lines, there is still room for improvement. The compounds were only investigated for their ability to compete with E2 for binding to the LBD of the ERs. They may also interact with the co-regulator binding domain of the ERs and should be examined for such activity. Understanding exactly how the compounds interact with the ERs will allow for optimization of their structure. As far as the development of a new compound for the treatment of breast cancer, the ideal ligand would act as an agonist when bound to ERβ and an antagonist when bound to ERα. Future efforts should work to make a compound that possesses both of these properties.

In aim 2, the NMPs that were demonstrated to be specifically altered in the antiestrogen resistant cell line should be investigated further. To confirm their role within the MCF-7 and MCF-7/LY2 cell lines, the levels of the proteins should be controlled. Overexpression of dynein heavy chain 5, hnRNP R, and Serpin H1 in the antiestrogen resistant cell line should, if the protein is playing a role in the development of resistance, restore their response to tamoxifen somewhat. Knockdown of these three proteins in the responsive MCF-7 line should in turn abolish the response of these cell lines to tamoxifen. Knockdown of NuMA in the MCF-7/LY2 cell line should sensitize these cells to tamoxifen, while overexpression of NuMA in the MCF-7 cell line should inhibit their response to tamoxifen. The alterations demonstrated in these cell lines should be confirmed using the iTRAQ methodology with other breast cancer cell lines that have progressed to antiestrogen resistance. Additionally, the levels of the proteins should be investigated in human tumor samples to confirm what was observed in the cell line models also occurs *in vivo*. The ability to detect the NMPs in the blood should also be determined in order to decide whether or not they could be applicable in the development of a clinical assay.

Knowledge of the alterations that occur to the NM in DCIS, the earliest identifiable lesion in breast cancer, was also gained through these studies. Most of the work was done using only one DCIS case, however. More DCIS lines need to be investigated using the iTRAQ method in order to validate the changes seen in the JL-DCIS-1 series. If these changes are validated in many DCIS cell lines, then focus should be turned to the detection of these proteins *in vivo* and their potential as biomarkers. Additionally, one of the major issues in DCIS is that there is no true understanding of whether or not the disease will become invasive (Kuerer, 2009). Therefore treatment of many women may be over-aggressive, as most women diagnosed with DCIS undergo surgery and often treatment with chemotherapy and tamoxifen. The transwell

invasion assay was optimized for use with the Latimer lines; therefore the invasive potential of other DCIS lines can be determined. In addition to determining their invasive potential, specific alterations to the NM and how these correspond to the line's invasive potential may allow for the development of a biomarker that could be used to customize treatment for a woman who is diagnosed with DCIS and thereby given the opportunity to avoid unnecessary treatment.

Finally, while the MCF-7 cell line has provided much information on breast cancer, including its use in investigating antiestrogen resistance as done in aim 2, the cell line does have its caveats. It is prone to genotypic and phenotypic variation, and the MCF-7 line used by one lab is not the same as the MCF-7 line used by most other labs, making it very hard to compare results using this line (Burdall, 2002). Additionally, the line came from a woman with very late stage disease and was made from her pleural effusion, not her actual breast tumor (Soule, 1973). Because of these reasons, the need for a system like that generated in the Latimer lab in breast cancer research is evident. The system allows for both the culture of normal breast reduction lines and the earlier stages of the disease in an environment that more resembles what is seen *in vivo*. These cell lines are more likely to represent what is truly occurring in the patient; therefore, their use in drug discovery and biomarker development should translate into patients more readily than what is generated using the later-stage cell lines. The future direction of breast cancer research is to understand the disease in its earliest stage and eventually work towards prevention.

APPENDIX A

NMPS IDENTIFIED IN MCF-7 BREAST CANCER CELLS

Table 14: NMPs identified in MCF-7 breast cancer cells.

Protein Name	Accession Number (IPI)	Gene Symbol
Beta actin variant (fragment)	00894498.1	ACTB
Actin, cytoplasmic 2	00021440.1	ACTG1
Highly similar to AF4/FRM2 family member 1, CDNA FLJ61397	00396310.5	AFF1
Putative uncharacterized protein ALB	00022434.4	ALB
ATP synthase subunit alpha	00440493.2	ATP5A1
ATP synthase subunit D, isoform 2	00456049.3	ATP5H
Uncharacterized protein DKFXP564G0422	00553153.1	ATPIF1
Uncharacterized protein C6ORF174	00647205.1	C6ORF174
Chromobox protein homolog 3	00297579.4	CBX3
24 kDa protein	00641672.1	CD320
Cofilin-1	00012011.6	CFL1
Cingulin-like protein 1, isoform 1	00307829.7	CGNL1
Charged multivesicular body protein 4b	00025974.3	CHMP4B
CDNA FLJ37462, Clone BRAWH2011343, highly similar to Cold-inducible RNA-binding protein	00641579.1	CIRBP
Clathrin light chain A, isoform 3	00790571.2	CLTA
Dynein heavy chain 5, axonemal	00152653.3	DNAH5
Desmoplakin, isoform DPI	00013933.2	DSP
Elongation factor 1-alpha 1	00396485.3	EEF1A1
Putative elongation factor 1-alpha-like 3	00472724.1	EEF1A1
Epiplakin	00010951.2	EPPK1
Enhancer of rudimentary homolog	00029631.1	ERH
Electron transfer flavoprotein subunit beta, isoform 2	00556451.2	ETFB
Ewing sarcoma breakpoint region 1	00879259.1	EWSR1

Protocadherin Fat 3, Isoform 1	00847978.2	FAT3
CDNA FLJ46111 fis, clone TEST2034913, moderately similar to Keratin, type II cytoskeletal 8	00396004.3	FLJ4611
53 kDa protein	00645208.3	FUS
Fus-like protein	00260715.5	FUS
CDNA FLJ58049, highly similar to RNA-binding protein FUS	00873762.1	FUS
Interferon-induced guanylate-binding protein 2	00848358.1	GBP2
48 kDa protein	00879060.1	GCAT
Histone H2AV	00018278.3	H2AFV
Probable E3 ubiquitin-protein ligase HECTD3, isoform 1	00456642.3	HECTD3
Histidine triad nucleotide-binding protein 1	00239077.5	HINT1
Histone H1.5	00217468.3	HIST1H1B
Histone H1.3	00217466.3	HIST1H1D
Histone H2A type 1-A	00045109.3	HIST1H2AA
Histone H3.1	00902514.1	HIST1H2AD
Histone H2A, type 1-J	00552873.2	HIST1H2AG
Histone H2B, type 1-N	00794461.1	HIST1H2BN
Histone H2B	00646240.3	HIST2H2BA
Putative Histone H2B type 2-C	00454695.4	HIST2H2BC
Similar to high mobility group 1 protein	00886784.1	HMG_HMG1/HMG2
19 kDa protein	00872915.1	HMG_HMGB1
High-mobility group protein B1	00645948.4	HMGB1
hnRNP A1, isoform A1-A	00215965.4	HNRNPA1
hnRNP A1, isoform A1-A	00465365.4	HNRNPA1
hnRNP A2/B1, Isoform B1	00396378.3	HNRNPA2B1
hnRNPA3, isoform 1	00419373.1	HNRNPA3
hnRNPA3, isoform 2	00216492.1	HNRNPA3
Putative uncharacterized protein HNRNPAB	00742926.1	HNRNPAB
CDNA FLJ53542, highly similar to hnRNP C	00909232.1	HNRNPC
P37 AUF1	00903278.1	HNRNPD
hnRNP D0, isoform 3	00220684.1	HNRNPD
hnRNP F	00003881.5	HNRNPF
51 kDa protein	00479191.2	HNRNPH1
hnRNP H2	00026230.1	HNRNPH2
hnRNP H3, isoform 1	00013877.2	HNRNPH3
hnRNP H3, isoform 2	00216482.1	HNRNPH3
CDNA FLJ54552, highly similar to hnRNP K	00910458.1	HNRNPK
hnRNPL, isoform a	00027834.3	HNRNPL
hnRNP M, isoform 1	00171903.2	HNRNPM
hnRNP M, isoform 2	00383296.5	HNRNPM
hnRNP R, isoform 1	00644055.3	HNRNPR
hnRNP U, long isoform	00883857.1	HNRNPU
CDNA FLJ54392, highly similar to heat shock 70 kDa protein	00845339.1	HSPA1B

Heat shock cognate 71 kDa protein, isoform 1	00003865.1	HSPA8
Stress-70 protein	00007765.5	HSPA9
Heat Shock Protein, Beta-1	00025512.2	HSPB1
Heat Shock Protein, 60 kDa	00784154.1	HSPD1
Interleukin enhancer-binding factor 3, isoform 4	00418313.3	ILF3
Keratin, type II cytoskeletal 1	00220327.3	KRT1
Keratin, type I cytoskeletal 15	00290077.1	KRT15
Keratin, type I cytoskeletal 16	00217963.3	KRT16
Keratin, Type II Cytoskeletal 18	00554788.5	KRT18
Keratin, Type II Cytoskeletal 19	00479145.2	KRT19
21 kDa protein	00794644.1	KRT19
Keratin, type I cytoskeletal 24	00004550.5	KRT24
Keratin, type II cytoskeletal 5	00009867.3	KRT5
Keratin 7	00847342.1	KRT7
Keratin 77	00376379.3	KRT77
Keratin, Type II Cytoskeletal 8	00554648.3	KRT8
Lamin-A/C, Isoform C	00216952.1	LMNA
Lamin-A/C, Isoform ADelta10	00216953.1	LMNA
Progerin	00644087.1	LMNA
Lamin-B1	00217975.4	LMNB1
Lamin-B2	00009771.6	LMNB2
Putative uncharacterized protein MATR3	00789551.1	MATR3
Myosin regulatory light chain MRCL3 variant	00604523.1	MRCL3
39S ribosomal protein L40	00099871.1	MRPL40
Myosin-10, isoform 3	00790503.3	MYH10
Myosin regulatory light chain	00719669.4	MYL12B
Non-muscle isoform of myosin light polypeptide 6	00335168.9	MYL6
CDNA FLJ56329, highly similar to myosin light polypeptide 6	00796366.2	MYL6B
Nucleosome assembly protein 1-like 1	00902909.1	NAP1L1
Nucleolin, isoform 1	00604620.3	NCL
32 kDa protein	00827674.1	NCL
Nucleoside diphosphate kinase B, isoform 3	00795292.1	NME2
Non-POU domain-containing octamer-binding protein	00304596.3	NONO
Nucleophosmin, isoform 1	00549248.4	NPM1
Nuclear ubiquitous casein and cyclin-dependent kinase substrate, isoform 1	00872944.1	NUCKS1
NUMA1 variant protein	00872028.2	NUMA1
Polyadenylate-binding protein1, isoform 1	00008524.1	PABPC1
Protein disulfide-isomerase A6, isoform 2	00299571.5	PDIA6
Protein pigeon homolog, isoform 1	00893006.1	PION
Peptidyl-prolyl cis-trans isomerase A	00419585.9	PPIA
Peroxiredoxin 3, isoform b	00374151.1	PRDX3
26S protease regulatory subunit 7	00021435.3	PSMC2
Paraspeckle component 1, isoform 1	00103525.1	PSPC1
RNA-binding protein 14, isoform 1	00013174.2	RBM14

RNA-binding protein 3, putative	00024320.1	RBM3
RNA-binding protein 8A, isoform 2	00216659.1	RBM8A
hnRNP G	00304692.1	RBMX
60S ribosomal protein L12, isoform 1	00024933.3	RPL12
60S ribosomal protein L12, isoform 2	00816063.1	RPL12
60S acidic ribosomal protein P1	00008527.3	RPLP1
60S acidic ribosomal protein P2	00008529.1	RPLP2
40S ribosomal protein S12	00847579.3	RPS12
40S ribosomal protein S14	00026271.5	RPS14
40S ribosomal protein S19	00215780.5	RPS19
40S ribosomal protein s20	00012493.1	RPS20
40S ribosomal protein S23	00218606.7	RPS23
40S ribosomal protein S25	00012750.3	RPS25
Putative uncharacterized protein RPS7	00893703.1	RPS7
Sin3A-associated protein	00011698.4	SAP18
Serpin H1	00032140.4	SERPINH1
Splicing factor, proline- and glutamine- rich	00010740.1	SFPQ
Splicing factor, arginine/serine-rich 3	00010204.1	SFRS3
SWI/SNF complex subunit SMARCC2, isoform 1	00216047.3	SMARCC2
Small nuclear ribonucleoprotein Sm D3	00017964.1	SNRNPD3
Spectrin alpha chain, isoform 1	00844215.1	SPTAN1
hnRNPQ, isoform 2	00402182.2	SYNCRIP
hnRNP Q, isoform 1	00018140.3	SYNCRIP
Transcription factor A	00020928.1	TFAM
THO complex subunit 4	00328840.9	THOC4
Transcription intermediary factor 1-b, isoform 1	00438229.2	TRIM28
Tau-tubulin kinase	00217437.6	TTBK2
TUBA1B protein	00793930.1	TUBA1B
Tubulin, Beta Chain	00011654.2	TUBB
Tubulin beta-2C chain	00007752.1	TUBB2C
HCG2042771	00152453.1	TUBB3
Tubulin alpha-1C chain	00218343.4	TUBA1C
Tu translation elongation factor	00027107.5	TUFM
Cytochrome B-C1 complex subunit 6	00296022.1	UQCRH
Vimentin	00418471.6	VIM
WD repeat-containing protein 21B	00295511.8	WDR21B
YBX1 Protein	00643351.1	YBX1
Zinc finger protein 595	00478170.1	ZNF595

APPENDIX B

NMPS ALTERED IN MCF-7/LY2 CELLS

Table 15: The ratio for NMP abundance in MCF-7/LY2 cells compared to MCF-7 cells.

Protein Name	Accession Number (IPI)	Gene Symbol	MCF-7/ LY2: MCF-7	Std Dev
Beta actin variant (fragment)	00894498.1	ACTB	0.7804	
Actin, cytoplasmic 2	00021440.1	ACTG1	0.8005	
Putative uncharacterized protein ALB	00022434.4	ALB	0.6308	
ATP synthase subunit alpha	00440493.2	ATP5A1	2.537	
ATP synthase subunit D, isoform 2	00456049.3	ATP5H	0.7142	
Dynein heavy chain 5, axonemal	00152653.3	DNAH5	0	
Desmoplakin, isoform DPI	00013933.2	DSP	0.3705	0.2411
Putative elongation factor 1-alpha-like 3	00472724.1	EEF1A1	0.7306	
Enhancer of rudimentary homolog	00029631.1	ERH	0.5597	
Fus-like protein	00260715.5	FUS	1.728	
Interferon-induced guanylate-binding protein 2	00848358.1	GBP2	0.6226	
Histone H2AV	00018278.3	H2AFV	1.588	
Histone H3.1	00902514.1	HIST1H2AD	3.439	2.114
Histone H2A, type 1-J	00552873.2	HIST1H2AG	1.595	
Histone H2B, type 1-N	00794461.1	HIST1H2BN	1.541	0.1151
Histone H2B	00646240.3	HIST2H2BA	2.301	
Similar to high mobility group 1 protein	00886784.1	HMG_HMG1/ HMG2	1.441	
High-mobility group protein B1	00645948.4	HMGB1	1.270	
hnRNP A2/B1, Isoform B1	00396378.3	HNRNPA2B1	0.7712	
P37 AUF1	00903278.1	HNRNPD	2.178	
hnRNP D0, isoform 3	00220684.1	HNRNPD	1.513	
hnRNP F	00003881.5	HNRNPF	0.5719	
51 kDa protein	00479191.2	HNRNPH1	1.106	

hnRNPL, isoform a	00027834.3	HNRNPL	0.7024	0.0059
hnRNP M, isoform 1	00171903.2	HNRNPM	0.7657	
hnRNP M, isoform 2	00383296.5	HNRNPM	0.8107	
hnRNP R, isoform 1	00644055.3	HNRNPR	0	
Heat Shock Protein, 60 kDa	00784154.1	HSPD1	1.391	
Interleukin enhancer-binding factor 3, isoform 4	00418313.3	ILF3	1.400	
Keratin, type II cytoskeletal 1	00220327.3	KRT1	0.2214	
Keratin, Type II Cytoskeletal 18	00554788.5	KRT18	0.5885	0.2307
Keratin, Type II Cytoskeletal 19	00479145.2	KRT19	0.5041	0.2666
Keratin, type I cytoskeletal 24	00004550.5	KRT24	1.377	
Keratin, Type II Cytoskeletal 8	00554648.3	KRT8	0.4466	0.08853
Lamin-A/C, Isoform C	00216952.1	LMNA	1.203	
Lamin-A/C, Isoform ADelta10	00216953.1	LMNA	1.136	
Progerin	00644087.1	LMNA	1.234	
Lamin-B1	00217975.4	LMNB1	1.438	0.2368
Lamin-B2	00009771.6	LMNB2	1.766	0.5235
Myosin regulatory light chain	00719669.4	MYL12B	0.7596	
32 kDa protein	00827674.1	NCL	0.7411	
Non-POU domain-containing octamer-binding protein	00304596.3	NONO	0.7291	
Nucleophosmin, isoform 1	00549248.4	NPM1	0.9076	
NUMA1 variant protein	00872028.2	NUMA1	9999	
60S acidic ribosomal protein P1	00008527.3	RPLP1	1.813	
40S ribosomal protein S19	00215780.5	RPS19	1.693	

APPENDIX C

NMP ALTERATIONS IN RESPONSE TO PPT

Table 16: Alterations to NMP abundance in MCF-7 cells in response to PPT.

Protein Name	Accession Number (IPI)	Gene Symbol	PPT : DMSO	Std Dev
Fus-like protein	00260715.5	FUS	1.453	
Interferon-induced guanylate-binding protein 2	00848358.1	GBP2	0.782	
Histone H3.1	00902514.1	HIST1H2AD	2.196	
Histone H2B, type 1-N	00794461.1	HIST1H2BN	1.063	
Histone H2B	00646240.3	HIST2H2BA	1.138	
19 kDa protein	00872915.1	HMG_HMGB1	1.413	
hnRNP A1, isoform A1-A	00465365.4	HNRNPA1	0.734	
hnRNP F	00003881.5	HNRNPF	0.657	
51 kDa protein	00479191.2	HNRNPH1	1.082	
Heat Shock Protein, Beta-1	00025512.2	HSPB1	1.287	
Keratin, Type II Cytoskeletal 18	00554788.5	KRT18	0.6695	0.3470
Keratin, Type II Cytoskeletal 19	00479145.2	KRT19	0.8676	0.1015
Keratin, Type II Cytoskeletal 8	00554648.3	KRT8	0.8263	0.0554
Lamin-A/C, Isoform C	00216952.1	LMNA	1.239	
Lamin-A/C, Isoform ADelta10	00216953.1	LMNA	1.100	
Lamin-B1	00217975.4	LMNB1	1.231	0.1292
Lamin-B2	00009771.6	LMNB2	1.206	
Non-muscle isoform of myosin light polypeptide 6	00335168.9	MYL6	1.484	
Non-POU domain-containing octamer-binding protein	00304596.3	NONO	0.8664	
Nucleophosmin, isoform 1	00549248.4	NPM1	0.9097	
Peroxiredoxin 3, isoform b	00374151.1	PRDX3	1.123	
hnRNP G	00304692.1	RBMX	1.507	
60S acidic ribosomal protein P1	00008527.3	RPLP1	2.100	

60S acidic ribosomal protein P2	00008529.1	RPLP2	1.308
40S ribosomal protein s20	00012493.1	RPS20	0.8136
40S ribosomal protein S25	00012750.3	RPS25	1.287
Small nuclear ribonucleoprotein Sm D3	00017964.1	SNRNPD3	1.593
TUBA1B protein	00793930.1	TUBA1B	1.739
Tubulin, Beta Chain	00011654.2	TUBB	1.475
YBX1 Protein	00643351.1	YBX1	1.352

Table 17: Alterations to NMP abundance in MCF-7/LY2 cells in response to PPT.

Protein Name	Accession Number (IPI)	Gene Symbol	PPT : DMSO	Std Dev
Histone H12AD	00902514.1	HIST1H2AD	0.8089	
Histone H2B, type 1-N	00794461.1	HIST1H2BN	1.233	
Histone 1 H2BJ	00515061.3	HIST1H2BJ	0.8619	
hnRNP A3	00419373.1	HNRNPA3	1.0977	
Heat Shock Protein, Beta-1	00025512.2	HSPB1	1.1718	
Keratin, Type II Cytoskeletal 18	00554788.5	KRT18	0.9538	
Keratin, Type II Cytoskeletal 19	00479145.2	KRT19	0.7879	0.02807
Keratin, Type II Cytoskeletal 8	00554648.3	KRT8	0.9254	
Small nuclear ribonucleoprotein Sm D3	00017964.1	SNRNPD3	0.6201	
Putative elongation factor 1-alpha-like 3	00472724.1	EEF1A1	0.8337	
Protein disulfide isomerase A6	00299571.5	PDIA6	1.1565	
Tu translation elongation factor	00027107.5	TUFM	1.1563	

APPENDIX D

NMP ALTERATIONS IN RESPONSE TO MPP

Table 18: Alterations to NMP abundance in MCF-7 cells in response to MPP.

Protein Name	Accession Number (IPI)	Gene Symbol	MPP : DMSO	Std Dev
Highly similar to AF4/FRM2 family member 1, CDNA FLJ61397	00396310.5	AFF1	21.10	
ATP synthase subunit alpha	00440493.2	ATP5A1	2.032	0.7981
ATP synthase subunit D, isoform 2	00456049.3	ATP5H	1.223	
Uncharacterized protein DKFXP564G0422	00553153.1	ATPIF1	1.167	
Cingulin-like protein 1, isoform 1	00307829.7	CGNL1	25.9	
Dynein heavy chain 5, axonemal	00152653.3	DNAH5	49.53	
Putative elongation factor 1-alpha-like 3	00472724.1	EEF1A1	0.6748	
Epiplakin	00010951.2	EPPK1	42.24	
Enhancer of rudimentary homolog	00029631.1	ERH	0.6234	
Interferon-induced guanylate-binding protein 2	00848358.1	GBP2	27.45	
48 kDa protein	00879060.1	GCAT	47.36	
Histone H2AV	00018278.3	H2AFV	1.198	
Histone H3.1	00902514.1	HIST1H2AD	1.401	
Histone H2A, type 1-J	00552873.2	HIST1H2AG	0.8286	
Histone H2B, type 1-N	00794461.1	HIST1H2BN	0.8655	
Histone H2B	00646240.3	HIST2H2BA	0.5326	
19 kDa protein	00872915.1	HMG_HMGB1	0.5358	
hnRNP A1, isoform A1-A	00465365.4	HNRNPA1	0.8873	
hnRNP A2/B1, Isoform B1	00396378.3	HNRNPA2B1	0.7661	0.1757
hnRNPA3, isoform 1	00419373.1	HNRNPA3	0.8028	
hnRNP F	00003881.5	HNRNPF	0.4017	
51 kDa protein	00479191.2	HNRNPH1	0.9079	
hnRNP R, isoform 1	00644055.3	HNRNPR	32.83	

Heat Shock Protein, Beta-1	00025512.2	HSPB1	0.7162	
Heat Shock Protein, 60 kDa	00784154.1	HSPD1	1.236	
Keratin, type I cytoskeletal 15	00290077.1	KRT15	141.5	
Keratin, type I cytoskeleral 16	00217963.3	KRT16	0.1578	
Keratin, Type II Cytoskeletal 18	00554788.5	KRT18	0.8870	0.4328
Keratin, Type II Cytoskeletal 19	00479145.2	KRT19	0.9695	0.5037
Keratin, type I cytoskeletal 24	00004550.5	KRT24	0.2323	
Keratin 7	00847342.1	KRT7	10.86	
Keratin, Type II Cytoskeletal 8	00554648.3	KRT8	0.9259	0.4946
Lamin-A/C, Isoform C	00216952.1	LMNA	0.6018	
Lamin-B1	00217975.4	LMNB1	0.8022	
Lamin-B2	00009771.6	LMNB2	1.286	
Myosin-10, isoform 3	00790503.3	MYH10	0.6519	
Non-POU domain-containing octamer-binding protein	00304596.3	NONO	0.6435	
Nucleophosmin, isoform 1	00549248.4	NPM1	0.7218	0.09143
NUMA1 variant protein	00872028.2	NUMA1	9999	
Peroxiredoxin 3, isoform b	00374151.1	PRDX3	1.171	
60S acidic ribosomal protein P1	00008527.3	RPLP1	4.651	
40S ribosomal protein s20	00012493.1	RPS20	1.749	
Splicing factor, proline- and glutamine-rich	00010740.1	SFPQ	0.829	
hnRNPQ, isoform 2	00402182.2	SYNCRIP	0.4418	
Tau-tubulin kinase	00217437.6	TTBK2	15.68	
Zinc finger protein 595	00478170.1	ZNF595	0.487	

Table 19: Alterations to NMP abundance in MCF-7/LY2 cells in response to MPP.

Protein Name	Accession Number (IPI)	Gene Symbol	MPP : DMSO	Std Dev
Dynein heavy chain 5, axonemal	00152653.3	DNAH5	9999	
Elongation factor 1-alpha 1	00396485.3	EEF1A1	0.6337	
Interferon-induced guanylate-binding protein 2	00848358.1	GBP2	0.3863	
Histone H3.1	00902514.1	HIST1H2AD	0.592	0.3067
Histone H2A, type 1-J	00552873.2	HIST1H2AG	0.8619	
Histone H2B, type 1-N	00794461.1	HIST1H2BN	1.233	
Histone H2B	00646240.3	HIST2H2BA	0.8263	
hnRNP A1, isoform A1-A	00215965.4	HNRNPA1	2.15	
hnRNP A2/B1, Isoform B1	00396378.3	HNRNPA2B1	1.95	
hnRNPA3, isoform 1	00419373.1	HNRNPA3	2.401	
hnRNPA3, isoform 2	00216492.1	HNRNPA3	1.11	
51 kDa protein	00479191.2	HNRNPH1	1.481	
hnRNPL, isoform a	0027834.3	HNRNPL	1.812	
hnRNP R, isoform 1	00644055.3	HNRNPR	9999	

Heat Shock Protein, Beta-1	0025512.2	HSPB1	0.932	0.3391
Keratin, Type II Cytoskeletal 18	00554788.5	KRT18	0.7855	0.2381
Keratin, Type II Cytoskeletal 19	00479145.2	KRT19	0.6963	0.1582
Keratin, Type II Cytoskeletal 8	00554648.3	KRT8	0.7454	0.2553
Lamin-A/C, Isoform C	00216952.1	LMNA	1.174	
Lamin-B1	00217975.4	LMNB1	1.444	
Peptidyl-prolyl cis-trans isomerase A	00419585.9	PPIA	1.157	
60S ribosomal protein L12, isoform 1	00024933.3	RPL12	1.846	
60S acidic ribosomal protein P2	00008529.1	RPLP2	2.855	
40S ribosomal protein S19	00215780.5	RPS19	1.495	
40S ribosomal protein s20	00012493.1	RPS20	1.224	
hnRNPQ, isoform 2	00402182.2	SYNCRIP	1.671	
Tu translation elongation factor	00027107.5	TUFM	1.156	
YBX1 Protein	00643351.1	YBX1	1.474	
Zinc finger protein 595	00478170.1	ZNF595	2.988	

APPENDIX E

NMP ALTERATIONS IN RESPONSE TO DPN

Table 20: Alterations to NMP abundance in MCF-7 cells in response to DPN.

Protein Name	Accession Number (IPI)	Gene Symbol	DPN : DMSO	Std Dev
Actin, cytoplasmic 2	00021440.1	ACTG1	0.689	
Highly similar to AF4/FRM2 family member 1, CDNA FLJ61397	00396310.5	AFF1	2.002	
Cofilin-1	00012011.6	CFL1	0.6621	
Cingulin-like protein 1, isoform 1	00307829.7	CGNL1	3.542	
Elongation factor 1-alpha 1	00396485.3	EEF1A1	1.225	
Enhancer of rudimentary homolog	00029631.1	ERH	0.343	
Interferon-induced guanylate-binding protein 2	00848358.1	GBP2	2.909	
48 kDa protein	00879060.1	GCAT	5.748	
Histone H2A type 1-A	00045109.3	HIST1H2AA	0	
Histone H2A, type 1-J	00552873.2	HIST1H2AG	0.8652	
Histone H2B	00646240.3	HIST2H2BA	1.995	
Putative Histone H2B type 2-C	00454695.4	HIST2H2BC	1.765	
19 kDa protein	00872915.1	HMG_HMGB1	0.5914	
High-mobility group protein B1	00645948.4	HMGB1	1.237	
hnRNP A1, isoform A1-A	00465365.4	HNRNPA1	0.5777	
hnRNP A2/B1, Isoform B1	00396378.3	HNRNPA2B1	0.7687	0.1644
hnRNPA3, isoform 1	00419373.1	HNRNPA3	0.8445	
Putative uncharacterized protein HNRNPAB	00742926.1	HNRNPAB	0.5888	
P37 AUF1	00903278.1	HNRNPD	1.748	
hnRNP F	00003881.5	HNRNPF	0.4783	
51 kDa protein	00479191.2	HNRNPH1	1.707	
hnRNPL, isoform a	00027834.3	HNRNPL	0.6865	
hnRNP M, isoform 1	00171903.2	HNRNPM	0.6445	

Heat Shock Protein, Beta-1	00025512.2	HSPB1	0.8039	
Keratin, Type II Cytoskeletal 18	00554788.5	KRT18	0.6249	0.6449
Keratin, Type II Cytoskeletal 19	00479145.2	KRT19	0.7857	0.4963
Keratin, type I cytoskeletal 24	00004550.5	KRT24	0.6479	
Keratin 7	00847342.1	KRT7	2.507	
Keratin, Type II Cytoskeletal 8	00554648.3	KRT8	0.6094	0.5604
Lamin-B1	00217975.4	LMNB1	1.07	
Lamin-B2	00009771.6	LMNB2	1.192	
Non-POU domain-containing octamer-binding protein	00304596.3	NONO	0.7414	
Nucleophosmin, isoform 1	00549248.4	NPM1	0.7831	0.05438
NUMA1 variant protein	00872028.2	NUMA1	9999	
Peroxiredoxin 3, isoform b	00374151.1	PRDX3	1.148	
60S ribosomal protein L12, isoform 1	00024933.3	RPL12	3.531	
60S acidic ribosomal protein P2	00008529.1	RPLP2	0.6056	
40S ribosomal protein s20	00012493.1	RPS20	1.575	1.069
40S ribosomal protein S23	00218606.7	RPS23	1.357	
Splicing factor, proline- and glutamine-rich	00010740.1	SFPQ	0.7821	

Table 21: Alterations to NMP abundance in MCF-7/LY2 cells in response to DPN.

Name	Accession Number (IPI)	Gene Symbol	DPN : DMSO	Std Dev
Actin, cytoplasmic 2	00021440.1	ACTG1	1.486	
Putative uncharacterized protein ALB	00022434.4	ALB	0.8555	
ATP synthase subunit alpha	00440493.2	ATP5A1	0.6799	0.04094
Dynein heavy chain 5, axonemal	00152653.3	DNAH5	9999	
Elongation factor 1-alpha 1	00396485.3	EEF1A1	0.6362	
Putative elongation factor 1-alpha-like 3	00472724.1	EEF1A1	1.769	
Fus-like protein	00260715.5	FUS	0.5103	
Interferon-induced guanylate-binding protein 2	00848358.1	GBP2	1.843	
Histone H2A type 1-A	00045109.3	HIST1H2AA	0	
Histone H3.1	00902514.1	HIST1H2AD	0.5117	0.4192
Histone H2B, type 1-N	00794461.1	HIST1H2BN	0.8394	
Histone H2B	00646240.3	HIST2H2BA	0.4359	
High-mobility group protein B1	00645948.4	HMGB1	0.6824	
hnRNP A1, isoform A1-A	00465365.4	HNRNPA1	1.45	
hnRNPA3, isoform 2	00216492.1	HNRNPA3	1.177	
P37 AUF1	00903278.1	HNRNPD	0.479	
hnRNP F	00003881.5	HNRNPF	1.627	
51 kDa protein	00479191.2	HNRNPH1	0.8714	
hnRNP H3, isoform 2	00216492.1	HNRNPH3	0.8147	
hnRNP R, isoform 1	00644055.3	HNRNPR	9999	

hnRNP U, long isoform	00883857.1	HNRNPU	0.8837	
Heat shock cognate 71 kDa protein, isoform 1	00003865.1	HSPA8	1.139	
Stress-70 protein	00007765.5	HSPA9	0.8767	
Heat Shock Protein, Beta-1	00025512.2	HSPB1	1.274	0.5374
Heat Shock Protein, 60 kDa	00784154.1	HSPD1	0.7283	0.0239
Keratin, type II cytoskeletal 1	00220327.3	KRT1	4.0085	
Keratin, Type II Cytoskeletal 18	00554788.5	KRT18	1.255	0.9309
Keratin, Type II Cytoskeletal 19	00479145.2	KRT19	1.842	1.937
Keratin, type I cytoskeletal 24	00004550.5	KRT24	0.7362	
Keratin, Type II Cytoskeletal 8	00554648.3	KRT8	1.432	1.222
Lamin-A/C, Isoform C	00216952.1	LMNA	0.8899	
Lamin-B1	00217975.4	LMNB1	0.8121	
Nucleophosmin, isoform 1	00549248.4	NPM1	1.177	
Peptidyl-prolyl cis-trans isomerase A	00419585.9	PPIA	1.415	
Peroxiredoxin 3, isoform b	00374151.1	PRDX3	1.272	
60S acidic ribosomal protein P2	00008529.1	RPLP2	1.624	0.0932
40S ribosomal protein S25	00012750.3	RPS25	1.514	
Serpin H1	00032140.4	SERPINH1	0.6679	
Splicing factor, proline- and glutamine-rich	00010740.1	SFPQ	1.624	
THO complex subunit 4	00328840.9	THOC4	1.226	
YBX1 protein	00643351.1	YBX1	1.332	

APPENDIX F

CHARACTERIZATION OF BREAST CANCER CELL LINES USED

Table 22: Characteristics of Latimer cell lines and commercially available cell lines.

Cell Line	Description	Karyotype	Molecular Characteristics
MDA-MB231	Stage IV Pleural Effusion Breast Cancer	56-61,X,X, +1,+2,+3,del(3)(q12q25)x2,+4,+5,del(6)(q21),add(7)(p21),+9,del(9)(p21)x2,+11x2,add(11)(p11.2),+12,+14,der(15)t(7;15)(q11.2;p11.2),dup(15)(q11.1q21),+17x2,i(17)(q10),i(18)(q10),+20,+0-7mar[21]	Basal ER- PR- Her2-
MCF-7	Stage IV Pleural Effusion Breast Cancer	82-83, X,add(X)(q26),+2,+2,+3,+4,+5,+5,+6,del(6)(q21),+8,+9,+9, add(9)(p13)x2,+10,+11,del(11)(p13),+12,del(12)(p11.2),+13,+14,+15,+15, +16,+17,del(17)(13)x2,+18,+19,der(19)t(12;19)(q13;q13.3),+21,del(22)(q13),+5-10mar[cp8]	Luminal ER+ PR+ Her2-
MCF-10A	Derived from normal breast epithelium; Transformed over time in culture; DCIS.com in some systems	45-48,XX,i(1)(q10),-3, del(3)(p13),+4,der(9), der(9),+19	Currently ER- Originally ER+
JLBTL-7	Stage II Breast tumor	33 chromosomes. Loss of 2 copies of chromosome 1 and loss of one copy of chromosomes 4,5,7,8,9,10,11,18,19, and 21.	ER- PR-
JLBTL-10	Stage II Breast tumor	46, XX, but contains double minutes indicative of gene amplification	ER- PR-
JLBTL-12	Stage III	49-75,X,-X	ER+

	Breast tumor	[17],del(X)(q23)[12],+1[12],+1[3],del(1)(q31)[16],del(1)(q31)x2[4],der(1)t(1;3;7)(1qter➔1p10::3q10➔3q24::7q11.2➔7qter)[18],der(1;3)(p10;q10)[15-1[15],del(2)(q12q22)[20],del(2)(q12q22)x2[15],+3[7],del(3)(q10)[20],der(3)del(3)(p10)t(3;?)(q26.1;?)[16],-4[7].del(4)(p13p15)[10],-5[7],+5[7],del(5)(q13.2q31.2)[19],de;(5)(q13.2q31.2)x2[5],-6[5],+6[9],add(6)(q24)[11],add(6)(p22.3)[8],+7[11],+7[5],-7[4],der(7)t(5;7)(q14;q31.3)[16],-8[5],del(8)(p22)[-9[17],del(9)(q33)[15],-10[9].del(10)(p12.3)[13],+11[9],add(11)(q23)[4],der(11;15)(q10;p10)[17],-12[10],del(12)(p10)[17],-13[19].-13[11],add(13)(p10)[5]del(13)(q13;q21.3)[5],-14[10],+14[5],-15[12],i(15)(q10)[14],i(15)(q10)x2[2],+16[8],add(16)(p12)[12],add(16)(p12)[12],add(16)(p12)x2[4],-17[11],add(17)(p10)[11],add(17)(p10)x2[4],-18[15],-18[6],-19[7],+19[5],-20[9],+20[4],del(20)(q13.2)[9],-21[8],-22[14],add(22)(q11.2)[18],+mar1[14],+mar2[6],+mar3[2][cp20]	PR+ Her2-
JL-DCIS4	DCIS with an invasive component	46,XX,16qh-[20] diploid or hypodiploid chromosome complement. All of the cells had absence of heterochromatin in the proximal long arm of chromosome 16	ER- PR- Her2+
JLDCIS-1A	DCIS, no evidence of invasion or recurrence	45,X,-X,der(14)t(5;14)(q11.2;p11.2)[3]/46,X,-X,der(14)t(5;14)(q11.2;p11.2)[3]/46,XX[10]	ER+ PR+
JLNTALDCIS-1	Adjacent to JLDCIS-1	47,XX,i(17)(q10)[3]/46,XX[17]	ER+ PR+
JLDCIS-1Contra	Contralateral breast to DCIS 1 series	46, XX	ER+ PR+
JLBRL-14	Breast reduction mammoplasty	46, XX	
JLBRL-23	Breast reduction mammoplasty	46, XX	
JLBRL-24	Breast reduction mammoplasty	46, XX	

APPENDIX G

NMPS IDENTIFIED IN DCIS CELL LINES

Table 23: NMPs identified in DCIS cell lines.

Protein Name	Accession Number (IPI)	Gene Symbol	Score	% Coverage
Vimentin	00418471.6	VIM	147	79.2
Isoform A of Lamin-A/C	00021405.3	LMNA	62.9	63.4
Neuroblast differentiation-associated protein AHNAK	00021812.2	AHNAK	61.0	48.5
Nucleolin	00604620.3	NCL	44.1	59.3
HSPA5 protein	00003362.2	HSPA5	42.7	52.7
Keratin, type II cytoskeletal 8	00554648.3	KRT8	39.3	68.7
Isoform B1 of hnRNP A2/B1	00396378.3	HNRNPA2B1	38.9	77.3
Lamin-B1	00217975.4	LMNB1	33.7	56.7
Annexin A2 isoform 1	00418169.3	ANXA2	33.4	69.5
p180/ribosome receptor	00856098.1	RRBP1	30.1	52.0
Histone H2B type 1-N	00794461.1	HIST1H2BN	29.8	73.5
Isoform 1 of Nucleophosmin	00549248.4	NPM1	27.5	61.6
Lamin-B2	00009771.6	LMNB2	26.9	45.3
Keratin, type I cytoskeletal 19	00479145.2	KRT19	25.6	55.8
Histone H1.2	00217465.5	HIST1H1C	25.4	87.8
Putative elongation factor 1-alpha-like	00472724.1	EEF1A1	24.8	36.1
60 kDa heat shock protein	00784154.1	HSPD1	24.0	59.7
High mobility group protein B1	00419258.4	HMGB1	22.4	64.6
Nuclease-sensitive element-binding protein 1	00031812.3	YBX1	22.0	44.4
Keratin, type I cytoskeletal 18	00554788.5	KRT18	21.9	48.6
cDNA FLJ56329, highly similar to myosin light polypeptide 6	00796366.2	MYL6B	21.9	64.3
Filamin A, alpha	00644576.1	FLNA	20.4	21.5

Isoform 3 of plectin-1	00398002.6	PLEC1	20.0	29.5
Isoform long of splicing factor, proline- and glutamine-rich	00010740.1	SFPQ	19.9	45.3
Isoform 1 of Heat shock cognate 71 kDa protein	00003865.1	HSPA8	19.5	40.9
60S ribosomal protein L8	00012772.8	RPL8	19.1	47.5
51 kDa protein	00479191.2	HNRNPH1	17.7	34.5
Beta actin variant (Fragment)	00894498.1	ACTB	17.6	36.5
Putative uncharacterized protein hnRNP AB	00742926.1	HNRNPAB	17.2	41.6
ATP synthase subunit alpha, mitochondrial	00440493.2	ATP5A1	16.4	29.8
Elongation factor 1-beta	00178440.3	EEF1B2	16.4	34.7
similar to peptidylprolyl isomerase A	00887678.1	LOC654188	14.9	65.9
Keratin 7	00847342.1	KRT7	14.5	45.6
Protein disulfide-isomerase A3	00025252.1	PDIA3	13.9	37.6
Isoform 1 of hnRNP Q	00018140.3	SYNCRIP Q	13.6	43.3
Histone H2A type 1	00291764.5	HIST1H2AG	13.6	57.7
Filamin B	00900293.1	FLNB	13.6	19.6
Putative uncharacterized protein SPTAN1	00879810.1	SPTAN1	13.3	18.3
TUBA1C protein	00166768.3	TUBA1C	13.3	37.7
Highly similar to hnRNP C	00909232.1	FLJ53542	13.2	53.8
Isoform HMG-I of high mobility group protein HMG-I/HMG-Y	00179700.3	HMGA1	12.8	73.8
Isoform ASF-1 of splicing factor, arginine/serine-rich 1	00215884.4	SFRS1	12.7	78.2
Peroxiredoxin-1	00000874.1	PRDX1	12.6	52.3
Tubulin beta chain	00011654.2	TUBB	12.5	30.6
Isoform 2 of hnRNP M	00383296.5	HNRNPM	12.1	36.9
Isoform 2 of polyadenylate-binding protein 1	00410017.1	PABPC1	12.1	35.8
Histone H1.4	00217467.3	HIST1H1E	11.6	91.8
Laminin subunit gamma-1	00298281.4	LAMC1	11.6	14.9
Isoform 3 of clathrin light chain A	00790571.2	CLTA	11.1	29.7
Transitional endoplasmic reticulum ATPase	00022774.3	VCP	11.0	34.5
Hepatoma-derived growth factor	00020956.1	HDGF	11.0	31.7
Isoform 3 of plasminogen activator inhibitor 1 RNA-binding protein	00470498.1	SERBP1	10.9	29.0
Glyceraldehyde-3-phosphate dehydrogenase	00219018.7	GAPDH	10.7	36.7
Heat shock protein beta-1	00025512.2	HSPB1	10.5	47.8
Isoform 1 of Myosin-9	00019502.3	MYH9	10.4	22.8
Myosin regulatory light chain MRLC2	00033494.3	MYL12B	10.3	45.4
Eukaryotic translation elongation	00789435.2	EEF1D	10.0	31.3

factor 1 delta isoform 3				
Putative uncharacterized protein ALB	00022434.4	ALB	9.75	20.4
28 kDa heat- and acid-stable phosphoprotein	00013297.1	PDAP1	9.63	58.6
Similar to 40S ribosomal protein S28	00887241.1	RPS28P9	9.52	53.9
34 kDa protein	00927677.1	HNRNPA3	9.50	61.6
Non-POU domain-containing octamer-binding protein	00304596.3	NONO	9.33	40.3
Histone H2A.Z	00218448.4	H2AFZ	9.10	64.1
40S ribosomal protein S23	00218606.7	RPS23	9.08	53.9
cDNA FLJ35087 fis, clone PLACE6005546, highly similar to polymerase I and transcript release factor	00924434.1	PTRF	8.98	38.8
Histone H1.5	00217468.3	HIST1H1B	8.04	80.1
Isoform 1 of triosephosphate isomerase	00465028.7	TPI1	8.01	36.4
Putative uncharacterized protein hnRNP D	00915340.1	HNRNPD	8.00	35.6
Annexin A1	00218918.5	ANXA1	8.00	31.2
Fus-like protein (Fragment)	00260715.5	FUS	7.74	40.9
Isoform A1-A of hnRNP A1	00465365.4	HNRNPA1	7.57	60.0
Histone H3.1	00465070.7	HIST1H3C	7.56	44.1
Endoplasmic reticulum protein ERp29	00024911.1	ERP29	7.11	22.2
hnRNP F	00003881.5	HNRNPF	6.96	35.9
Putative uncharacterized protein DKFZp564G0422	00553153.1	ATPIF1	6.75	54.2
Stress-70 protein, mitochondrial	00007765.5	HSPA9	6.70	30.9
Isoform 1 of hnRNP H3	00013877.2	HNRNPH3	6.61	43.1
Putative uncharacterized protein MSN (Fragment)	00872814.1	MSN	6.54	31.9
Upstream of NRAS isoform 3	00844264.7	CSDE1	6.52	24.9
40S ribosomal protein S19	00215780.5	RPS19	6.47	66.9
Tu translation elongation factor	00027107.5	TUFM	6.46	29.7
HSPA1A cDNA FLJ54392, highly similar to heat shock 70 kDa protein 1	00845339.1	HSPA1B	6.25	24.8
Endoplasmin	00027230.3	HSP90B1	6.24	15.2
Keratin, type II cytoskeletal 1	00220327.3	KRT1	6.19	20.6
Splicing factor, arginine/serine-rich 3, isoform CRA_a	00843996.1	SFRS3	6.17	71.0
45 kDa protein	00796333.1	ALDOA	6.15	23.0
Putative uncharacterized protein MECP2 (Fragment)	00872623.1	MECP2	6.05	26.2
Isoform 2 of DNA-binding protein A	00219147.4	CSDA	6.03	36.0
Sperm protein associated with the nucleus on the X chromosome B/F	00148062.1	SPANXF1	6.03	64.1
Protein disulfide isomerase family A,	00878546.1	PDIA2	6.02	23.4

member 2				
30 kDa protein	00472119.2	30 kDa protein	6.01	24.2
34 kDa protein	00872944.1	NUCKS1	6.00	29.6
Stathmin 1 isoform b	00921996.1	STMN1	6.00	31.6
cDNA FLJ52570, highly similar to splicing factor, arginine/serine-rich 2	00796848.1	SFRS2	6.00	40.2
cDNA, FLJ96792, highly similar to Homo sapiens calmodulin 2 (phosphorylase kinase, delta) (CALM2), mRNA	00916768.1	CALM2	6.00	40.3
Similar to ribosomal protein L23	00795408.1	RPL23	5.74	40.7
THO complex subunit 4	00328840.9	THOC4	5.62	40.1
Transcription factor A, mitochondrial	00020928.1	TFAM	5.57	33.3
heat shock 90kDa protein 1, alpha isoform 1	00382470.3	HSP90AA1	5.50	32.8
Isoform UBF2 of nucleolar transcription factor 1	00220833.1	UBTF	5.33	17.9
Enhancer of rudimentary homolog	00029631.1	ERH	5.32	44.2
Isoform 1 of eukaryotic translation initiation factor 5A-1	00411704.9	EIF5A	5.31	44.8
CFL1 Cofilin-1	00012011.6	CFL1	5.30	66.3
40S ribosomal protein S4, X isoform	00217030.1	RPS4X	5.10	29.7
Charged multivesicular body protein 4b	00025974.3	CHMP4B	5.05	18.8
Isoform 1 of RNA-binding protein raly	00216044.1	RALY	5.02	40.0
Activated RNA polymerase II transcriptional coactivator p15	00221222.7	SUB1	4.90	43.3
Isoform 2 of 60S ribosomal protein L11	00746438.2	RPL11	4.89	45.2
Isoform 8 of titin	00759542.1	TTN	4.88	8.10
Protein disulfide-isomerase	00010796.1	P4HB P	4.88	19.5
Isoform 1 of protein disulfide-isomerase A6	00644989.2	PDIA6	4.83	29.1
60S ribosomal protein L7a	00299573.1	RPL7A	4.77	28.2
PKM2 cDNA FLJ56065, highly similar to pyruvate kinase isozyme M1	00479186.6	PKM2	4.75	13.7
27 kDa protein	00926903.1	CHCHD3	4.69	25.4
Isoform 1 of caldesmon	00014516.1	CALD1	4.68	29.5
High mobility group protein B2	00219097.4	HMGB2	4.55	49.3
Laminin subunit beta-1	00013976.3	LAMB1	4.46	8.20
Histone H2B type 1-J	00515061.3	HIST1H2BJ	4.44	92.1
Histone H4	00453473.6	HIST1H4D	4.41	66.0
Peptidyl-prolyl cis-trans isomerase B	00646304.4	PPIB	4.39	33.8
18 kDa protein	00176755.4	Ribosomal 23	4.22	41.7

Isoform 1 of 60S ribosomal protein L12	00024933.3	RPL12	4.21	49.1
DnaJ homolog subfamily B member 11	00008454.1	DNAJB11	4.19	26.5
40S ribosomal protein S3	00011253.3	RPS3	4.17	30.0
Similar to RPL13 protein	00397611.2	RPL13P12	4.16	29.4
High mobility group protein B3	00217477.5	HMGB3	4.15	56.5
40S ribosomal protein S7	00013415.1	RPS7	4.07	32.0
Putative uncharacterized protein DKFZp686J1372	00642042.3	TPM3	4.04	29.3
Peroxiredoxin-2	00027350.3	PRDX2	4.02	36.9
Isoform 1 of cytoskeleton-associated protein 4	00141318.2	CKAP4 I	4.01	27.2
Serpin H1	00032140.4	SERPINH1	4.01	21.1
Profilin-1	00216691.5	PFN1	4.01	47.9
Histone H2A.x	00219037.5	H2AFX	4.00	58.7
Tubulin beta-2C chain	00007752.1	TUBB2C	4.00	27.2
26S protease regulatory subunit 7	00021435.3	PSMC2	4.00	24.7
46 kDa protein	00791301.1	TMPO	4.00	16.4
40S ribosomal protein S12	00013917.3	RPS12	4.00	31.1
60S ribosomal protein L14	00925323.1	RPL14 6	4.00	22.1
Ribosomal protein S21	00387084.1	RPS21	4.00	58.9
cDNA FLJ31776 fis, clone NT2RI2008141, highly similar to Calumenin	00789155.1	CALU	4.00	11.2
Chromobox protein homolog 3	00297579.4	CBX3	4.00	20.2
Small acidic protein	00003419.1	C11orf58	4.00	18.6
26S protease regulatory subunit 6A	00018398.4	PSMC3	3.98	12.5
40S ribosomal protein S30	00397098.1	FAU	3.70	49.1
Na(+)/H(+) exchange regulatory cofactor NHE-RF1	00003527.5	SLC9A3R1	3.70	16.2
40S ribosomal protein S14	00026271.5	RPS14	3.70	33.1
Sin3A-associated protein, 18kDa	00011698.4	SAP18	3.62	23.8
Cytochrome c oxidase subunit 5B	00021785.2	COX5B	3.52	48.1
interleukin enhancer binding factor 3 isoform d	00418313.3	ILF3	3.42	15.5
Isoform long of hnRNP U	00883857.1	HNRNPU	3.02	15.4
10 kDa heat shock protein	00220362.5	HSPE1	3.01	71.6
18 kDa protein	00796600.1	UBC	2.94	36.9
Putative uncharacterized protein RPL31	00917298.1	RPL31	2.93	34.6
cDNA FLJ59206, highly similar to Eukaryotic translation initiation factor 4B	00908588.1	FLJ59206	2.90	18.1
60S ribosomal protein L3	00550021.4	RPL3	2.90	14.9
Isoform 2 of polyadenylate-binding protein 2	00414963.2	PABPN1	2.85	16.6

Isoform 2 of Na(+)/H(+) exchange regulatory cofactor NHE-RF2	00398293.1	SLC9A3R2	2.82	26.4
NADH-ubiquinone oxidoreductase flavoprotein 3 isoform a precursor	00291016.8	NDUFV3	2.72	17.3
Alpha-2-macroglobulin receptor-associated protein	00026848.3	LRPAP1	2.66	24.1
Poly(rC)-binding protein 1	00016610.2	PCBP1	2.65	24.2
Ribosomal protein L28 isoform 3	00914529.1	RPL28	2.62	13.6
Isoform brain of clathrin light chain B	00014589.1	CLTB	2.49	20.1
ATP synthase subunit beta	00303476.1	ATP5B	2.38	17.6
Dihydrolipoyllysine-residue succinyltransferase component of 2-oxoglutarate dehydrogenase complex, mitochondrial	00420108.5	DLST	2.35	13.2
Isoform 3 of hnRNP K	00807545.1	HNRNPK	2.34	34.8
Splicing factor, arginine/serine-rich 9	00012340.1	SFRS9	2.33	29.9
LOC653884 hypothetical protein	00887543.1	LOC653884	2.33	51.4
Nascent polypeptide-associated complex subunit alpha-2	00007471.2	NACA2	2.33	18.1
Isoform 2 of filamin-C	00413958.4	FLNC	2.30	10.0
highly similar to 40S ribosomal protein S20	00794659.1	RPS20	2.25	18.3
Hypoxia up-regulated protein 1	00000877.1	HYOU1	2.24	12.6
RPS2 40S ribosomal protein S2	00013485.3	RPS2	2.21	35.5
Isoform 2 of nucleoside diphosphate kinase A	00375531.2	NME1	2.19	24.9
LIM domain and actin binding 1 isoform a	00883896.1	LIMA1	2.18	13.3
highly similar to Histone H2B type 2-F	00419833.8	HIST1H2BK	2.14	86.6
SRA stem-loop-interacting RNA-binding protein	00009922.3	C14orf156	2.11	34.9
hnRNP H2	00026230.1	HNRNPH2	2.10	32.1
Heat shock protein HSP 90-beta	00414676.6	HSP90AB1	2.10	21.0
60S ribosomal protein L22	00219153.4	RPL22	2.09	44.5
Alpha-enolase	00465248.5	ENO1	2.09	23.0
Similar to hCG1812668	00887758.1	RPL26P14	2.09	57.9
Ubiquinol-cytochrome c reductase hinge protein, isoform CRA_c	00872952.1	UQCRH	2.07	42.4
60S ribosomal protein L21	00247583.5	RPL21	2.05	46.3
Cystatin-B	00021828.1	CSTB	2.05	18.4
Highly similar to neutral alpha-glucosidase AB	00383581.4	GANAB	2.04	11.7
Nucleoprotein TPR	00742682.2	TPR	2.03	10.7
FK506-binding protein 3	00024157.1	FKBP3	2.03	13.8
20 kDa protein	00852745.1	MRPL40	2.03	22.2
Isoform 1 of hnRNP D-like	00011274.3	HNRPDL	2.02	21.9

glutamyl-prolyl tRNA synthetase	00923606.1	EPRS	2.02	9.90
Isoform 1 of histone deacetylase complex subunit SAP130	00748953.2	SAP130 I	2.02	3.70
Elongation factor 2	00186290.6	EEF2	2.02	16.7
hnRNP G	00304692.1	RBMX	2.01	28.9
Similar to 60S ribosomal protein L17	00844321.1	Ribosomal L22	2.01	24.5
Phosphoglycerate kinase 1	00169383.3	PGK1	2.01	18.7
11 kDa protein	00793102.1	RPL35A	2.01	24.5
Actin, cytoplasmic 2	00021440.1	ACTG1	2.00	36.5
Isoform 2 of hnRNP A3	00455134.1	HNRNPA3	2.00	50.0
Isoform HMG-Y of High mobility group protein HMG-I/HMG-Y	00177716.7	HMGA1	2.00	70.8
PRDX4 Protein	00639945.1	PRDX4	2.00	26.7
69 kDa protein	00872684.1	EZR	2.00	24.1
High mobility group protein B3-like-1	00006437.2	HMGB3L1	2.00	49.2
Histone H1x	00021924.1	H1FX	2.00	25.8
cDNA FLJ38664 fis, clone HLUNG2002334, highly similar to Homo sapiens KH domain containing, RNA binding, signal transduction associated 2 (KHDRBS2)	00903310.1	FLJ38664 KHDRBS2	2.00	16.7
Isoform 2 of ATP synthase subunit d, mitochondrial	00456049.3	ATP5H	2.00	25.5
LisH domain-containing protein C16orf63	00043563.3	C16orf63	2.00	14.4
hnRNP A0	00011913.1	HNRNPA0	2.00	27.9
Serine hydroxymethyltransferase	00002520.1	SHMT2	2.00	26.8
Electron transfer flavoprotein, alpha polypeptide isoform b	00895865.1	ETFA	2.00	14.8
Staufen isoform c	00643664.1	STAU1	2.00	27.9
NUMA1 variant protein	00872028.1	NUMA1	2.00	15.6
Isoform 7 of transcription factor TFIIIB component B homolog	00893272.1	BDP1	2.00	7.90
EBNA1 binding protein 2	00745955.3	EBNA1BP2	2.00	38.8
Kinesin-1 heavy chain	00012837.1	KIF5B	2.00	14.7
cDNA FLJ57496, moderately similar to tubulin-specific chaperone A	00909626.1	FLJ57496	2.00	17.8
cDNA FLJ60539, highly similar to Nucleosome assembly protein 1-like 1	00797545.2	NAP1L1	2.00	5.70
Isoform 1 of calcyclin-binding protein	00395627.3	CACYBP	2.00	8.80
Prohibitin variant (fragment)	00791634.1	PHB	2.00	29.8
Putative uncharacterized protein DKFZp686E2459	00375731.1	RBM10	2.00	6.30
Highly similar to major vault protein	00910019.1	FLJ53437	2.00	8.40
19 kDa protein	00883946.1	LASP1	2.00	40.4
Septin 9 isoform c	00784936.1	SEPT9	2.00	9.00

Ribosomal protein S8	00645201.1	RPS8	2.00	30.3
UPF0027 protein C22orf28	00550689.3	C22orf28	2.00	6.90
Prohibitin-2	00027252.6	PHB2	2.00	22.1
Isoform 3 of protein LSM14 homolog B	00471933.5	LSM14B	2.00	30.1
11 kDa protein	00794121.1	RPL30	2.00	26.0
GP2 cDNA FLJ56017, highly similar to pancreatic secretory granule membrane major glycoprotein GP2	00299429.8	FLJ56017	2.00	10.7
Proteasome subunit alpha type-6	00029623.1	PSMA6	2.00	13.4
Small nuclear ribonucleoprotein D2	00017963.1	SNRPD2	2.00	26.3
Isoform 2 endothelial differentiation-related factor 1	00006362.1	EDF1	2.00	28.8
Putative uncharacterized protein WIBG (Fragment)	00914992.1	WIBG	2.00	19.2
- cDNA FLJ57742	00910288.1	FLJ57742	2.00	16.3
Putative uncharacterized protein HBE1	00853641.1	HBE1	2.00	27.6
Cysteine and glycine-rich protein 1	00442073.5	CSRP1	2.00	9.80
Prefoldin subunit 4	00015891.1	PFDN4	2.00	29.1
21 kDa protein	00644034.1	CD99	2.00	11.4
PHD finger-like domain-containing protein 5A	00005511.1	PHF5A	2.00	12.7
NADH dehydrogenase [ubiquinone] 1 alpha subcomplex subunit 5	00554681.2	NDUFA5	2.00	8.60
Eukaryotic translation initiation factor 3 subunit I	00012795.3	EIF3I	2.00	3.40
cDNA FLJ60076, highly similar to ELAV-like protein 1	00301936.4	ELAVL1	1.93	24.9
Major histocompatibility complex, class I, A	00785070.4	HLA-A	1.77	19.1
Topoisomerase (DNA) I	00902597.2	TOP1	1.76	29.0
Isoform 1 of apoptotic chromatin condensation inducer in the nucleus	00007334.1	ACIN1	1.75	23.0
Keratin, type I cytoskeletal 10	00009865.2	KRT10	1.74	11.3
Protein CTF18 homolog	00178203.1	CHTF18	1.73	10.0
Histone H2B type 1-M	00554798.2	HIST1H2BM	1.70	93.7
Histone H1.3	00217466.3	HIST1H1D	1.70	66.5
hnRNP R isoform 1	00644055.3	HNRNPR	1.70	31.8
DnaJ homolog subfamily A member 1	00012535.1	DNAJA1	1.70	33.0
Isoform 1 of SLIT and NTRK-like protein 2	00176104.1	SLITRK2	1.70	3.80
Isoform 1 of protein SET	00072377.1	SET	1.70	20.0
41 kDa protein	00794875.1	PA2G4	1.70	18.5
Vitronectin	00298971.1	VTN	1.70	11.3
Isoform 1 of synemin	00299301.1	SYNM	1.59	14.5

Isoform 4 of nesprin-1	00247295.3	SYNE1	1.57	10.1
Reticulocalbin-1	00015842.1	RCN1	1.55	11.2
Stomatin-like protein 2	00334190.4	STOML2	1.52	17.7
LOC728470 similar to hCG1736317	00887971.1	LOC728470	1.52	6.80
Isoform 1 of centrosomal protein of 290 kDa	00784201.1	CEP290	1.42	14.0
Proteasome 26S ATPase subunit 6	00926977.1	PSMC6	1.41	19.6
Tankyrase-2	00019270.1	TNKS2	1.40	6.90
Peroxisome proliferator-activated receptor gamma coactivator 1-alpha	00033138.1	PPARGC1A	1.40	15.0
- 19 kDa protein	00445053.1	- 19 kDa protein	1.40	7.10
N-acetyltransferase 5 isoform c	00375483.2	NAT5	1.40	6.30
Teneurin-2	00182194.7	ODZ2	1.34	6.70
BAI1-associated protein 3	00828007.1	BAIAP3	1.34	5.80
Isoform 1 of ATP-binding cassette sub-family A member 8	00479296.2	ABCA8	1.31	5.80
Isoform 1 of protein phosphatase 1 regulatory subunit 14A	00059135.1	PPP1R14A	1.30	46.9
Highly similar to probable ATP-dependent RNA helicase DDX5	00798375.2	DDX5	1.30	13.8

APPENDIX H

QUANTIFICATION OF NMPS IN DCIS CELL LINES

Table 24: Ratios obtained for NMPs in several cell line in comparison to the JLDCIS-1Contra line.

Protein Name	JLBRL-14	JLBRL-24	JL NTAL DCIS-1	JL DCIS-1A	MCF-7	MDA-MB 231
- 19 kDa protein	0.0111					
18 kDa protein				0.112		
26S protease regulatory subunit 6A		0.0112				0.0126
26S protease regulatory subunit 7	0.0631					
40S ribosomal protein S19	0.142			0.119		
40S ribosomal protein S3	0.3162		0.661	0.661		
40S ribosomal protein S30			0.0111			
40S ribosomal protein S7	0.0291					
51 kDa protein		0.0421				
60 kDa heat shock protein			0.106		6.03	
60S ribosomal protein L7a				7.24		
60S ribosomal protein L8	5.50	8.09	8.55	9.20		
69 kDa protein	0.0111					
Activated RNA polymerase II transcriptional coactivator p15	0.0759		0.0225			
Annexin A1					0.565	
Annexin A2 isoform 1			0.0679	0.187	1.906	
ATP synthase subunit alpha, mitochondrial		6.98			8.32	
cDNA FLJ31776 fis, clone NT2RI2008141, highly similar to Calumenin					0.0661	
cDNA FLJ52570, highly similar to splicing factor, arginine/serine-rich 2	8.71	6.19		7.66	28.3	13.9
cDNA FLJ60076, highly similar to	0.129		0.0111			0.136

ELAV-like protein 1						
Chromobox protein homolog 3	0.0277					
Elongation factor 1-beta	0.233		0.0387	0.0319	0.172	0.236
Eukaryotic translation elongation factor 1 delta isoform 3				0.0545	0.247	
Filamin B					0.145	0.184
Fus-like protein (Fragment)				0.0350		
glutamyl-prolyl tRNA synthetase	0.0126					
Glyceraldehyde-3-phosphate dehydrogenase	0.597					
heat shock 90kDa protein 1, alpha isoform 1				0.331	3.53	1.87
Heat shock protein beta-1			4.45			
Heat shock protein HSP 90-beta	0.384	0.258				
High mobility group protein B1	0.161	0.111	0.0711		1.91	
High mobility group protein B2	0.092	0.020	0.047			
Histone H1.2			0.409	0.0322	0.366	0.506
Histone H1.4	0.515			0.040	0.146	0.413
Histone H4	0.229	0.0474			0.340	0.511
hnRNP F	0.738	1.24	0.143	0.147		
hnRNP H2						0.0187
HSPA1A cDNA FLJ54392, highly similar to heat shock 70 kDa protein 1	0.110					
HSPA5 protein					3.10	3.37
Hypoxia up-regulated protein 1	0.0511					
Isoform 1 of eukaryotic translation initiation factor 5A-1	0.0111					
Isoform 1 of Heat shock cognate 71 kDa protein		0.0955	0.161			
Isoform 1 of hnRNP Q	0.0912		0.0296		13.1	0.105
Isoform 1 of Nucleophosmin	0.179	0.151	0.0322	0.0316	0.0592	0.138
Isoform 1 of protein disulfide-isomerase A6			87.9		86.3	
Isoform 1 of RNA-binding protein raly	6.08	3.44	4.49	0.724	4.06	8.79
Isoform 1 of synemin	0.0114					
Isoform 1 of triosephosphate isomerase	0.637	6.98		5.70	4.74	4.61
Isoform 2 of hnRNP M		0.294				
Isoform 2 of polyadenylate-binding protein 1			0.0196	0.0766	1.854	
Isoform 3 of hnRNP K			0.0417	0.101		0.146
Isoform 3 of plectin-1		0.090				
Isoform A of Lamin-A/C	0.203		0.0766		0.160	
Isoform ASF-1 of splicing factor, arginine/serine-rich 1			0.470		7.80	

Isoform B1 of hnRNP A2/B1		0.141	0.0231	0.0211	0.545	1.98
Isoform brain of clathrin light chain B	0.100	0.256		0.138		
Isoform HMG-I of high mobility group protein HMG-I/HMG-Y		0.0380				
Isoform long of hnRNP U	0.194		0.0113			0.0113
Isoform long of splicing factor, proline- and glutamine-rich			0.119			
Isoform UBF2 of nucleolar transcription factor 1					22.3	
Keratin 7				0.0608		
Keratin, type I cytoskeletal 18					6.14	
Keratin, type II cytoskeletal 8	0.115	2.81		0.242		0.115
Lamin-B1						5.20
Lamin-B2						7.94
Laminin subunit gamma-1		36.3	5.01	4.21		
LOC653884 hypothetical protein	0.0655					
LOC728470 similar to hCG1736317	0.0191		0.0191			
NADH-ubiquinone oxidoreductase flavoprotein 3 isoform a precursor	0.0581					
Neuroblast differentiation-associated protein AHNAK	0.0887	0.0328	0.0377	0.0809	0.0409	0.196
Nuclease-sensitive element-binding protein 1		0.0449	0.363	0.360	0.215	
Nucleolin	0.0920	0.0643	0.0256	0.0545	0.344	0.154
p180/ribosome receptor					0.187	
Peroxiredoxin-1						0.0497
Peroxiredoxin-2	0.0946					
PKM2 cDNA FLJ56065, highly similar to pyruvate kinase isozyme M1	1.05	20.0	15.7	29.1	30.8	22.7
Prohibitin-2						0.0156
Proteasome subunit alpha type-6			0.0118			
Putative elongation factor 1-alpha-like	0.413		0.121		0.0802	0.366
Putative uncharacterized protein ALB	1.66	10.0	2.63		1.85	1.41
Putative uncharacterized protein DKFZp564G0422					3.56	
Putative uncharacterized protein DKFZp686J1372	0.0111					
Putative uncharacterized protein hnRNP AB			0.056	0.353	2.83	0.413
Putative uncharacterized protein hnRNP D			0.028			
Putative uncharacterized protein SPTAN1	0.126					
Ribosomal protein S21			0.0111			

Serine hydroxymethyltransferase	0.0158					
Similar to 40S ribosomal protein S28					0.357	
Similar to ribosomal protein L23	0.809					
Sperm protein associated with the nucleus on the X chromosome B/F			1.01	13.8		
Splicing factor, arginine/serine-rich 3, isoform CRA_a	0.809				2.94	
SRA stem-loop-interacting RNA-binding protein						0.0724
THO complex subunit 4		0.297	0.118		0.137	
Transcription factor A, mitochondrial					12.7	
Tu translation elongation factor					5.55	
Tubulin beta chain		0.766				
Ubiquinol-cytochrome c reductase hinge protein, isoform CRA_c	0.0149					
Vimentin	0.133	0.461	0.0619	0.109	0.129	0.305

BIBLIOGRAPHY

Akiyama, T.; Ishida, J.; Nakagawa, S.; Ogawara, H.; Watanabe, S.; Itoh, N.; Shibuya, M.; Fukami, Y. Genistein, a specific inhibitor of tyrosine-specific protein kinases. J Biol Chem, 1987, 262, 5592-5595.

Albini, A.; Benelli, R.; Noonan, D.M.; Brigati, C. The "chemoinvasion assay": a tool to study tumor and endothelial cell invasion of basement membranes. Int J Dev Bio, 2004, 48, 563-571.

Alexander, R.B.; Greene, G.L.; Barrack, E.R. Estrogen receptors in the nuclear matrix: direct demonstration using monoclonal antireceptor antibody. Endocrinology, 1987, 120, 1851-1856.

Allen, S.; Berezney, R.; Coffey, D.S. Phosphorylation of nuclear matrix proteins during rat liver regeneration. Biochem Biophys Res Comm, 1977, 75, 111-116.

American Cancer Society Breast Cancer Facts and Figures 2007-2008; ACS 2007.

American Cancer Society Cancer Facts & Figures 2009. Atlanta: ACS, 2009.

Asai, D.J.; Koonce, M.P. The dynein heavy chain: structure, mechanics and evolution. Trends Cell Biol, 2001,11, 196-202.

Badve, S.; Wiley, E.; Rodriguez, N. Assesment of utility of ductal lavage and ductoscopy in breast cancer -- A retrospective analysis of mastectomy specimens. Mod Pathol, 2003, 16, 206-209.

Bagatell, R.; Khan, O.; Paine-Murrieta, G.; Taylor, C.W.; Akinaga, S.; Whitesell, L. Destabilization of steroid receptors by heat shock protein 90-binding drugs. Clin Cancer Res, 2001, 7, 2076-2082.

Bahia, H.; Ashman, J.N.; Cawkwell, L.; Lind, M.; Monson, J.R.; Drew, P.J.; Greenman, J. Karyotypic variation between independently cultured strains of the cell line MCF-7 identified by multicolor fluorescence in situ hybridization. Int J Oncol, 2002, 20, 489-494.

Balasubramani, M.; Day, B.W.; Schoen, R.E.; Getzenberg, R.H. Altered expression and localization of creatine kinase B, heterogeneous nuclear ribonucleoprotein F, and high

mobility group box 1 protein in the nuclear matrix associated with colon cancer. Cancer Res, 2006, 66, 763-769.

Barbaro,P.; D'Arrigo, C.; Repaci, E.; Bagnasco, L.; Oreccha, P.; Carnemoola, B.; Patrone, E.; Balbi, C. Proteomic analysis of the nuclear matrix in the early stages of rat liver carcinogenesis: identification of differentially expressed MAR-binding proteins. Exp Cell Res, 2009, 315, 226-239.

Bardin, A.; Boulle, N.; Lazennec, G.; Vignon, F.; Pujol, P. Loss of ERβ expression as a common step in estrogen-dependent tumor progression. Endocr Relat Cancer, 2004, 11, 537-551.

Barrack, E.R.; Coffey, D.S. Biological properties of the nuclear matrix: steroid hormone binding. Recent Prog Horm Res, 1982, 38, 133-195.

Barrack, E.R.; Coffey, D.S. The specific binding of estrogens and androgens to the nuclear matrix of sex hormone responsive tissues. J Biol Chem, 1980, 255, 7265-7275.

Barrack, E.R.; Hawkins, E.F.; Allen, S.L.; Hicks, L.; Coffey, D.S. Concepts related to salt-resistant estradiol receptors in rat uterine nuclei: nuclear matrix. Biochem Biophys Res Comm, 1977, 79, 829-836.

Berezney, R., J. Basler, B. B. Hughes, S. C. Kaplan. Isolation and characterization of the nuclear matrix from Zajdela ascites hepatoma cells. Cancer Res, 1979, 39, 3031-3039.

Berezney, R.; Coffey, D.S. Identification of a nuclear matrix protein. Biochem Biophys Res Comm, 1974, 60, 1410-1417.

Berezney, R.; Coffey, D.S. Nuclar protein matrix: association with newly synthesized DNA. Science, 1975, 189, 291-293.

Berg, W.A.; Guierrez, L.; NessAiver, M.S.; Carter, W.B.; Bhargavan, M.; Lewis, R.S.; Ioffe, O.B. Diagnostic accuracy of mammography, clinical examinatione, US, and MR imagingin preoperative assesment of breast cancer. Radiology, 2004, 233, 830-849.

Berry, M.; Nunez, P.; Chambon, P. Estrogen response element of the human pS2 gene is an imperfectly palindromic sequence. Proc Natl Acad Sci USA, 1989, 139, 1981-1990.

Berx, G.; Roy, F.V. He E-cadherin/catenin complex: an important gatekeeper in breast cancer tumorigenesis and malignant progression. Breast Cancer Res, 2001, 3, 289-293.

Boos, G.; Stopper, H. Genotoxicity of several clinically used topoisomerase II inhibitors. Toxicol Lett, 2006, 116, 7-16.

Borquist, S.; Holm, C.; Stendahl, M.; Anagnostake, L.; Landberg, G.; Jirström. Oestrogen receptors alpha and beta show different associations to clinicopathological parameters and their co-expression might predict a better response to endocrine treatment in breast cancer. J Clin Pathol, 2008, 61, 197-203.

Bronzert, D.A.; Greene, G.L.; Lippman, M.E. Selection and characterization of a breast cancer cell line resistant to the antiestrogen LY 117018. Endocrinology, 1985, 117, 1409-1417.

Brünagel, G.; Schoen, R.E.;Bauer, A.J.; Vietmeier, B.N.; Getzenberg, R.H. Nuclear matrix protein alterations associated with colon cancer metastasis to the liver. Clin Cancer Res, 2002B, 8, 3039-3045.

Brünagel, G.; Vietmeier, B.N.; Bauer, A.J.; Schoen, R.E.; Getzenberg, R.H. Identification of nuclear matrix protein alterations associated with human colon cancer. Cancer Res, 2002A, 62, 2437-2442.

Brunner, N.; Frandsen, T. L.; Holst-Hansen, C.; Bei, M.; Thompson, E. W.; Wakeling, A. E.; Lippman, M. E.; Clarke, R. MCF7/LCC2: a 4-hydroxytamoxifen resistant human breast cancer variant that retains sensitivity to the seteroidal antiestrogen ICI 182,780. Cancer Res 1993, 53, 3229-3232.

Brzozowski, A.M.; Pike, A.C.; Dauter, Z.; Hubbard, R.E.; Bonn, T.; Engström, O.; Ohman, L.; Greene, G.L.; Gustafsson, J.A.; Carlquist, M. Molecular basis of agonism and antagonism in the oestrogen receptor. Nature, 1997, 389, 753-758.

Bunone, G.; Birand, P.A.; Miksicek, R.J.; Picard, D. Activation of the unliganded estrogen receptor by EGF involves the MAP kinase pathway and direct phosphorylation. EMBO J, 1996, 15, 2174-2183.

Burdall, S.E.; Hanby, A.M.; Lansdown, M.R.J.; Speirs, V. Breast cancer cell lines: friend or foe? Breast Cancer Res, 2002, 5, 89-95.

Burnside, E.S.; Park, J.M.; Fine, J.P.; Sisney, G.A. The use of batch reading to improve the performance of screening mammography. Am J Roentgenol, 2005, 185, 790-796.

Cailleau, R.; Olivé, M.; Cruciger, Q.V.J. Long-term human breast carcinoma cell lines of metastatic origin: preliminary characterization. In Vivo Cell Dev Biol, 1978, 14, 911-915.

Campbell, R.A.; Bhat-Naksatri, P.; Patel, N.M.; Constantinidou, D.; Ali, S. Phosphatidylinositol 3-kinase/AKT-mediated activation of estrogen receptor alpha: a new model for anti-estrogen resistance. J Biol Chem, 2001, 276, 9817-9824.

Carpenter, B.; MacKay, C.; Alnabulsi, A.; MacKay, M.; Telfer, C.; Melvin, W.T.; Murray, G.I. The roles of heterogeneous nuclear ribonucleoproteins in tumour development and progression. Biochim Biophys Acta, 2006, 1765, 85-100.

Carroll, J.S.; Brown, M. Estrogen receptor target gene: an evolving concept. Mol Endocrinology, 2006, 20, 1707-1714.

Chan, K.K.L.; Wei, N.; Liu, S.S.; Xiao-Yun, L.; Cheung, A.N.; Ngan, H.Y.S. Estrogen receptor subtypes in ovarian cancer: a clinical correlation. Obstetr Gynecol, 2008, 111, 144-151.

Cheung, J.; Smith, D.F. Molecular chaperone interactions with steroid receptors: an update. Mol Endocrinology, 2000, 14, 939-946.

Cho, M.A.; Lee, M.K.; Nam, K.; Chung, W.Y.; Park, C.; Lee, J.H.; Noh, T.; Yang, W.; Rhee, Y.; Lim, S.; Lee, H.C.; Lee, E.J. Expression and role of estrogen receptor α and β in medullary thyroid carcinoma: different roles in cancer growth and apoptosis. J Endocrinology, 2007, 195, 255-263.

Choi, Y.D.; Dreyfuss, G. Isolation of the heterogeneous nuclear RNA-ribonucleoprotein complex (hnRNP): a unique supramolecular assembly. Proc Natl Acad Sci USA, 1984, 81, 7471-7475.

Ciejek, E.M.; Nordstrom, J.L.; Tsai, M.J.; O'Malley, B.W. Ribonucleic acid precursors are associated with the chick oviduct nuclear matrix. Biochemistry, 1982, 22, 4945-4953.

Clark, G.M.; McGuire, W.L.; Hubay, C.L.; Pearson, O.H.; Carter, A.C. The importance of estrogen and progesterone receptor in primary breast cancer. Prog Clin Biol Res, 1983, 132E, 183-190.

Clark, J.H; W.T. Schrader and B.W. O'Malley, Mechanisms of action of steroid hormones. In: J.D. Wilson and D.W. Foster, Editors, Williams Textbook of Endocrinology, W. B. Saunders, New York, U.S.A. (1992), pp. 35–90.

Clarke, R.; Brunner, N. Acquired estrogen independence and antiestrogen resistance in breast cancer: estrogen receptor driven phenotypes? Trends Endocrinology Metab, 1996, 7, 291-301.

Cobleigh, M.A; Vogel, C.L.; Tripathy, D.; Robert, N.J.; Scholl, S.; Fehrenbacher, L.; Wolter, J.M.; Paton, V.; Shak, S.; Lieberman, G.; Slamon, D.J. Multifunctional study of the efficacy and safety of humanized anti-HER2 monoclonal antibody in women who have HER2-overexpressing metastatic breast cancer that has progressed after chemotherapy for metastatic disease. J Clin Oncol, 1999, 17, 2639-2648.

Cottone, E.; Orso, F.; Biglia, N.; Sismondi, P.; De Bortoli, M. Role of coactivators and corepressors in steroid and nuclear receptor signaling: potential markers of tumor growth and drug sensitivity. Int J Biol Markers, 2001, 16, 151-166.

Coutts, A.S.; Davie, J.R.; Dotzlaw, H.; Murphy, L.C. Estrogen regulation of nuclear matrix-intermediate filament proteins in human breast cancer cells. J Cell Biochem, 1998, 63, 174-184.

Creighton, C.J.; Hilger, A.M.; Murthy, S.; Rae, J.M.; Chinnaiyan, A.M.; El-Ashry, D. Activation of mitogen-activated protein kinase in estrogen receptor alpha-positive breast cancer cells in vitro induces an in vivo molecular phenotype of estrogen receptor alpha-negative human breast tumors. Cancer Res, 2006, 66, 3903-3911.

Cronin, M.; Pho, M.; Dutta, D.; Stephans, J.C.; Shak, S.; Kiefer, M.C.; Esteban, J.M.; Baker, J.B. Measurement of gene expression in archival paraffin-embedded tissues. Am J Pathol, 2004, 164, 35-42.

Dang, C.V. C-Myc target genes involved in cell growth, apoptosis, and metabolism. Mol Cell Biol, 1999, 19, 1-11.

Davido, T.; Getzenberg, R.H. Nuclear matrix proteins as cancer markers. J Cell Biochem, 2000, 35, 136-141.

De Bortoli, M.; Castellino, R.C.; Lu, X.; Deyo, J.; Sturla, L.M.; Adesina. A.M.; Perlaky, L.; Pomeroy, S.L.; Lau, C.C.; Man, T.; Rao, P.H.; Kim, J.Y.H. Medulloblastoma outcome is adversely associated with overexpression of EEF1D, RPL30, and PRS20 on the long arm of chromosome 8. BMC Cancer, 2006, 6, 233.

Dillner, N.B.; Sanders, M.M. The zinc finger/homeodomain protein δEf1 mediates estrogen-specific induction of the ovalbumin gene. Mol Cell Endocrinology, 2002, 192, 85-91.

Dillner, N.B.; Sanders, M.M.; Transcriptional activation by the zinc-finger homeodomain protein δEF1 in estrogen signaling cascades. DNA Cell Biol, 2004, 23, 25-34.

Dinney, C.; Fishbeck, R.; Singh, R.; Eve, B.; Pathak, S.; Brown, N.; Xie, B.; Dan, D.; Bucana C.; Fidler, I. Isolation and characterization of etastatic variants from human transitional cell carcinoma passaged by orthotopic implantatin in athymic nude mice. J Urol, 1995, 154, 1532-1538.

Djabeli, K.; Portier, M.M.; Gros, F.; Biobel, G.; Georgatos, S.D. Network antibodies identify nuclear lamin B as a physiological attachment site for peripherin intermediate filaments. Cell, 1991, 11, 109-121.

Dobrzycka, K.M.; Townson, S.M.; Jiang, S.; Oesterreich, S. Eestrogen receptor corepressors – a role in human breast cancer? Endocr Relat Cancer, 2003, 10, 517-536.

Dubik, D.; Dembinski, T.C.; Shiu, R.P.C. Stimulation of c-myc oncogene expression associated with estrogen-induced proliferation of human breast cancer cells. Cancer Res, 1987, 47, 6517-6521.

Early Breast Cancer Trialists' Collaborative Group. Effects of chemotherapy and hormonal therapy for early breast cancer on recurrence and 15-year survival: an overview of the randomised trails. Lancet, 2005, 365,1687-1717.

Earnshaw, W.C.; Heck, M.M. Localization of topoisomerase I in mitotic chromosomes. J Cell Biol, 1985, 100, 1716-1725.

Edsall Jr., R.J.; Harris, H.A.; Manas, E.S.; Mewshaw, R.E. Erβ ligands, part 1: the discovery of ERβ selective ligands which embrace the 4-hydroxy-biphenyl template. Bioorg Med Chem, 2003, 11, 3457-3474.

Eeckhoute, J.; Carroll, J.S.; Geistlinger, T.R.; Torres-Arzayus, M.I.; Brown, M. A cell-type-specific transcriptional network reguired for estrogen regulation of cyclin D1 and cell cycle progression in breast cancer. Genes Dev, 2006, 20, 2513-2526.

Eger, A.; Aigner, K.; Sonderegger, S.; Dampier, B.; Oehler, S.; Schreiber, M.; Berx, G.; Cano, A.; Beug, H.; Foisner, R. DeltaEF1 is a transcriptional repressor of E-cadherin and regulates epithelial plasticity in breast cancer cells. Oncogene, 2005, 24, 2375-2385.

Eger, A.; Stockinger, A.; Schaffhauser, B.; Beug, H.; Foisner, R. J Cell Biol, 2000, 148, 173-188.

Emmen, J.M.A.; Couse, J.F.; Elmore, S.A.; Yates, M.M.; Kissling, G.E.; Korach, K.S. In vitro growth and ovulation of follicles from ovaries of estrogen receptor (ER)α and ERβ null mice indicate a role for ERβ in follicular maturation. Endocrinology, 2005, 146, 2817-2826.

Enmark, E.; Pelto-Huikko, M.; Grandien, K.; Lagercrantz, S.; Lagercrantz, J.; Fried, G.; Nordenskjold, M.; Gustafsson, J.A. Human estrogen receptor beta-gene structure, chromosomal localization and expression pattern. J Clin Endocrinology Metab, 1997, 82, 4258-4265.

Esslimani-Sahla, M.; Simony-Lafontaine, J.; Kramar, A.; Lavaill, R.; Mollevi, C.; Warner, M.; Gustafsson, J.; Rochefort, H. Estrogen receptor β (Erβ) level but not its Erβcx variant helps to predict tamoxifen resistance in breast cancer. Clin Cancer Res, 2004, 10, 5769-5776.

Etzioni, R.; Urban, N.; Ramsey, S.; McIntosh, M.; Schwartz, S.; Reid, B.; Radich, J.; Anderson, G.; Hartwell, L. The case for early detection. Nat Rev Cancer, 2003, 3, 243-252.

Evans, C.T.; Ledesma, D.B.; Schulz, T.Z.; Simpson, E.R.; Mendelsen, C.R. Isolation and characterization of a complementary DNA specific human aromatase-system cytochrome P-450 mRNA. Proc Natl Acad Sci USA, 1986, 83, 6387-6391.

Evinger, A.J.; Levin, E.R. Requirements for estrogen receptor a membrane localization and function. Steroids, 2005, 70, 361-363.

Fan, P.; Wang, J.; Santen, R.J.; Yue, W. Long-term treatment with tamoxifen facilitates translocation of estrogen receptor alpha out of the nucleus and enhances its interaction with EGFR in MCF-7 breast cancer cells. Cancer Res, 2007, 67, 1352-1360.

Fawell S.E.; White, R.; Hoare, S.; Sydenham, M.; Page, M.; Parker, M.G. Inhibition of estrogen receptor-DNA binding by the "pure" antiestrogen ICI 164,384 appears to be mediated by impaired receptor dimerization. Proc Natl Acad Sci USA, 1990, 87, 6883-6887.

Fey, E.G.; Penman, S. Nuclear matrix proteins reflect cell type origin in cultured human cells. Proc Natl Acad Sci USA, 1988, 85, 121-125.

Frasor, J.; Danes, J.M.; Komm, B.; Chang, K.C.N.; Lyttle, C.R.; Katzenellenbogen, B.S. Profiling of estrogen up- and down-regulated gene expression in human breast cancer cells: insights into gene networks and pathways underlying estrogenic control of proliferation and cell phenotype. Endocrinology, 2003, 144, 4562-4574.

Fukuda, A.; Nakadi, T.; Shimada, M.; Hisatake, K. Heterogeneous nuclear ribonucleoprotein R enhances transcription from the naturally-configured c-fos promoter in vitro. J Biol Chem, 2009, doi 10.1074.

Gee, J.M.; Harper, M.E.; Hutchenson, I.R.; Madden, T.A.; Barrow, D.; Knowlden, J.M.; McClelland, R.A.; Jordan, N.; Wakeling. A.E.; Nicholson, R.I. The antiepidermal growth factor receptor agent gefitinib (ZD 1839/Iressa) improves antihormone response and prevents development of resistance in breast cancer in vitro. Endocrinology, 2003, 144¸1032-1044.

Georgatos, S.D.; Blobel, G. Lamin B constitutes an intermediate filament attachment site at the nuclear envelope. J Cell Biol, 1987, 105, 117-125.

Getzenberg, R.H.; Pienta, K.J.; Coffey, D.S. The tissue matrix: cell dynamics and hormone action. Endocr Rev, 1990, 11, 399-417.

Getzenberg, R.H.; Pienta, K.J.; Huang, E.Y.W.; Coffey, D.S. Identification of nuclear matrix proteins in the cancer and normal rat prostate. Cancer Res, 1991B, 51, 6514-6520.

Getzenberg, R.H.; Pienta, K.J.; Huang, E.Y.W.; Murphy, B.C.; Coffey, D.S. Modifications of the intermediate filament and nuclear matrix networks by the extracellular matrix. Biochem Biophys Res Comm, 1991A, 179, 340-344.

Girault, I.; Lerebours, F.; Amarir, S.; Tozlu, S.; Tubiana-Hulin, M.; Lidereau, R.; Bièche. Expression analysis of estrogen receptor alpha coregualtors in breast carcinoma: evidence that NCOR1 expression is predictive of the response to tamoxifen. Clin Cancer Res, 2003, 9, 1259-1266.

Glen, A., C. S. Gan, F. C. Hamdy, C. L. Eaton, S. S. Cross, J. W. F. Catto, P. C. Wright, I. Rehman. iTRAQ-facilitated proteomic analysis of human prostate cancer cells identifies proteins associated with progression. J Proteome Res, 2008, 7, 897-907.

Gobert, G.N.; Hueser, C.N. Curran, E.M.; Sun, Q.; Glinsky, V.V.; Welshons, W.V.; Eisentark, A.; Schatten, H. Immunolocalization of NuMA and phosphorylated proteins during the cell cycle in human breast and prostate cancer cells as analyzed by immunofluorescence and postembedding immunoelectron microscopy. Histochem Cell Biol, 2001, 115, 381-395.

Graham, K.A.; Richardson, C.L.; Minden, M.D.; Trent, J.M.; Buick, R.N. Varying degrees of amplification of the N-ras oncogene in the human breast cancer cell line MCF-7. Cancer Res, 1985, 45, 2201-2205.

Graham, K.A.; Trent, J.M.; Osborne, C.K.; McGrath, C.M.; Minden, M.D.; Buick, R.N. The use of restriction fragment polymorphisms to identify the cell line MCF-7. Breast Cancer Res Treat, 1986, 8, 29-34.

Green, S.; Walter, P.; Greene, G.; Krust, A.; Goffin, C.; Jensen, E.; Scrace, G.; Waterfield, M.; Chambon, P. Cloning of the human oestrogen receptor cDNA. J Steroid Biochem, 1986B, 24, 77-83

Green, S.; Walter, P.; Kumar, V.; Krust, A.; Bornert, J.M.; Argos, P.; Chambon, P. Human oestrogen receptor cDNA: sequence, expression, and homology to v-erb-A. Nature, 1986A, 320, 134-139.

Greene, G.L.; Gilna, P.; Waterfield, M.; Baker, A.; Hort, Y.; Shine, J. Sequence and expression of human estrogen receptor complementary DNA. Science, 1986, 231, 1150-1154.

Gruber, C.J.; Gruber, D.M.; Gruber, I.M.; Wieser, F.; Huber, J.C. Anatomy of the estrogen response element. Trends Endocrinology Metab, 2004, 15, 73-78.

Gutierrez, M.C.; Detre, S.; Johnston, S.; Mohsin, S.K.; Shou, J.; Allred, D.C.; Schiff, R.; Osborne, C.K.; Dowsett, M. Molecular changes in tamoxifen-resistant breast cancer: relationships between estrogen receptor, HER2, and p38 mitogen-activated protein kinase. J Clin Oncol, 2005, 23, 2469-2476.

Hall, J.M.; Couse, J.F.; Korach, K.S. The multifactorial mechanisms of estradiol and estrogen receptor signalling. J Biol Chem, 2001, 276, 36869-36872.

Hammerich-Hill, S.; Bardout, V.J.; Hilsenbeck, S.G.; Osborne, C.K.; Osterreich, S. Low SAFB levels are associated with worse outcome in breast cancer patients. Breast Cancer Res Treat, 2009,

Harris, H.A. Estrogen receptor-β: recent lessons from in vivo studies. Mol Endocrinology, 2007, 21, 1-13.

Harris, H.A.; Albert. L.M.; Leathurby, Y.; Malamas, M.S.; Mewshaw, R.E.; Miller, C.P.; Kharode, Y.P.; Marzolf, J.; Komm, B.S.; Winneker, R.C.; Frail, D.E.; Henderson, R.A.; Zhu, Y.; Keith Jr, J.C. Evaluation of an estrogen receptor-β agonist in animal models of human disease. Endocrinology, 2003, 144, 4241-4249.

Harris, L.; Fritsche, H.; Mennel, R.; Norton, L.; Ravdin, P.; Taube, S.; Sommerfield, M.R.; Hayes, D.F.; Bast Jr., R.C. American society of clinical ocology 2007 update of recommendations for the use of tumor markers in breast cancer. J Clin Oncol, 2007, 25. 5287-5312.

Hartman, J.; Lindberg, K.; Morani, A.; Inzunza, J.; Ström, A.; Gustafsson, J. Estrogen receptor β inhibits angiogenesis and growth of T47D breast cancer xenografts. Cancer Res, 2006, 66, 11207-11213.

Hendrix, M.J.C.; Seftor, E.A.; Chu, Y.W.; Trevor, K.T.; Seftor, R.E.B. Role of intermediate filaments in migration, invasion, and metastasis. Cancer Metastasis Rev, 1996, 15, 507-525.

Herynk, M.H.; Fuqua, S.A. Estrogen receptor mutations in human disease. Endocr Rev, 2004, 25, 869-898.

Hopp, T.A.; Weiss, H.L.; Parra, I.S.; Cui, Y.; Osborne, C.K.; Fuqua, S.A. Low levels of estrogen receptor beta protein predicts resistance to tamoxifen therapy in breast cancer. Clin Cancer Res, 2004, 10, 7490-7499.

Hornef, N.; Olbrich, H.; Horvath, J.; Zariwala, M.A.; Fliegauf, M.; Loges, N.T.; Wildhaber, J.; Noone, P.G.; Kennedy, M.; Antonarakis, S.E.; Blouin, J.; Bartoloni, L.; Nüsslein, T.; Ahrens, P.; Griese, M.; Kuhl, H.; Sudbrak, R.; Knowles, M.R.; Reinhardt, Omran, H. DNAH5 mutations are a common cause of primary ciliary dyskinesia with outer dynein arm defects. Am J Respir Crit Care Med, 2006, 174, 120-126.

Howell, A.; Cuzick, J.; Baum, M.; Buzdar, A., Dowesett, M.; Forbes, J.F.; Hoctin-Boes, G.; Houghton, J.; Locker, G.Y.; Tobias, J.S.; ATAC Trialists' Group. Results of the ATAC (arimidex, tamoxifen, alone or in combination) trial after completion of 5 years' adjuvant treatment for breast cancer. Lancet, 2005, 365, 60-62.

Hozak, P.; Sasseville, A.M.; Raymond, Y.; Cook, P.R. Lamin proteins form an internal nucleoskeleton as well as a peripheral lamina in human cells. J Cell Sci, 1995, 108, 635-644.

Hughes, L.; Malone, C.; Chumsri, S.; Burger, A.M.; McDonnell, S. Characterization of breast cancer cell lines and establishment of a novel isogenic subclone to study migration, invasion, and tumorigenicity. Clin Exp Metast, 2008, 25, 549-557.

Ingber, D.E. The riddle of morphogenesis: a question of solution chemistry or molecular cell engineering? Cell, 1993, 75, 1249-1252.

Itoh, K.; Wakabayashi, N.; Katoh, H. ET AL. Keap1 represses nuclear activation of antioxidant responsive elements by Nrf2 through binding to the amino-terminal Neh2 domain. Genes Dev, 199, 13, 76-86.

Izzo, R.S.; Pellecchia, C. Comparison of nuclear matrix protein composition in colon cancer and dysplasia. Scand J Gastroenterol, 1998, 33, 191-194.

Jackson, D.A.; McCready, S.J.; Cook, P.R. RNA is synthesized at the nuclear cage. Nature, 1981, 292, 552-555.

Janjic, J. Design, synthesis and biologcail evaluation of new agents targeting estrogen receptor-alpha and -beta. 2005B, (PhD dissertation, University of Pittsburgh)

Janjic, J.; Mu, Y.; Kendall, C.; Stephenson, C.R.J.; Balachandran, R.; Raccor, B.S.; Lu, Y.; Zhu, G.; Xie, W.; Wipf, P.; Day, B.W. New antiestrogeens from a library screen of

homoallylic amides, allylic amides, and *C*-cyclopropylalkylamides. Bioorg Med Chem, 2005A, 13, 157-164.

Jarvinen, T.; Pelto-Huikko, M.; Holli, K.; Isola, J. Estrogen receptor beta is coexpressed with ERalpha and PR and associated with nodal status grade and proliferation rate in breast cancer. Am J Pathol, 2000, 156, 29-35.

Jensen, E.V.; Jacobsen, H.I. Basic guidelines to the mechanism of estrogen action. Rec Prog Horm Res, 1962, 18, 387-414.

Jensen, E.V.; Jordan, V.C. The estrogen receptor, a model for molecular medicine. Clin Cancer Res, 2003, 9, 1950-1989.

Ji, Q.; Liu, P.I.; Eishimali, Y.; Stolz, A. Frequent loss of estrogen and progesterone receptors in human prostatic tumors determined by qantitative real-time PCR. Mol Cell Endocrinology, 2005, 229, 103-110.

Jin, S.; Mao, H.; Schnepp, R.W.; Sykes, S.M.; Silva, A.C.; D'Andrea, A.D.; Hua, X. Menin associate with FANCD2, a protein involved in repair of DNA damage. Cancer Res, 2003, 63, 4204-4210.

Johnson, J.M. Molecular Mechanism of Nucleotide Excision Repair Deficiency in Novel Breast Cancer Cell Lines. 2006, (PhD Dissertation, University of Pittsburgh)

Johnston, S.R.; Saccani-Jotti, G.; Smith, I.E.; Salter, J.; Newby, J.; Coppen, M.; Ebbs, S.R.; Dowsett, M. Changes in estrogen receptor, progesterone receptor, and pS2 expression in tamoxifen-resistant human breast cancer. Cancer Res, 1995, 55, 3331-3338.

Jones, C. Comparative genomic hybridization reveals extensive variation among different mcf-7 cell stocks. Cancer Genetics Cytogenetics, 2000, 117, 153-158.

Jordan, V. C.; Brodie, A.M. Development and evolution of therapies targeted to the estrogen receptor for the treatment and prevention of breast cancer. Steroids 2007, 72, 7-25.

Jordan, V.C. Tamoxifen: a most unlikely pioneering medicine. Nat Rev Drug Discovery, 2003, 2 205-213.

Jordan, V.C.; O'Malley, B.W. Selective estrogen-receptor mdulators and anti-hormonal resistance in breast cancer. J Clin Oncol, 2007, 25, 5815-5824.

Joseph, P.; O'Kernick, C.M.; Othumpangat, S.; Lei, Y.X.; Yuan, B.Z.; Ong, T.M. Expression profile of eukaryotic translation factors in human cancer tissues and cell lines. Mol Carcinogenesis, 2004, 40, 171-179.

Jost, J.; Seldran, M. Association of transcriptionally active vitellogenin II gene with the nuclear matrix of chicken liver. EMBO J, 1984, 3, 2005-2008.

Kahlert, S.; Nuedling, M.; van Eickels, M.; Vetter, H.; Meyer, R.; Grohe, C. Estrogen receptor alpha rapidly activates the IGF-1 receptor pathway. J Biol Chem, 2000, 275, 18447-18453.

Kammerer, S.; Roth, R.B.; Hoyal, C.R.; Reneland, R.; Marnellos, G.; Kiechle, M.; Schwarz-Boeger, U.; Griffiths, L.R.; Ebner, F.; Rehbock, J.; Cantor, C.R.; Nelson, M.R.; Braun, A. Association of the NuMA region on chromosome 11q13 with breast cancer susceptibility. Proc Natl Acad Sci USA, 2005, 102, 2004-2009.

Kato, S.; Endoh, Y.; Masuiro, T.; Kitamoto, S.; Uchiyama, H.; Sasaki, S.; Masushige, Y.; Gotoh, E.; Nishida, H.; Kawashima, H.; Metzger, D.; Chambon, P. Activation of the unliganded estrogen receptor by EGF through phosphorylation by mitogen-activated protein kinase. Science, 1995, 270, 1491-1494.

Keenan, J.; Murphy, L.; Henry, M.; Meleady, P.; Clynes, M. Proteomic analysis of multidrug-resistance mechanisms in adriamycin-resistant variants of DLKP, a squamous lung cancer cell line. Proteomics, 2009, 9, 1556-1566.

Keesee, S.K.; Marchese, J.; Meneses, A.; Potz, D.; Garcia-Cuellar, C.; Szaro, R.P.; Solorza, G.; Osornio-Vargas, A.; Mohar, A.; de la Garza, J.G.; Wu, Y.J. Human cervical cancer-associated nuclear matrix proteins. Exp Cell Res, 1998, 244, 14-25.

Khanuja, P. S., J. E. Lehr, H. D. Soule, S. K. Gehani, A. C. Noto, S. Choudhury, R. Chen, K. J. Pienta. Nuclear matrix proteins in normal and breast cancer cells. Cancer Res, 1993, 53, 3394-3398.

Kim, T.A.; Lim, J.; Ota, S.; ET AL. NRP/B, a novel nuclear matrix protein, associates with p110(RB) and is involved in neuronal differentiation. J Cell Biol, 1998, 141, 553-566.

Klein-Hitpass, L.; Ryffel, G.U.; Heitlinger, A.C.; Cato, A.C. A 13 bp palindrome is a functional estrogen receptor element and interacts specifically with estrogen receptor. Nucleic Acid Res, 1988, 16, 647-663.

Knowlden, J.M.; Hutcheson, I.R.; Jones, H.E.; Madden, T.; Gee, J.M.; Harper, M.E.; Barrow, D.; Wakeling, A.E.; Nicholson, R.I. Elevated levels of epidermal growth factor receptor/c-erbB2 heterodimers mediate an autocrine growth regulatory pathway in MCF-7 breast cancer cells. Endocrinology, 2003, 144, 1032-1044.

Kobayashi, Y.; Kitamoto, T.; Masuhito, Y.; Watanabe, M.; Kase, T.; Metzger, D.; Yanagisawa, J.; Kato, S. P300 mediates functional synergism between AF-1 and AF-2 of estrogen receptor alpha and beta by interacting directly with the N-terminal A/B domains. J Biol Chem, 2000, 275, 15645-15651.

Koide, A.; Zhao, C.; Naganuma, M.; Abrams, J.; Deighton-Collins, S.; Skafar, D.F.; Koide, S. Identification of regions within the F domain of the human estrogen receptor α that are important for modulating transactivation and protein-protein interactions. Mol Endocrinology, 2007, 21, 829-842.

Konety, B.; Nguyen, T.; Brenes, G.; Sholder, A.; Lewis, N.; Bastacky, S.; Potter, D.; Getzenberg, R. Clinical usefulness of the novel marker BLCA-4 for the detection of bladder cancer. J Urol, 2000B, 164, 634-639.

Konety, B.R.; Nguyen, T.S.; Dhir, R.; Day, R.S.; Becich, M.J.; Stadler, W.M.; Getzenberg, R.H. Detection of bladder cancer using a novel matrix protein, BLCA-4. Clin Cancer Res., 2000A, 6, 2618-2625.

Kousteni, S.; Chen, J.R.; Bellido, T.; Han, L.; Ali. A.A.; O'Brien, C.A.; Plotkin, L.; Fu, Q.; Mancino, A.T.; Wen, Y. Reversal of bone loss in mice by nongenotypic signaling of sex steroids. Science, 2002, 298, 843-846.

Kuerer, H.M.; Albarracin, C.T.; Yang, W.T.; Cardiff, R.D.; Brewster, A.M.; Fraser Symmans, W.; Hylton, N.M.; Middleton, L.P.; Krishnamurthy, S.; Perkins, G.H.; Babiera, G.; Edgerton, M.E.; Czerniecki, B.J.; Arun, B.K.; Hortobagyi, G.N. Ductal carcinoma in situ: state of the science and roadmap to advance the field. J Clin Oncol, 2009, 27, 279-288.

Kuiper, G.G.; Enmark, E.; Pelto-Huikko, M.; Nilsson, S.; Gustafson, J.A. Cloning of a novel receptor expressed in rat prostate and ovary. Proc Natl Acad Sci USA, 1996, 93, 5925-5930.

Kuiper, G.G.; Lemmen, J.G.; Carlsson, B.; Corton, J.C.; Safe, S.H.; van der Saag, P.T.; van der Burg, B.; Gustafsson, J.A. Interaction of estrogenic chemicals and phytoestrogens with estrogen receptor beta. Endocrinology, 1998, 139, 4252-4263.

Kuiper, G.G.J.M.; Carlsson, B.; Grandien, K.; Enmark, E.; Häggblad, J.; Nilsson, S.; Gustafsson, J. Comparison of the ligand binding specificity and transcript distribution of estrogen receptors α and β. Endocrinology, 1997, 138, 863-870.

Kumar, V.; Green, S.; Stack, G.; Berry, M.; Jin, J.; Chambon, P. Functional domains of the human estrogen receptor. Cell, 1987, 51, 941-951.

Kushner, P.J.; Agard, D.A.; Greene, G.L.; Scanlan, T.S.; Shiau, A.K.; Uht, R.M.; Webb, P. Estrogen receptor pathways to AP-1. J Steroid Biochem Mol Biol, 2000, 74, 311-317.

Latimer, J.J. 2002. Epithelial cell cultures for in vitro testing. U.S. Patent 6,383,805, filed 04/11/2000, and issued 05/07/2002.

Lazennee, G. Estrogen receptor beta, a possible tumor suppressor involved in ovarian carcinogenesis. Cancer Lett, 2006, 231, 151-157.

Lebkowski, J.S.; Laemmli, U.K. Evidence for two levels of DNA folding in histone-depleted HeLa interphase nuclei. J Mol Biol, 1982, 156, 309-324.

Lees, J.A.; Fawell, S.E.; Parker, M.G. Identification of two transactivation domains in the mouse oestrogen receptor. Nucleic Acids Res, 1989, 17, 5477-5488.

Leman, E.S.; Getzenberg, R.H. Nuclear structure as a source of cancer specific biomarkers. J Cell Biochem, 2008, 104, 1988-1993.

Leman, E.S.; Madigan, M.C.; Brünagel, G.; Takaha, N.; Coffey, D.S.; Getzenberg, R.H. Nuclear matrix localization of high mobility group protein I(Y) in a transgenic mouse model for prostate cancer. J Cell Biochem, 2002, 88, 599-608.

Lemieux, P.; Lawrence, J.; Steeg, P.; Oesterreich, S.; Fuqua, S.A.W. Transfection of hsp27 overexpression affects growth and motility of an estrogen receptor negative human breast cancer cell line. Proc Amer Assoc Cancer Res 1996, 37, 68.

Levenson, V.V. Biomarkers for early detection of breast cancer: what, when, and where? Biochim Biophys Acta, 2007, 1770, 847-856.

Leygue, E.; Dotzlaw, H.; Watson, P.; Murphy, L. Altered estrogen receptor alpha and beta mRNA expression during human breast tumorigenesis. Cancer Res, 1998, 58, 3197-3201.

Liao, D.J.; Dickson, R.B. C-Myc in breast cancer. Endocr Relat Cancer, 2000, 7, 143-164.

Liu, M.; Albanese, C.; Anderson, C.A.; Hilty, K.; Webb, P.; Uht, R.M.; Price Jr., R.H.; Pestell, R.G.; Kushner, P.J. Opposing action of estrogen receptors α and β on vyclin D1 gene expression. J Biol Chem, 2002, 27, 24353-24360.

Longcope, C.; Baker, R.; Johnston Jr., C.C. Androgen and estrogen metabolism: relationship to obesity. Metabolism, 1986, 35, 235-237.

Ludérus, M.E.E.; de Graff, A.; Mattia, E.; den Balen, J.L.; Grande, M.A.; de Jong, L.; Van Driel, R. Binding of matrix attachment regions to lamin B1. Cell, 1992, 70, 949-959.

Lyderson, B.K.; Pettijohn, D.E. Human-specific nuclear protein that associates with the polar region of the mitotic apparatus: distribution in a human/hamster hybrid cell. Cell, 1980, 22, 489-499.

Mader, S.; Chambon, P.; White, J.H. Defining a minimal estrogen receptor DNA binding domain. Nucleic Acids Res, 1993, 21, 1125-1132.

Maitra A.; Iacobuzio-Donahue, C.; Rahman, A.; Sohn, T.A.; Argani, P.; Meyer, R.; Yeo, C.J.; Cameron, J.L.; Goggins, M.; Kern, S.E.; Ashfaq, R.; Hruban, R.H.; Wilentz, R.E. Immunohistochemical validation of a novel epithelial and a novel stromal marker of pancreatic ductal adenocarcinoma identified by global expression microarrays: sea urchin fascin homolog and heat shock protein 47. Am J Clin Pathol, 2002, 118, 52-59.

Mancini, M.A.; Shan, B.; Nickerson, J.A.; Penman, S.; Lee, W. The retinoblastoma gene product is a cell cycle-dependent, nuclear matrix-associated protein. Proc Natl Acad Sci, 1994, 91, 418-422.

Maor, S.; Mayer, D.; Yarden, R.I.; Lee, A.V.; Sarfstein, R.; Werner, H.; Papa, M.Z. Estrogen receptor regulates insulin-like growth factor-I receptor gene expression in breast tumor cells: involvement of transcription factor Sp1. J Endocrinology, 2006, 191, 605-612.

Marino, M.; Ascenzi, P. Membrane association of estrogen receptor a and b influences 17b-estradiol-mediated cancer cell proliferation. Steroids, 2008, 73, 853-858.

Markovits, J.; Linassier, C.; Fossé, P.; Couprite, J.; Jacquemin-Sablon, A.; Saucier, J.; Le Pecq, J.; Larsen, A.K. Inhibitory effects of the tyrosine kinase inhibitor genistein on mammalian DNA topoisomerase II. Cancer Res, 1989, 49, 5111-5117.

McCready, S.J.; Krigg, A.; Cock, P.R. Electron-microscopy of intact nuclear DNA from human cells. J Cell Sci, 1979, 39, 53-62.

McDonnell, D. The molecular pharmacology of SERMs. Trends Endocrinology Metab 1999, 10, 301-311.

McInerney, E.M.; Weis, K.E.; Sun, J.; Mosselman, S.; Katzenellenbogen, B.S. Transcription activation by the human estrogen receptor subtype β (ERβ) studied with ERβ and ERα receptor chimeras. Endocrinology, 1998, 139, 4513-4522.

McKenna, N.J.; Lanz, R.B.; O'Malley, B.W. Nuclear receptor coregulators: cellular and molecular biology. Endocr Rev, 1999, 20, 321-344.

Mersereau, J.E.; Levy, N.; Staub, R.E.; Baggett, S.; Zogric, T.; Chow, S.; Ricke, W.A.; Tagliaferri, M.; Cohen, I.; Bjeldanes, L.F.; Leitman, D.C. Liquiritigenin is a plant-derived highly selective estrogen receptor β agonist. Mol Cell Endocrinology, 2008, 283, 49-57.

Meyers, M.J.; Sun, J.; Carlson, K.E.; Marriner, G.A.; Katzenellenbogen, B.S.; Katzenellenbogen, J.A. Estrogen receptor-β potency-selective ligands: structure-activity relationship studies on diarylpropionitriles and their acetylene and polar analogues. J Med Chem, 2001, 44, 4230-4251.

Miller, T.E., L. A. Beausung, L. F. Winchell, G. P. Lidgard. Detection of nuclear matrix proteins in serum from cancer patients. Cancer Res, 1992, 52, 422-427.

Miller, W.R.; Hawkins, R.A.; Forrest, A.P. Significance of aromatase activity in human breast cancer. Cancer Res, 1982, 42, 3365s-3368s.

Ming, J.; Axe, T.; Holgate, R.; Rubbi, C.P.; Okorokov, A.L.; Mee, T.; Milner, J. P53 binds the nuclear matrix in normal cells: binding involves the proline-rich domain of p53 and increases following genotoxic stress. Oncogene, 2001, 20, 5449-5458.

Moretti-Rojas, I.; Fuqua S.A.W.; Montgomery III, R.A.; McGuire, W.L. A cDNA for the estradiol-regulated 24K protein: Control of mRNA levels in MCF-7 cells. Breast Cancer Res Treat, 1988, 11, 155-163.

Murdoch, F.E.; Gorski, J. The role of ligand in estrogen receptor regulation of gene expression. Mol Cell Endocrinology, 1991, 78, C103-C108.

Murphy, L.C.; Peng, B.; Lewis, A.; Davie, J.R.; Leygue, E.; Kemp, A.; Ung, K.; Vendetti, M.; Shiu, R. Inducible upregulation of oestrogen receptor-β1 affects oestrogen and tamoxifen respnsiveness in MCF7 human breast cancer cells. J Mol Endocrinolpgy, 2005, 34, 553-566.

Murphy, L.C.; Watson, P.H. Is oestrogen receptor-β a predictor of endocrine therapy responsiveness in human breast cancer? Endocr Relat Cancer, 2006, 13, 327-334.

National Cancer Institue. Breast Cancer Treatment (PDQ®). 2009.

Nelson, L.R.; Bulun, S.E. Estrogen production and action. J Am Acad Dermatol, 2001, 45, S116-S124.

Nettles, K.W.; Greene, G.L. Ligand control of coregulator recruitment to nuclear receptors. Ann Rev Physiol, 2005, 67, 309-333.

Nickerson, J.A.; Krockmalnic, G.; He, D.C.; Penman, S. Immunolocalization in three dimensions: immunogold staining of cytoskeletal and nuclear matrix proteins in resinless elecron microscopy sections. Proc Natl Acad Sci, 1990, 87, 2259-2263.

Normanno, N.; Ciardiello, F.; Brandt, R.; Salomon, D.S. Epidermal growth factor-related peptides in the pathogenesis of human breast cancer. Breast Cancer Res, 1994, 29, 11-27.

O'Lone, R.; Frith, M.C.; Karlsson, E.K.; Hansen, U. Genomic targets of nuclear estrogen receptors. Mol Endocrinology, 2004, 18, 1859-1875.

Oesterreich S.; Allredl, D.C.; Zhang, Q.; Wong, H.; Lee, A.V.; Osborne, C.K.; O'Connell, P.O. High rates of loss of heterozygosity on chromosome 19p13 in human breast cancer. Br J Cancer, 2001, 84, 493-498.

Oesterreich, S.; Hilsenbeck, S.G.; Allred, D.C.; Ciocca, D.; Chambness, G.C.; Osborne, C.K.; Fuqua, S.A.W. The small heat shock protein hsp27 is not an independent prognostic marker in axillary lymph node-negative breast cancer patients. Clin Cancer Res, 1996, 2, 1199-1206.

Oesterreich, S.; Lee, A.V.; Sullivan, T.M.; Samuel, S.K.; Davie, J.R.; Fuqua, S.A.W. Novel nuclear matrix protein HET binds to and influences activity of the HSP27 promoter in human breast cancer cells. J Cell Biochem 1997, 67, 275-286.

Oesterreich, S.; Weng. C-N.; Qiu, M.; Hilsenbeck, S.G.; Osborne, C.K.; Fuqua, S.A.W. The small heat shock protein hsp27 is correlated with growth and drug resistance in human breast cancer cell lines. Cancer Res 1993, 53, 4443-4448.

Oesterreich, S.; Zhang, Q.; Hopp, T.; Fuqua, S.A.W.; Michealis, M.; Zhao, H.H.; Davie, J.R.; Osborne, C.K.; Lee, A.V. Tamoxifen-bound estrogen receptor (ER) strongly interacts with the nuclear matrix protein HET/SAF-B, a novel inhibitor of ER-mediated transactivation. Mol Endocrinology, 2000, 3, 369-381.

Ogawa, K.; Utsunomiya, T.; Mimori, K.; Tanaka, Y.; Tanaka, F.; Inoue, H.; Murayama, S.; Mori, M. Clinical significance of elongaation factor-1 delta mRNA expression in oesophageal carcinoma. Br J Cancer, 2004, 91, 282-286.

Omoto, Y.; Eguchi, H.; Yamamoto-Yamaguchi, Y.; Hayashi, S. Estrogen receptor (ER) beta 1 and ER betacx/beta2 inhibit Eralpha function differently in breast cancer cell line MCF7 . Oncogene, 2003, 22, 5011-5020.

Osborne, C.K. Tamoxifen in the treatment of breast cancer. N Engl J Med, 1998, 339, 1609-1618.

Osborne, C.K.; Hobbs, K.; Trent, J.M. Biological differences among MCF-7 breast cancer cell lines from different laboratories. Breast Cancer Res Treat, 2005B, 9, 111-121.

Osborne, C.K.; Pippen, J.; Jones, S.E.; Parker, L.M.; Ellis, M.; Come, S.; Gertler, S.Z.; May, J.T.; Burton, G.; Dimery, I.; Webster, A.; Morris, C.; Elledge, R.; Buzdar, A. Double-blind, randomized trial comparing the efficacy and tolerability of fulvestrant versus amastrozole in postmenopausal women with advanced breast cancer progressing on prior endocrine therapy: results of a north American trial. J Clin Oncol, 2002, 20, 3386-3395.

Osborne, C.K.; Schiff, R. Estrogen-receptor biology: continuing progress and therapeutic implications. J Clin Oncol, 2005A, 23, 1616-1622.

Osborne, C.K.; Schiff, R.; Fuqua, S.A.W.; Shou, J. Estrogen receptor: current understanding of its activation and modulation. Clin Cancer Res, 2001, 7, 4338s-4342s.

Ottaviano, Y.L.; Issa, J.P.; Parl, F.F.; Smith, H.S.; Baylin, S.B.; Davidson, N.E. Methylation of the estrogen receptor CpG island marks loss of estrogen receptor expression in human breast cancer cells. Cancer Res, 1994, 54, 2552-2555.

Ozaki, T.; Saijo, M.; Murakami, K.; Enomoto, H.; Taya, Y.; Sakiyama, S. Complex formation between lamin A and the retinoblastoma gene product: identification of the domain lamin A required for its interaction. Oncogene, 1994, 9, 2649-2653.

Paech, K.; Webb, P. Kuiper, G.G.J.M.; Nilsson, S.; Gustafsson, J.; Kushner, P.J.; Scanlan, T.S. Differential ligand activation of estrogen receptors ERα and ERβ at AP1 sites. Science, 1997, 1508-1510.

Park, B.W.; Kim, K.S.; Heo, M.K.; Ko, S.S.; Hong, S.W.; Yang, W.I.; Kim, J.H.; Kim, G.E.; Lee, K.S. Expression of estrogen receptor-beta in normal mammary and tumor tissues: is it protective in breast carcinogenesis? Breast Cancer Res Treat, 2003, 80, 79-85.

Parker, G.J.; Law, T.L.; Lenoch, F.J.; Bolger, R.E. Development of high throughput screening assays using flourescence polarization: nuclear receptor-ligand-binding and kinase/phosphatase assays. J Biomed Screen, 2000, 5, 77-88.

Parl, F.F. Multiple mechanisms of estrogen receptor gene repression contribute to ER-negative breast cancer. Pharmacogenomics J, 2003, 2003, 251-253.

Paruthiyil, S.; Parmar, H.; Kerekatee, V.; Cunha, G.R.; Firestone, G.L.; Letiman, D.C. Estrogen receptor β inhibits human breast cancer cell proliferation and tumor formation by causing a G2 cell cycle arrest. Cancer Res, 2004, 423-428.

Peale, F.V.; Ludwig, L.B.; Zain, S.; Hilf, R.; Bambara, R.A. Properties of a high-affinity DNA binding site for estrogen receptor. Proc Natl Acad Sci, 1988, 85, 1038-1042.

Pearce, S.T.; Jordan, V.C. The biological role of estrogen receptors alpha and beta in cancer. Crit Rev Oncol Hematol, 2004, 50, 3-22.

Pedram, A.; Razandi, M.; Levin, E.R. Nature of functional estrogen receptors at the plasma membrane. Mol Endocrinology, 2006, 20, 1996-2009.

Pedram, A.; Razandi, M.; Sainson, R.C.; Kim, J.K.; Hughes, C.C.; Levin, E.R. A conserved mechanism for steroid receptor translocation to the plasma membrane. J Biol Chem, 2007, 282, 22278-22288.

Pettersson, K.; Delaunay, F.; Gustafsson, J. Estrogen receptor β acts as a dominant regulator of estrogen signaling. Oncogene, 2000, 19, 4970-4978.

Picard, D.; Kumar, V.; Chambon, P.; Yamamoto, K.R. Signal transduction by steroid hormones: nuclear localization is differentially regulated in estrogen and glucocorticoid receptors. Cell Regulation, 1990, 1, 291-299.

Pick, E.; Kluger, Y.; Giltnane, J.M.; Moeder, C.; Camp, R.L.; Rimm, D.L.; Kluger, H.M. High HSP90 expression is associated with decreased survival in breast cancer. Cancer Res, 2007, 67, 2932-2937.

Pienta, K.J., D.S. Coffey. Nuclear-cytoskeletal interactions: Evidence for physical connections between the nucleus and cell periphery and their alterations by transformation. J Cell Biochem, 1992. 49, 357-365.

Pike, A.C.; Brzozowski, A.M.; Walton, J.; Hubbard, R.E.; Thorsell, A.G.; Li, Y.L.; Gustafsson, J.; Calquist, M. Structural insight into the mode of action of a pure antiestrogen. Structure, 2001, 9, 145-153.

Piñol-Roma, S.; Swanson, M.S.; Gall, J.G.; Dreyfuss, G. A novel heterogeneous nuclear RNP protein with a unique distribution on nascent transcripts. J Cell Biol, 1989, 109, 2575-2587.

Poschmann, G.; Sitek, B.; Sipos, B.; Ulrich, A.; Wiese, S.; Stephan, C.; Warscheid, B.; Klöppel, G.; Borght, A.V.; Ramaekers, F.C.S.; Meyer, H.E.; Stühler, K. Identification of proteomic differences between squamous cell carcinoma of the lung and bronchial epithelium. Mol Cell Proteomics, 2009, 8, 1105-1116.

Prall, O.W.J.; Rogan, E.M.; Musgrove, E.A.; Watts, C.K.W.; Sutherland, R.L. C-myc or cyclin D1 mimics estrogen effects on cyclin e-cdk2 activation and call cycle reentry. Mol Cell Biol, 1998, 18, 4499-4508.

Prall, O.W.J.; Sarcevic, B.; Musgrove, E.A.; Watts, C.K.W.; Sutherland, R.L. Estrogen-induced activation of cdk4 and cdk2 during G1-S phase progression is accompanied by an increased cyclin D1 expression and decreased cyclin-dependent kinase inhbitor association with cyclin-e-cdk2. J Biol Chem, 1997, 272, 10882-10894.

Pravettoni, A.; Mornati, O.; Martni, P.G.V.; Marino, M.; Colciago, A.; Celotti, F.; Motta, M.; Negri-Cesi, P. Estrogen receptor beta (ERbeta) and inhibition of prostate cancer cell proliferation: studies on the possible mechanism of action in DU145 cells. Mol Cell Endocrinology, 2007, 263, 46-54.

Privalsky, ML. The role of corepressors in transcriptional regulation by nuclear hormone receptors. Ann Rev Physiol, 2004, 66, 315-360.

Proud, C.G. Peptide-chain elongation in eukaryotes. Mol Bio Reports, 1994, 19, 161-170.

Ravaioli, A.; Bagli, L.; Zucchini, A.; Monti, F. Prognosis and prediction of reseponse in breast cancer: the current role of the main biological markers. Cell Prolif, 1998, 31, 113-126.

Rayala, S.K.; Hollander, P.; Balasenthil, S.; Yang, Z.; Broaddus, R.R. Functional regulation of oestrogen receptor pathway by the dynein light chain 1. EMBO Reports, 2005, 6, 538-545.

Razandi, M.; Pedram, A.; Park, S.T.; Levin, E.R. Proximal events in signaling by plasma membrane estrogen receptors. J Biol Chem, 2003, 278, 2701-2712.

Replogle-Schwab, T.S., K. J. Pienta, R. H. Getzenberg. The utilization of nuclear matrix proteins for cancer diagnosis. Crit Rev Eukaryot Gene Expr, 1996, 6, 103-113.

Robinson, M.J.; Corbett, A.H.; Osheroff, N. Effects of topoisomease II-targeted drugs on enzyme-mediated DNA cleavage and ATP hydrolysis: evidence for distinct drug interaction domains on topoisomerase II. Biochemistry, 1993, 32, 3638-3643.

Robinson, S.I.; Small, D.; Idzerda, R.; McKnight, G.S.; Vogelstein, B. The association of transcriptionally active genes with the nuclear matrix of the chicken oviduct. Nucleic Acids Res, 1983, 11, 5113-5130.

Roger, P.; Sahla, M.E.; Mäkelä, S.; Gustafsson, J.A.; Baldet, P.; Rochefort, H. Decreased expression of estrogen rececptor β protein in proliferative preinvasive mammary tumors. Cancer Res, 2001, 61, 2537-2541.

Romond, E.H.; Perez, E.A.: Bryant, J.; Suman, V.J.; Geyer Jr., C.E.; Davidson, N.E.; Tan-Chiu, E.; Martino, S.; Paik, S.; Kaufman, P.A.; Swain, S.M.; Pisansky, T.M.; Fehrenbacher, L.; Kutteh, L.A.; Vogel, V.G.; Visscher, D.W.; Yothers, G.; Jenkins, R.B.; Brown, A.M.; Dakhil, S.R.; Mamounas, E.P.; Lingle, W.L.; Klein, P.M.; Ingle, J.N.; Wolmark, N. Trastuzumab plus adjuvant chemotherapy for operable HER2-positive breast cancer. N Engl J Med, 2005, 16, 1673-1684.

Ross, P.L.; Huang, Y.N.; Marchese, J.N.; Williamson, B.; Parker, K.; Hattan, S.; Khainovski, N.; Pillai, S.; Dey, S.; Daniels, S. Purkayastha, S.; Juhasz, P.; Martin, S.; Bartlet-Jones, M.; He, F.; Jacobson, A.; Pappin, D.J. Multiplexed protein quantitation in Saccharomyces cerevisiae using amine-reactive isobaric tagging reagents. Mol Cell Prot, 2004, 3, 1154-1169.

Sabbah, M.; Courilleau, D.; Mester, J.; Redeuilh, G. Estrogen induction of the cyclin D1 proomoter: involvement of a cAMP response-like element. PNAS, 1999, 96, 11217-11222.

Samuel, S. K.; Mimish, M. M.; Davie, J. R. Nuclear matrix proteins in well and poorly differentiated human breast cancer cell lines. J Cell Biochem 1997, 66, 9-15.

Santen, R.J.; Song, R.X.; Zhang, Z.; Kumar, R.; Jeng, M.H.; Masamura, S.; Lawrence, J.; Berstein, L.; Yue, W. Long-term estradiol deprivation in breast cancer cells up-regulates growth factor signaling and enhances estrogen sensitivity. Endocr Relat Cancer, 2005, 12, S61-S73.

Santen, R.J.; Song, R.X.; Zhang, Z.; Kumar, R.; Jeng, M.H.; Masamura, S.; Yue, W.; Berstein, L. Adaptive hypersensitivity to estrogen: mechanisms for superiority of aromatase inhibitors over selector estrogen receptor modulators for breast cancer treatment and prevention. Endocr Relat Cancer, 2003, 10, 111-130.

Saredi, A.; Howard, L.; Compton, D.A. Phosphorylation regulates the assembly of NuMA in a mammalian mitotic extract. J Cell Sci, 1997, 110, 1287-1297.

Sauk, J.J.; Nikitakis, N.; Siavash, H. HSP47 a novel collagen binding serpin chaperone, autoantigen and therapeutic target. Fronteirs Bioscience, 2005, 10, 107-118.

Saville, B.; Wormke, M.; Wang, F.; Nguyen, T.; Enmark, E.; Kuiper, G.; Gustafsson, J.A.; Safe, S. Ligand-, cell-, and estrogen receptor subtype (α/β)-dependent activation at GC-rich (Sp1) promoter elements. J Biol Chem, 2000, 275, 5379-5387.

Schiff, R.; Massarweh, S.; Shou, J.; Bharwani, L.; Mohsin, S.K.; Osborne, C.K. Cross-talk between estrogen receptor and growth factor pathways as a molecular target for overcoming endocrine resistance. Clin Cancer Res, 2004, 10, 331S-336S.

Sekido, R.; Murai, K.; Kamachi, Y.; Kondoh, H. Two mechanisms in the activation of repressor deltaEF1: binding site competition with an activator and active repression. Genes Cells, 1997, 2, 771-783.

Seng, S.; Avraham, H.K.; Jiang, S.; Yang, S.; Sekine, M.; Kimelman, N.; Li, H.; Avraham, S. The nuclear matrix protein, NRP/B, enhances Nrf-2 mediated oxidative stress responses in breast cancer cells. Cancer Res, 2007, 67, 8596-8604.

Seymour, L.; Bezwoda, W.R.; Meyer, K. Tumor factors predicting for prognosis in metastatic breast cancer: The prsence of p24 predicts for response to treatment and the duration of survival. Cancer, 2006, 66, 2390-2394.

Shaaban, A.M.; O'Neil, P.A.; Davies, M.P.; Sibson, R.; West, C.R.; Smith, P.H.; Foster, C.S. Declining estrogen receptor-beta expression defines malignant progression of human breast neoplasia. Am J Surg Pathol 2003, 17, 1502-1512.

Shang, Y.; Brown, M. Molecular determinants for the tissue specificity of SERMs. Science, 2002, 295, 2465-2468.

Shaw, J.A.; Udokang, K.; Mosquera, J.; Chauhan, H.; Jones, J.L. Oestreogen receptors alpha and beta differ in normal human breast and breast carcinomas. J Pathol, 2002, 198, 450-457.

Shiau. A.K.; Barstad, D.; Loria, P.M.; Chen, L.; Kushner, D.A.; Agard, D.A.; Green, G.L. The structural basis of estrogen receptor/coactivator recognition and the antagonism of this interaction by tamoxifen. Cell, 1998, 95, 927-937.

Shou, J.; Massarweh, S.; Osborne, C.K.; Wakeling, A.E.; Ali, S.; Weiss, H.; Schiff, R. Mechanisms of tamoxifen resistance: increased estrogen receptor-HER2/neu cross-talk in ER/HER2 positive breast cancer. J Natl Cancer Inst, 2004, 96, 926-935.

Sjakste, N.; Sjakste, T.; Vikmanis, U. Role of the nuclear matrix proteins in malignant transformation and cancer diagnosis. Exp Oncol, 2004, 26, 170-178.

Skafar, D.F.; Zhao, C. The multifunctional estrogen receptor-alpha F domain. Endocrine, 2008, 33, 1-8.

Skiliris, G.P.; Munot, K.; Bell, S.M.; Carder, P.J.; Lane, S.; Horgan, K.; Lansodwn, M.R.; Parkes, A.T.; Hanby, A.M.; Markham, A.F.; Speirs, V. Reduced expression of oestrogen receptor beta in invasive breast cancer and its re-expression using DNA methyl transferase inhibitors in a cell line model. J Pathol, 2003, 201, 213-220.

Slamon, D.J.; Leyland-Jones, B.; Shak, S.; Fuchs, H.; Platon, V.; Bajamonde, A.; Fleming, T.; Eiermann, W.; Wolter, J.; Pegram, M.; Baslega, J.; Noron, L. Use of chemotherapy plus a monoclonal antibody against HER2 for metastatic breast cancer that overexpress HER2. N Eng J Med, 2001, 11, 783-792.

Smith, C.L.; Nawaz, Z.; O'Malley, B.W. Coactivator and corepressor regulation of the agonist: antagonistic activity of the mixed antiestrogen, 4-hydroxytamoxifen. Mol Endocrinology, 1997, 11, 657-666.

Smith, C.L.; O'Malley, B.W. Coregulator function: a key to understanding tissue specificity of selective receptor modulators. Endocr Rec, 2004, 25, 45-71.

Smith, I.E.; Dowsett, M. Aromatase inhibitors in breast cancer. N Eng J Med, 2003, 348, 2431-2442.

Soule, H.D.; Vazguez, J.; Long, A.; Albert, S.; Brennan, M. A human cell line from a pleural effusion derived from a breast carcinoma. J Natl Cancer Inst, 1973, 51, 1409-1416.

Speirs, V.; Malone, C.; Walton, D.S.; Kerin, M.J.; Atkin, S.L. Increased expression of estrogen receptor beta mRNA in tamoxifen-resistant breast cancer patients. Cancer Res, 1999, 59, 5421-5424.

Spencer, V. A., A. S. Coutts, S. K. Samuel, L. C. Murphy, J. R. Davie. Estrogen regulates the association of intermediate filament proteins with nuclear DNA in human breast cancer cells. J Biol Chem, 1998. 273: 29093-29097.

Spencer, V.A., S. K. Samuel, J. R. Davie. Nuclear matrix proteins associated with DNA in Situ in Hormon-dependent and Hormone-independent human breast cancer cell lines. Cancer Res, 2000. 60: 288-292.

Spencer, V.A.; Samuel, S. K.; Davie, J. R. Altered profiles in nuclear matrix proteins associated with DNA in Situ during progression of breast cancer cells. Cancer Res 2001, 61, 1362-1366.

Stauffer, S.R.; Coletta, C.J.; Tedesco, R.; Nishiguchi, G.; Carlson, K.; Sun, J.; Katzenellenbogen, B.S.; Katzenellenbogen, J.A. Pyrazole ligands: structure-affinity/activity relationships and estrogen receptor-α-selective agonists. J Med Chem, 2000, 43, 4934-4947.

Stossi, F.; Barnett, D.H.; Frasor, J.; Komm, B.; Lyttle, C.R.; Katzenellenbogen, B.S. Transcriptional profiling of estrogen-regulated gene expression via estrogen receptor (ER) alpha or Erbeta in human osteosarcoma cells: distinct and commno targets for these receptors. Endocrinology, 2004, 145, 3473-3486.

Ström, A.; Hartman, J.; Foster, J.; Kietz, S.; Wimalasena, J.; Gustafsson, J. Estrogen receptor β inhibits 17β-estradiol-stimulated proliferation of the breast cancer cell line T47D. Proc Natl Acad Sci, 2004, 101, 1566-1571.

Subong, E.N.; Shue, M.J.; Epstein, J.I.; Briggman, J.V.; Chan, P.K.; Partin, A.W. Monoclonal antibody to prostate cancer nuclear matrix protein (PRO: 4-216) recognizes nucleophosmin/B23. Prostate, 1999, 29, 298-304.

Sugiura, H.; Toyama, T.; Hara, Y.; Zhang, Z.; Kobayashi, S.; Fujii, Y.; Iwase, H.; Yamashita, H. Expression of estrogen receptor β wild-type and its variant ERβcx/β2 is correlated with better prognosis in breast cancer. Jpn J Clin Oncol, 2007, 37, 820-828.

Sun, J.; Baudry, J.; Katzenellenbogen, J.A.; Katzenellenbogen, B.S. Molecular basis for the subtype discrimination of the estrogen receptor-β-selective ligand, diarylpropionitrile. Mol Endocrinology, 2003, 17, 247-258.

Sun, J.; Huang, Y.R.; Harrington, W.R.; Sheng, S.; Katzenellenbogen, J.A.; Katzenellenbogen, B.S. Antagonists selective for estrogen receptor α. Endocrinology, 2002, 143, 941-947.

Taimen, P.; Viljamaa, M.; Kallajoki, M. Preferential expression of NuMA in the nuclei of proliferating cells. Exp Cell Res, 2000, 256, 140-149.

Thijssen, J.H.; Blankenstein, M.A. Endogenous oestrogens and androgens in normal and malignant endometrial and mammary tissues. Eur J Clin Oncol, 1989, 25, 1953-1959.

Thomas, R.S.; Sarwar, N.; Phoenix, F.; Coombes, R.C.; Ali, S. Phosphorylation at serine 104 and 106 by Erk1/2 MAPK is important for estrogen receptor-alpha activity. J Mol Endocrinology, 2008, 40, 173-184.

Thompson, E.W.; Reich, R.; Shima, T.B.; Albini, A.; Graf, J.; Martin, G.R.; Dickson, R.B.; Lippman, M.E. Differential regulation of growth and invasiveness of MCF-7 breast cancer cells by antiestrogens. Cancer Res, 1988, 48, 6764-6768.

Tora, L.; White, J.; Brou, C.; Tasset, D.; Webster, N.; Scheer, E.; Chambon, P. The human estrogen receptor has two independent nonacidic transcriptional activation functions. Cell, 1989, 59, 477-487.

Townson, S.M.; Sullivan, T.; Zhang, Q.; Clark, G.M.; Osborne, C.K.; Lee, A.V.; Oesterreich, S. HET/SAF-B overexpression causes growth arrest and multinuclearity and is associated with aneuploidy in human breast cancer. Clin Cancer Res, 2000, 6, 3788-3796.

Treeck, O.; Lattrich, C.; Springwald, A.; Ortmann, O. Estrogen receptor beta exerts growth-inhibitory effects on human mammary epithelial cells. Breast Cancer Res Treat, 2009, doi 10.1007/s10549-009-0413-2.

Uozaki, H.; Ishida, T.; Kakiuchi, C.; Horiuchi, H.; Gotoh, T.; Iijima, T.; Imamura, T.; Machinami, R. Expression of heat shcok proteins in osteosarcoma and its relationship to prognosis. Pathol Res Pract, 2000, 196, 665-673.

Van Den Bemb, G.J.; Kuiper, G.G.; Pols, H.A.; Van Leeuwen, J.P. Distinct effects on the conformation of estrogen receptor alpha and beta by both the antiestrogen ICI 164, 384 and ICI 182,780 leading to opposite effects on receptor stability. Biochem Biophys Res Commun, 1999, 261, 1-5.

Veeneman, G.H. Non-steroidal subtype selective estrogens. Curr Med Chem, 2005, 12, 1077-1136.

Venugopal, R.; Jaiswal, A.K. Nrf1 and Nrf2 positively and c-Fos and Fra1 negatively regulate the human antioxidant response element-mediated expression and antioxidant induction

of NAD(P)H: quinine oxidoreductase1 gene. Proc Natl Acad Sci USA, 1996, 93, 14960-14965.

Vogel, C.L.; Cobleigh, M.A.; Tripathy, D.; Gutheil, J.C.; Harris, L.N.; Fehrenbacher, L.; Slamon, D.J.; Murphy, M.; Novotny, W.F.; Burchmore, M.; Shak, S.; Stewart, S.J.; Press, M. Efficacy and safety of traustuzumab as a single agent in first-line treatment of HER2-overexpressing metastatic breast cancer. J Clin Oncol, 2002, 20, 719-726.

Vogel, V.G. Effects on tamoxifen vs raloxifene on the risk of developing invasive breast cancer and other disease outcomes. JAMA-Express, 2006, 295, 2727-2926.

Vogelstein, B.; Pardoll, D.M.; Coffey, D.S. Supercoiled loops and eucaryotic DNA replication. Cell, 1980, 22, 79-85.

Wang, Z.H.; Ding, M.X.; Chew-Cheng, S.B.; Yun, J.P.; Chew, E.C. Bcl-2 and bax proteins are nuclear matrix associated proteins. Anticancer Res, 1999, 19, 5445-5449.

Weatherman, R.V.; Scanlan, T.S. Unique protein determinants of the subtype-selective ligand responses of the estrogen receptors (ERα and ERβ) at AP-1 sites. J Biol Chem, 2001, 3827-3832.

Webb, D.K.; Moulton, B.C.; Khan, S.A. Estrogen induces expression of c-jun and jun-B protooncogenes in specific rat uterine cells. Endocrinology, 1993, 133, 20-28.

Webb, P.; Nguyen, P.; Shinsako, J.; Anderson, C.; Feng, W.; Nguyen, M.P.; Chen, D.; Huang, S.M.; Subramanian, S.; McKinereney, E.; Katzenellenbogen, B.S.; Stallcup, M.R.; Kushner, P.J. Estrogen receptor activation function 1 works by binding p160 coactivator proteins. Mol Endocrinology, 1998, 12, 1605-1618.

Webb, P.; Valentine, C.; Nguyen, P.; Price Jr., R.H.; Marimuthu, A.; West, B.L.; Baxter, J.D.; Kushner, P.J. ERβ binds N-CoR in the presence of estrogens via an LXXLL-like motif in the N-CoR C-terminus. Nucl Recept, 2003, 1, 4-19.

Weidner, N.; Weinberg, D. S.; Hardy, S. C.; Hollister, K. A.; Lidgard, G. P. Localization of nuclear matrix proteins (NMPs) in tissue types with NM-200.4™ (An antibody strongly reactive with NMPs found in breast carcinoma). Am J Pathol 1991, 138, 1293-1298.

Welch, W.J.; Feramisco, J.R. Purification of the major mammalian heat shock proteins. J Biol Chem, 1982, 257, 14949-14959.

Wenger, S.L.; Senft, J.R.; Sargent, L.M.; Bamezai, R.; Bairwa, N.; Grant, S.G. Comparison of established cell lines at different passages by jaryotupe and comparative genomic hybridization. Biosci Rep,2004, 24, 631-639.

Williams, C.;Edvardsson, K.; Lewandowski, S.A.; Ström, A.; Gustafsson, J. A genome-wide study of the repressive effects of estrogen receptor beta on estrogen receptor alpha signaling in breast cancer cells. Oncogene, 2008, 27, 1019-1032.

Wipf, P.; Coleman, C.M.; Janjic, J.M.; Iyer, P.S.; Fodor, M.D.; Shafer, Y.A.; Stephenson, C.R.J.; Kendall, C.; Day, B.W. Microwave-assisted "libraries from libraries" approach toward the synthesis of allyl- and C-cycopropylalkylamides. J Comb Chem, 2005, 7, 322-330.

Wolff, A.C.; Hammond, M.E.; Schwartz, J.N.; Hagerty, K.N.; Allred, D.C.; Cote, R.J.; Dowsett, M.; Fitzgibbons, P.L.; Hanna, W.M.; Langer, A.; McShane, L.M.; Paik, S.; Pegram, M.D.; Perez. E.A.; Press, M.F.; Rhodes, A.; Sturgeon, C.; Taube, S.E.; Tubbs, R.; Vance, G.H.; Vijver, M.; Wheeler, T.M.; Hayes, D.F. American Society of Clinical Oncology/College of American Pathologists guideline recommendations for human epidermal growth factor receptor 2 testing in breast cancer. Arch Pathol Lab Med 2007, 131, 18.

Wong, C.W.; McNally, C.; Nickbarg, E.; Komm, B.S.; Cheskis, B.J. Estrogen receptor-interacting proteins that modulates its nongenomic ativity-crosstalk with Src/Erk phosphorylation cascade. Proc Natl Acad Sci USA, 2002, 99, 14783-14788.

Wood, J.R.; Likhite, M.A.; Loven, A.M. Nardulli, A.M. Allosteric modulation of estrogen receptor confirmation by different estrogen response elements. Mol Endocrinology, 2001, 15, 1114-1126.

Yam, H.F.; Wang, Z.H.; Or, P.C.; Wang, S.W.; Li, J.; Chew, E.C. Effect of glucocorticoid hormone on nuclear matrix in cervical cancer cells in vitro. Anticancer Res, 1998, 18, 209-216.

Yang, C.; Edsall Jr, R.; Harris, H.A.; Zhang, X.; Manas, E.S.; Mewshaw, R.E. Erbeta ligands. Part 2: synthesis and structure-activity relationshops of a series of 4-hydroxy-biphenyl-carbaldehyde oxime derivatives. Bioorg Med Chem, 2004, 15, 2553-2570.

Yang, L.; Yam, H.F.; Cheng-Chew, S.B.; Wong, S.W.; Loog, E.P.; Chew, E.C. The association of HPV 16 DNA with specific nuclear matrix proteins of nuclear matrix proteins of normal and cervical carcinoma cell. Anticancer Res, 1997, 17, 343-347.

Yang, S.; Du, J.; Wang, Z.; Yuan, W.; Qiao, Y.; Zhang, M.; Zhang, J.; Gao, S.; Yin, J.; Sun, B.; Zhu, T. BMP-6 promotes E-cadherin expression through repressing δEFI in breast cancer cells, BMC Cancer, 2007, 7, 211.

Yang, X.; Phillips, D.L.; Ferguson, A.T.; Nelson, W.G.; Herman, J.G.; Davidson, N.E. Synergistic activation of functional estrogen receptor (ER)-alpha by DNA methyltransferase and histone deacetylase inhibitor in human ER-alpha-negative breast cancer cells. Cancer Res, 2001, 61, 7025-7029.

Yano, M. Expression of hsp90 and cyclin D1 in human breast cancer. Cancer Lett, 1999, 137, 45-51.

Yarden, R.L.; Wilson, M.A.; Chrysogelos, S.A. Estrogen suppression of EGFR expression in breast cancer cells: a possible mechanism to modulate growth. J Cell Biochem, 2001, 81, 232-246.

Yi, P.; Drischoll, M.D.; Huang, J.; Bhagat, S.; Hilf, R.; Bambara, A.; Muyan, M. The effects of estrogen-responsive element- and ligand-induced structural changes on the recruitment of cofactors and transcriptional responses by ERa and ERb. Mol Endocrinology, 2002, 16, 674-693.

Zagouri, F.; Nonni, A.; Sergentanis, T.N.; Papadimitriou, C.A.; Michalpoulos, N.V.; Lazaris, A.C.; Patsouris, E.; Zografos, G.C. Heat shock protein 90 in lobular neoplasia of the breast. BMC Cancer, 2008, 8, 312.

Zeng, C. NuMA: A nuclear protein involved in mitotic centrosome function. Microscopy Res Tech, 2000, 49, 467-477.

Zeng, C.; He, D.; Brinkley, D.B.R. Localization of NuMA protein isoforms in the nuclear matrix of mammalian cells. Cell Motil Cytoskel, 1994, 29, 167-176.

Zilli, M.; Grassadonia, A.; Tinari, N.; Di Gioacobbe, A.; Gildetti, S.; Giampietro, J.; Natoli, C.; Iacobelli, S. Molecular mechanisms of endocrine resistance and their implication in the therapy of breast cancer. Biochim Biophys Acta Rev Cancer, 2009, 1795, 62-81.

Zink, D.; Fischer, A.H.; Nickerson, J.A. Nuclear structure in cancer cells. Nat Rev Cancer, 2004, 4, 677-687.